PDR

UCRL-15272
PSA #7249809

SEISMIC SAFETY MARGINS RESEARCH PROGRAM
(Phase I)

LINEAR SOIL-STRUCTURE INTERACTION

J. E. Luco
University of California, San Diego

July 1980

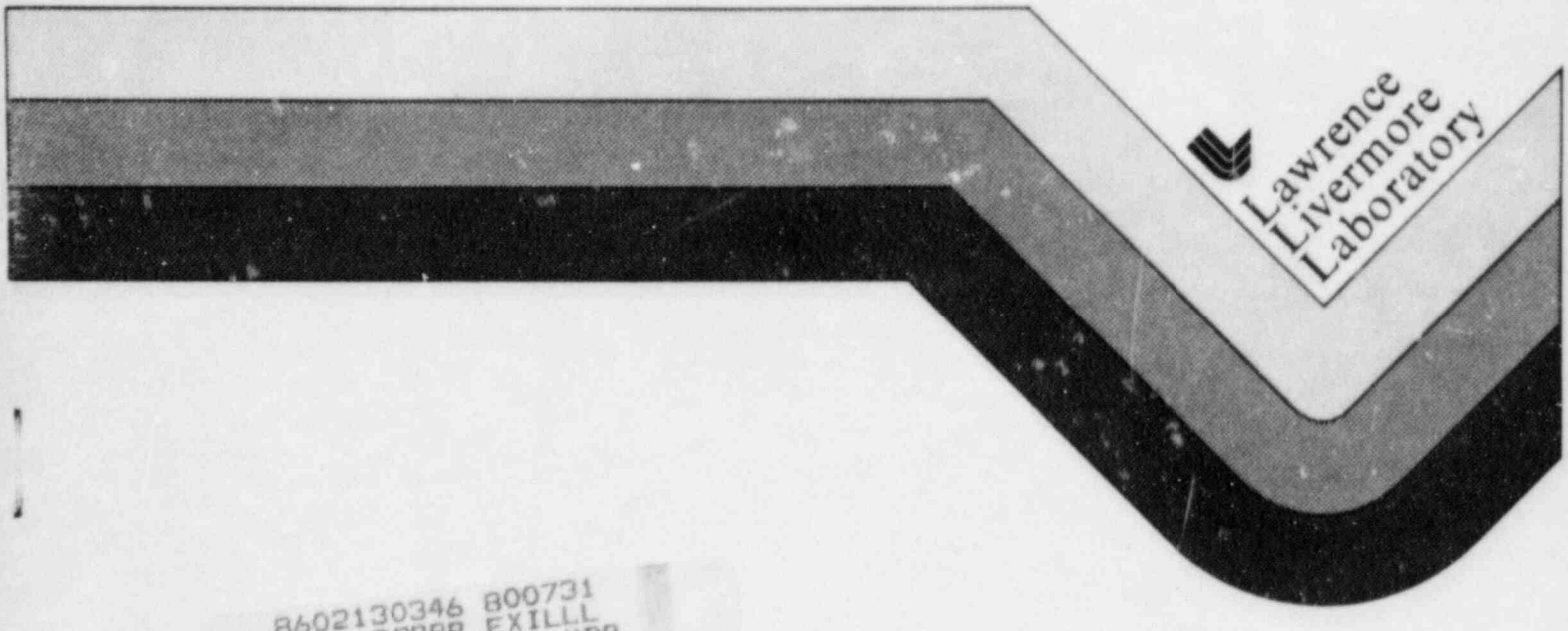

8602130346 800731
PDR TOPRP EXILLL PDR
C

DISCLAIMER

This book was prepared as an account of work sponsored by an agency of the United States Government. Neither the United States Government nor any agency thereof, nor any of their employees, makes any warranty, expressed or implied, or assumes any legal liability or responsibility for the accuracy, completeness, or usefulness of any information, apparatus, product, or process disclosed, or represents that its use would not infringe privately owned rights. Reference herein to any specific commercial product, process, or service by trade name, trademark, manufacturer, or otherwise, does not necessarily constitute or imply its endorsement, recommendation, or favoring by the United States Government or any agency thereof. The views and opinions of authors expressed herein do not necessarily state or reflect those of the United States Government or any agency thereof.

This work was supported by the United States Nuclear Regulatory Commission under a Memorandum of Understanding with the United States Department of Energy.

SEISMIC SAFETY MARGINS RESEARCH PROGRAM

(PHASE I)

LINEAR SOIL-STRUCTURE INTERACTION

July 1980

Prepared by

J. E. Luco

University of California, San Diego
Department of Applied Mechanics and
Engineering Sciences

Prepared for

Nuclear Test Engineering Division
Mechanical Engineering Department
Lawrence Livermore Laboratory
Livermore, California

NRC	LLL
Program Manager	Program Leader
J. E. Richardson	F. J. Tokarz
Branch Chief	Program Manager
G. Bagchi	P. D. Smith
Project Manager	Project Manager
J. F. Costello	J. J. Johnson

*This work was supported by the U. S. Nuclear Regulatory Commission under a memorandum of understanding with the U. S. Department of Energy.

TABLE OF CONTENTS

LINEAR SOIL-STRUCTURE INTERACTION

ABSTRACT

The formulation and analysis techniques for the linear three-dimensional soil-structure interaction problem are discussed. In particular, subsystem or substructure formulations of the interaction problem for isolated flexible structures supported on rigid and flexible foundations as well as for the case of several elastic structures interacting through the soil are presented and reviewed. Emphasis is given to the description of the analytical and numerical techniques used to determine the response of the various elements entering into a subsystem formulation. Some of the physical characteristics of these elements (free-field motion, foundation input motion, compliance and impedance functions, etc.) are also described.

1. INTRODUCTION

In the last few years significant advances have been made in the development of procedures to evaluate the seismic response of nuclear power plants and other structures including the effects of the interaction of each structure and the soil as well as the interaction through the soil among adjacent structures. In this report, the most important advances in the analysis of linear three-dimensional soil-structure interaction models are reviewed and an attempt at organizing these developments into a coherent whole is made.

A complete soil-structure interaction model must represent in a realistic fashion the geometry as well as the mechanical behavior of structures, foundations and soils. In particular, the geometrical arrangement of adjacent structures in a plant, the symmetry or lack of symmetry of each structure, the geometry of foundations, soil surface and soil strata must be preserved. In terms of the mechanical characterization, the model must properly account for the different structural elements (shells, slabs, walls, frames) and must accurately represent the material behavior of concrete, steel and soils. In addition, the conditions at each foundation-soil interface must be properly modelled including the possibility of lateral separation and foundation uplift. Finally, the model must be capable of considering seismic excitations in the form of internal waves arriving at any angle of incidence, and in the form of Rayleigh and Love surface waves.

The requirements just described imply that a complete soil-structure interaction model must be fully three-dimensional and nonlinear (inelastic). Although nonlinear three-dimensional finite-element and finite-difference schemes are presently available, they are not generally used due to the elevated cost, lack of generally accepted inelastic constitutive relationships for soils and lack of knowledge as to the values, for a particular site, of the associated constants appearing in these relationships.

At the present time the analyst is faced with two alternatives, the first of which is to include an approximation to the nonlinear behavior at the expense of restricting the analysis to two-dimensional geometrical configurations. Generally used computer programs such as LUSH, FLUSH and PLUSH are examples of this first alternative. These two-dimensional programs attempt to represent the nonlinear soil behavior by use of an equivalent linear model obtained by an iterative process. The intrinsic two-dimensional nature of the models on which these programs are based raises serious doubts as to their

applicability to three-dimensional configurations. In particular, these and other two-dimensional models do not account for the torsional response of structures and for the response to nonvertically incident SH and Love waves. In addition, two-dimensional models severely distort the interaction effects between adjacent structures.

The second alternative, reviewed here, is to consider models which preserve the three-dimensional nature of the problem while being restricted to linear material behavior. The analysis of the linear three-dimensional soil-structure interaction problem may be conducted on the basis of a direct finite-element approach or by use of a substructure or subsystem procedure. In the first approach, a finite-element model of the entire system is made and the response of the model is evaluated in one stage. Fully three-dimensional linear analyses performed on the basis of the direct approach have essentially the same cost disadvantages as three-dimensional nonlinear analyses. For this reason, only the subsystem approach will be described here.

In the subsystem approach the problem is solved in two stages: in the first stage, elements of the response of superstructures, foundations and soil are obtained independently. In the second stage, the individual responses are combined so as to satisfy the interaction conditions and the response of the complete system is obtained. This approach is particularly convenient when the foundations may be assumed to be rigid or when the deformation of the foundations may be described by a small number of degrees of freedom. One of the advantages of the subsystem approach is that the analysis of each subsystem (superstructure, foundation, soil) can be performed by the analytical technique best suited to that particular part of the total problem. In addition, the substructure approach provides intermediate results which help in developing an understanding of the interaction effects and in testing the correctness of the final results.

The emphasis in this review is placed on the discussion of the complete formulation of the three-dimensional linear soil-structure interaction problem. The properties of the elements entering into the formulation as well as the analytical or numerical techniques employed to analyze the different subsystems are presented in some detail. No attempt has been made to discuss the extent of the interaction effects under various conditions. It is hoped, however, that this work will assist the reader in developing an appreciation for the nature of the possible interaction effects.

REFERENCES (1)

Hadjian, A.H., J.E. Luco and N.C. Tsai (1974). Soil-Structure Interaction: Continuum or Finite Element?, *Nuclear Engineering and Design, 31,* 151-167.

Howard, G.E., P. Ibanez and C.B. Smith (1976). Seismic Design of Nuclear Power Plants - An Assessment, *Nuclear Engineering and Design, 38,* 385-461.

Lee, T.H. (1976). Soil-Structure Interaction - Nuclear Reactors, The Continuum Approach, *Shock and Vibration Digest, 6,* 15-23.

2. FORMULATION OF THE LINEAR THREE-DIMENSIONAL SOIL-STRUCTURE INTERACTION PROBLEM

To guide the discussion, the formulation of the soil-structure interaction problem for the case of an isolated structure on a rigid foundation supported on a layered viscoelastic medium is summarized here. The problem is illustrated in Fig. 2.1. Based on the assumed linearity of the model, the response of the soil-structure system may be obtained in two stages. In the first stage, the frequency response of the system for harmonic excitation with time dependence of the type $\exp(i\omega t)$ is obtained. The second stage corresponds to the evaluation of the response in time by means of the Fourier synthesis given by

$$u(t) = \frac{1}{2\pi} \int_{-\infty}^{\infty} U(\omega) e^{i\omega t} d\omega \qquad (2.1)$$

In this equation, $u(t)$ denotes the response in time, while $U(\omega)$ represents the frequency response. The Fourier synthesis described by Eq. (2.1) is readily calculated by use of the Fast Fourier Transform algorithm (Liu and Fagel, 1971).

The approach used to obtain the frequency response for the complete soil-structure system is illustrated in Fig. 2.2 and it consists of subdividing the complete problem into a set of simpler problems that may be solved independently. Once the solution for each of the basic problems is known, the response of the interacting soil-structure system may be easily obtained.

The first basic problem that needs to be considered corresponds to the evaluation of the free-field motion, i.e., the determination of the response of the soil deposit for a given incident seismic wave before the cavity for the foundation has been excavated. For uniform or horizontally layered soil deposits and for plane incident waves, the free-field motion on the soil surface may be characterized by the three-component displacement vector $\{U_g\}e^{i\omega t}$ at a reference point, by the horizontal direction of propagation of the incident wave, and by the apparent horizontal velocity c of the incident wave in the direction of propagation. For a given seismic excitation the three components of the free-field motion vector of the soil surface $\{U_g\}$ may not be independent. In addition, for surface wave excitation in a layered soil model, the apparent horizontal velocity c is frequency dependent. The characteristics of the free-field motion are discussed in Chapter 3.

The second basic problem is associated with the evaluation of the harmonic response of the rigid foundation bonded to the soil and subjected to the incident seismic wave in absence of the superstructure. In this step, the foundation is assumed massless, the inertia of the foundation being incorporated at a later stage. The presence of the rigid foundation modifies the free-field motion and the resulting response of the massless foundation, called here foundation input motion, may be represented by a six-component vector

$$\{U_o^*\} = (\Delta_x^*, \Theta_y^*, \Delta_y^*, \Theta_x^*, \Delta_z^*, \Theta_z^*)^T \quad , \qquad (2.2)$$

in which Δ_x^*, Δ_y^* and Δ_z^* represent the translational components of the response at a reference point while Θ_x^*, Θ_y^* and Θ_z^* represent the rotational components of the response about the x, y and z axes, respectively. The foundation input motion $\{U_o^*\}$ depends on the frequency of the excitation, geometry of the foundation, characteristics of the soil deposit and on the type of seismic excitation. The characteristics of the foundation input motion are discussed in Chapter 4.

When the inertia of the foundation and the presence of the superstructure are taken into account, the total response $\{U_o\} = (\Delta_x, \Theta_y, \Delta_y, \Theta_x, \Delta_z, \Theta_z)^T$ at a reference point in the rigid foundation may be written in the form

$$\{U_o\} = \{U_o^*\} + \{U_s\} \qquad (2.3)$$

in which the 6×1 vector $\{U_s\}$ corresponds to the additional motion of the foundation associated with

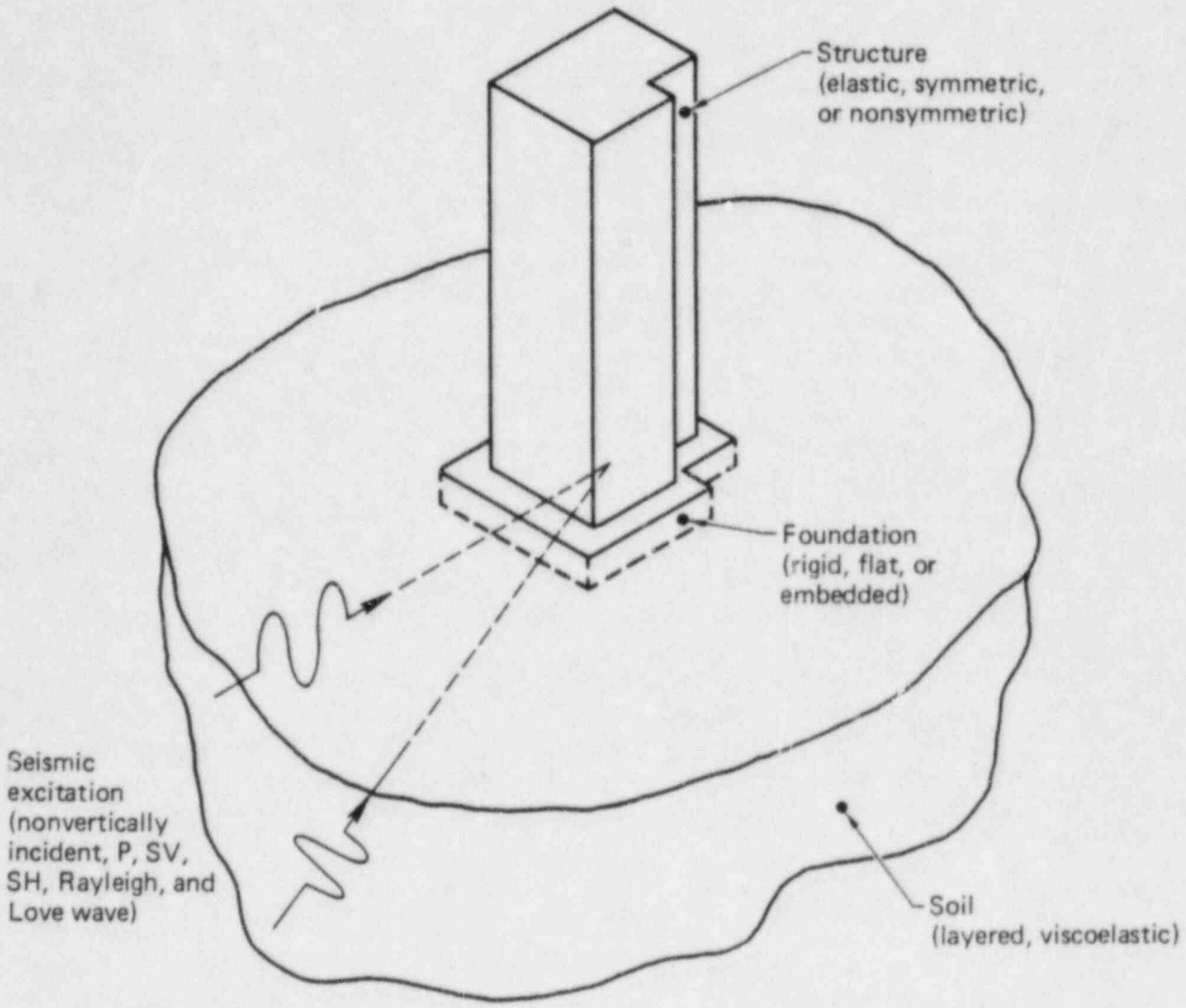

FIG. 2.1. Description of the soil-structure system.

deformation of the soil caused by the forces and moments that the foundation exerts on the soil. The forces and moments that the foundation exerts on the soil can be represented by the 6 × 1 vector $\{F_s\} = (F_{xs}, M_{ys}, F_{ys}, M_{xs}, F_{zs}, M_{zs})^T$, in which F_{xs}, F_{ys} and F_{zs} represent the components of the resultant force, while M_{xs}, M_{ys} and M_{zs} denote the components of the resultant moment about the point of reference in the foundation.

The motion $\{U_s\}$ of the foundation caused by the generalized force $\{F_s\}$ is given by

$$\{U_s\} = [C(\omega)]\{F_s\} \tag{2.4}$$

where $[C(\omega)]$ is the 6 × 6 compliance matrix for the rigid foundation. The third basic problem corresponds, then, to the evaluation of the compliance matrix for the rigid foundation. The compliance matrix depends on the frequency of the excitation, the geometry of the foundation and on the characteristics of the underlying soil deposit (Chapter 5).

If $\{F_b\} = (F_{xb}, M_{yb}, F_{yb}, M_{xb}, F_{zb}, M_{zb})^T$ represents the resultant forces and moments that the superstructure exerts on the foundation, then, the equation of motion for the rigid foundation can be written in the form

$$\{F_s\} = \omega^2[M_o]\{U_o\} + \{F_b\} \tag{2.5}$$

where $[M_o]$ is the 6 × 6 mass matrix for the rigid foundation.

It can be shown that the generalized force $\{F_b\}$ that the superstructure exerts on the foundation can be expressed in terms of the total motion of the foundation $\{U_o\}$ through the relation

$$\{F_b\} = \omega^2[M_b(\omega)]\{U_o\} \tag{2.6}$$

where $[M_b(\omega)]$ plays the role of a 6 × 6 frequency-dependent equivalent mass matrix. This matrix depends on the geometry, mass distribution and elastic properties of the superstructure. The fourth basic problem, discussed in Chapter 6, entails the construction of the equivalent mass matrix $[M_b(\omega)]$.

Once the basic sub-problems have been solved, the total motion $\{U_o\}$ of the foundation, including the soil structure interaction effects, can be obtained by eliminating $\{F_b\}$, $\{F_s\}$ and $\{U_s\}$ from Eqs. (2.3) through (2.6). The resulting expression is

$$\{U_o\} = \left([I] - \omega^2[C(\omega)]([M_o] + [M_b(\omega)])\right)^{-1}\{U_o^*\} \tag{2.7}$$

in which [I] denotes the 6 × 6 identity matrix. Equation (2.7) clearly separates the different interaction effects. The effects of scattering of the incident seismic waves by the rigid foundation are included in the foundation input motion vector $\{U_o^*\}$ which, in the case of non-vertically incident waves, involves translational and rotational components. The interaction effects between the superstructure, foundation and soil are represented in Eq. (2.7) by the term $[C(\omega)]([M_o] + [M_b(\omega)])$. The total motion of the foundation $\{U_o\}$ results from a combination of both types of effects as shown in the feedback block diagram of Fig. 2.2.

Once the total motion at foundation level has been obtained, the response in the frequency and time domains at any level of the superstructure can be easily obtained by standard techniques (Chapter 7).

The formulation just described is also valid for the case of several structures interacting through the soil (Chapter 8). In this case, the foundation response vector $\{U_o\}$ includes six degrees of freedom for each of the N foundations, and the matrices $[M_o]$ and $[M_b(\omega)]$ are block diagonal of dimensions 6N × 6N. The coupling between foundations is incorporated in the compliance matrix $[C(\omega)]$ and in the foundation input motion $\{U_o^*\}$. The case of a structure supported on a flexible foundation or on several footings can be formulated in a similar manner (Chapter 9).

The techniques available to determine the fundamental elements entering in the formulation, i.e. the

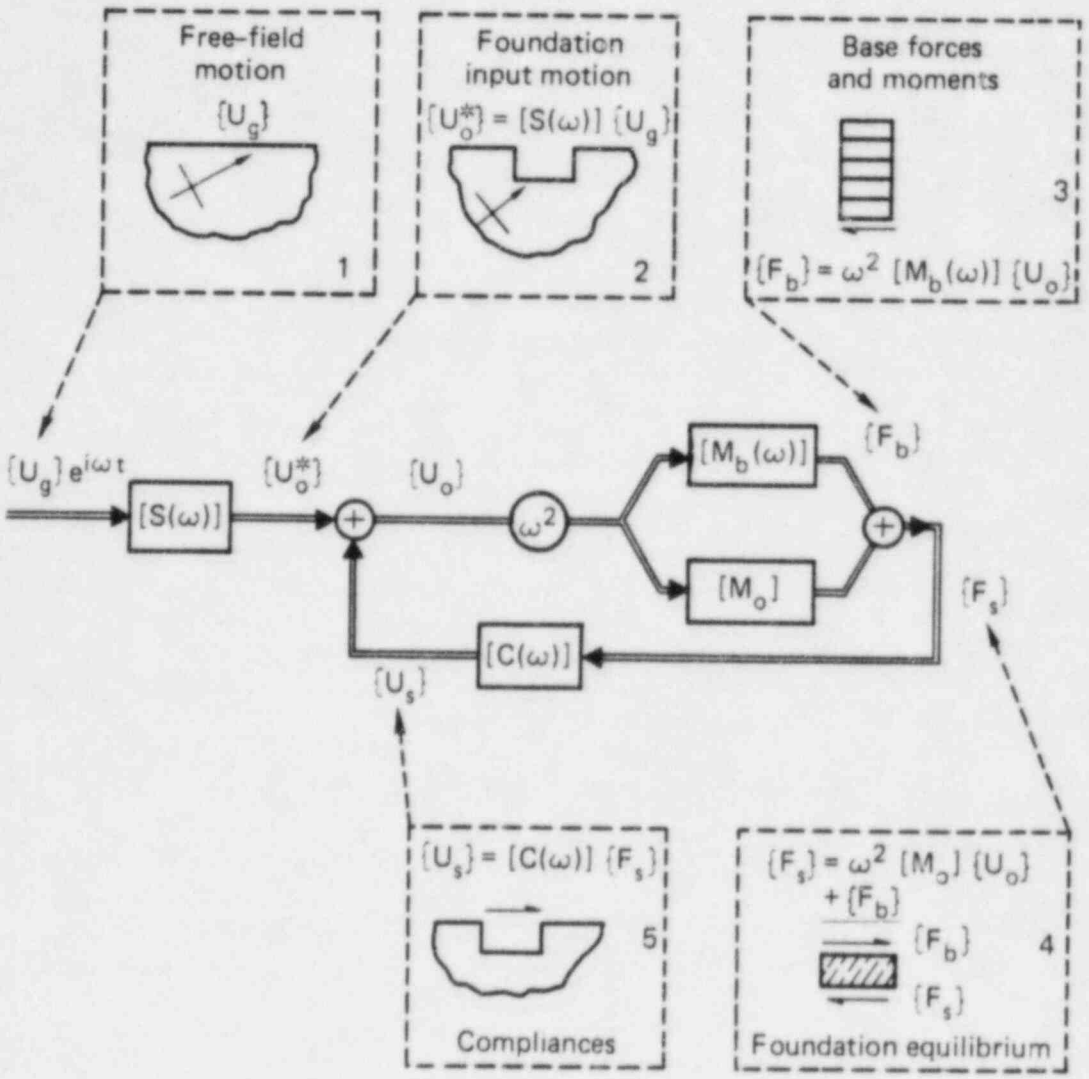

FIG. 2.2. Interaction block diagram.

free-field motion, foundation input motion, foundation compliance matrix and equivalent mass matrix for the superstructure, as well as the physical characteristic of these elements are described in some detail in Chapters 3, 4, 5 and 6. As example of the evaluation of the complete response of the soil-structure system, the response of structures subjected to nonvertically incident waves is discussed in Chapter 7. The application of the formulation described above to the case of several structures interacting through the soil is presented in Chapter 8. Finally, the modification of the basic formulation for the case of structures supported on various types of flexible foundations are presented in Chapter 9.

The formulation presented above [Wong and Luco (1977, 1978), Luco and Wong (1978)] has evolved from the formulations presented by Parmelee (1967), Thau (1967), Luco (1969), Lee and Wesley (1971) and Luco, Wong and Trifunac (1975). Other formulations applicable to the linear three-dimensional soil-structure interaction problem are discussed in Chapters 10 and 11.

REFERENCES (2)

Lee, T.H., and D.A. Wesley (1971). Soil-Foundation Interaction of Reactor Structures Subjected to Seismic Excitation, *Proc. 1st Int. Conf. Struct. Mech. in Reactor Technology*, Berlin, Paper K3/5.

Liu, S.C., and L.W. Fagel (1971). Earthquake Interaction by Fast Fourier Transform, *J. Engrg. Mech. Div. ASCE, 97*, EM4, 1223-1237.

Luco, J. E. (1969). Dynamic Interaction of a Shear Wall with the Soil, *J. Engrg. Mech. Div. ASCE, 95*, 333-346.

Luco, J.E., and H.L. Wong (1979). *Response of Structures to Nonvertically Incident Seismic Waves*. Report, Dept. of Appl. Mechs. and Engrg Sci., Univ. of California San Diego, La Jolla.

Luco, J.E., H.L. Wong and M.D. Trifunac (1975). A Note on the Dynamic Response of Rigid Embedded Foundations, *Earthquake Engrg. Struct. Dynamics, 4*, 119-129.

Parmelee, R. A. (1967). Building-Foundation Interaction Effects, *J. Engrg. Mech. Div. ASCE, 93*, 131-152.

Thau, S. A. (1967). Radiation and Scattering from a Rigid Inclusion in an Elastic Medium, *J. of Applied Mechanics, 89*, 509-511.

Wong, H.L., and J.E. Luco (1977). The Application of Standard Finite Element Programs in the Analysis of Soil-Structure Interaction, *Proc. 2nd SAP User's Conf.*, Univ. of Southern California, Los Angeles.

Wong, H.L., and J.E. Luco (1978). Dynamic Response of Rectangular Foundations to Obliquely Incident Seismic Waves, *Earthquake Engrg. Struct. Dynamics, 6*, 3-16.

3. FREE-FIELD MOTION

A basic assumption in many of the presently available methods to analyze the soil-structure interaction problem is that the seismic excitation can be represented by plane vertically propagating compressional or shear waves. Recent analyses of strong motion records as well as several theoretical investigations indicate that the motion recorded on the soil surface results from a complex superposition of different types of waves impinging on the free surface with different angles of incidence. In particular, it has been found that surface waves of the Rayleigh and Love types may represent an important contribution to the total free-field motion. Since these studies tend to invalidate a basic assumption of most soil-structure interaction analyses, it becomes a necessity to consider free-field motion representations that include non-vertically incident waves.

The present strong motion instrumentation of structures is such that one typically finds only one accelerograph per floor. Under these conditions it is difficult to find unambiguous evidence for non-vertically incident waves. In particular, it is not possible to separate the torsional response of symmetric structures, or to identify the rocking response. This situation will remain until buildings are properly instrumented with several instruments per floor.

In spite of the conditions just described there is some experimental evidence for the existence of non-vertically incident waves. Housner (1957) in a study of the response of the Hollywood Storage Building to the Arvin-Tehachapi earthquake of 1952 found a marked reduction of the intermediate and high frequency components of the recorded basement motion as compared with the motion recorded in the free-field and advanced the hypothesis that such reductions could be explained by non-vertically incident waves. Crouse (1973) noted similar effects on the same structure for the San Fernando earthquake of 1971 and showed that the reduction of the high frequency components could not be explained on the basis of vertically incident waves impinging on an assumed flat foundation. Duke et al. (1971) have shown that the observed reduction of the high-frequency components could be explained by the embedment of the foundation, but their study does not rule out the possibility of non-vertically incident waves. Analysis of the Hollywood Storage Building roof response reveals the existence of a torsional component that could only be generated by non-vertically incident waves given the symmetry of the structure.

Reductions of the peak accelerations recorded on the base of structures as compared with free-field values have been noted by Yamahara (1970). Again, non-vertically incident waves could explain these reductions although other effects such as embedment could also be contributing.

A different type of experimental information results from the analysis of the El Centro 1940 records made by Trifunac (1971). Trifunac found that the arrival times of many of the significant pulses coincided with the arrival times of Rayleigh and Love waves and concluded that surface waves are responsible for major contributions to the total accelerograms.

It seems then, from both the theoretical and experimental points of view, that it is not possible to ignore the existence of non-vertically incident seismic waves. It must be emphasized that the particular representation selected for the free-field motion has a marked effect on the structural response.

The description of the free-field motion at a site, i.e. the description of the motion that would take place before the cavity for the foundation has been excavated, involves several aspects. In the first place, a complete description of the motion at a point, usually on the ground surface, must be provided. In addition, the variation of the motion over the ground surface and into the soil to the depth of the base of the foundation must also be given. The conventional assumption of vertically incident SH-and P-waves drastically simplifies the problem. In this case, if the motion at a point on the ground surface is given, then all other points on the ground surface would experience simultaneously the same motion. The variation of motion with depth can be easily calculated by use of one-dimensional wave propagation analysis. For a more general seismic environment the problem of describing the free-field motion is considerably more complex. The different procedures generally used to specify the seismic ground mo-

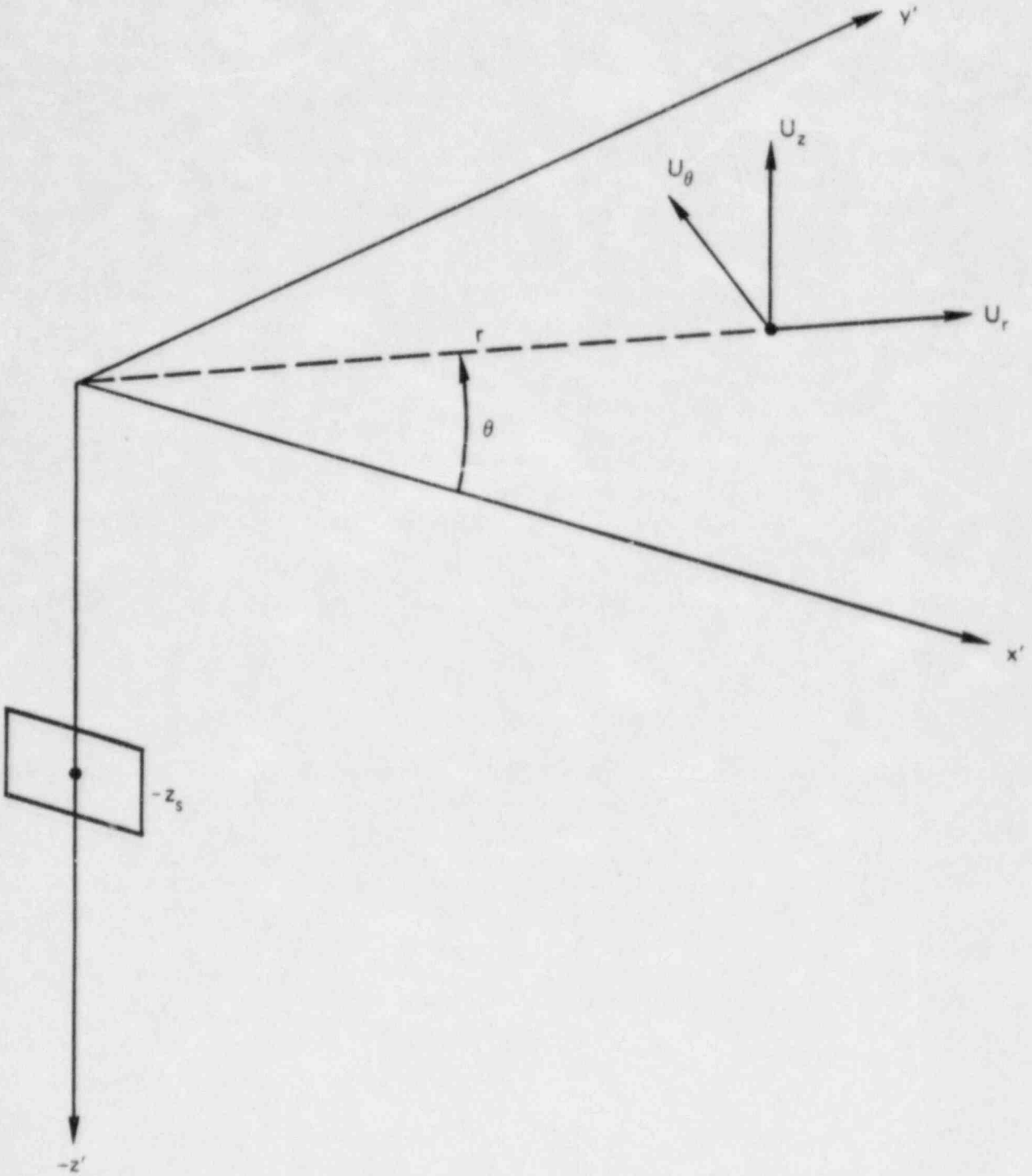

FIG. 3.1. Description of the source-observer geometry.

tion at a point will not be reviewed here; the emphasis will be placed on the description of the possible variation of motion over the ground surface and at depth. It must be noted, however, that the control motion is the most important single factor affecting the seismic response of the structure.

After the vertically incident wave model, the most parsimonious model of the free-field motion of a higher order of complexity would be as follows:

(i) The horizontal component of motion in the direction normal line connecting the site and the presumed epicenter would be represented by an equivalent nonvertically incident plane SH-wave with a given phase velocity. This plane wave would represent the contributions of SH and Love waves.

(ii) The other horizontal component and the vertical component of motion would be represented by a combination of a plane nonvertically incident SV-wave and a plane nonvertically incident P-wave both with the same phase velocity. These two equivalent waves would reflect the P-, SV- and Rayleigh waves arriving at the site.

This model requires the specification of the three components of motion at a point, of two equivalent phase velocities and of the epicenter-site direction. The free-field motion derived from this model would be such that the amplitude of motion at different points on the ground surface would remain uniform but phase differences between the motion at different points would be obtained. In depth, the free-field motion would vary both in amplitude and in phase. The critical parameters in this model would be the equivalent phase velocities.

The feasibility of a free-field model of this type has been explored by Luco and Sotiropoulos (1980). In that study the seismic source was represented by a small vertical fault located at a depth z_s from the surface of a layered viscoelastic half-space as shown in Fig. 3.1. In this case, the Fourier transforms of the radial, tangential and vertical components of acceleration at a point on the ground surface can be written in the form

$$\begin{aligned}
\ddot{U}_r(r,\Theta,\omega) &= \ddot{M}_x(\omega)\Sigma_{rx}(r,\omega)\sin 2\Theta + \ddot{M}_z(\omega)\Sigma_{rz}(r,\omega)\sin\Theta \\
\ddot{U}_\Theta(r,\Theta,\omega) &= \ddot{M}_x(\omega)\Sigma_{\Theta x}(r,\omega)\cos 2\Theta + \ddot{M}_z(\omega)\Sigma_{\Theta z}(r,\omega)\cos\Theta \qquad (3.1) \\
\ddot{U}_z(r,\Theta,\omega) &= \ddot{M}_x(\omega)\Sigma_{zx}(r,\omega)\sin 2\Theta + \ddot{M}_z(\omega)\Sigma_{zz}(r,\omega)\sin\Theta
\end{aligned}$$

where r and Θ denote epicentral distance and azimuth, respectively. The terms $\ddot{M}_x(\omega)$ and $\ddot{M}_z(\omega)$ correspond to the Fourier transforms of the second derivative with respect to time of the seismic moments $M_x(t)$ and $M_z(t)$. The seismic moment $M_x(t)$ is associated with strike-slip while $M_z(t)$ is associated with dip-slip. The terms $\Sigma_{rx}(r,\omega)$, ..., $\Sigma_{zz}(r,\omega)$ correspond to the radial dependence of the Green's functions for a double couple at depth z_s. The representation of the free-field motion given by Eq. (3.1) factorizes the effects of the seismic source $[M_x(\omega), M_z(\omega)]$, propagation path $[\Sigma_{rx}(r,\omega), \ldots, \Sigma_{zz}(r,\omega)]$ and radiation pattern $[\Theta]$.

The representation given by Eq. (3.1) indicates that the variation of the free-field motion on the ground surface will be controlled by the variation of the Green's functions with epicentral distance r. To study the behavior of the Green's functions $\Sigma_{\alpha\beta}(r,\omega)$ ($\alpha = r,\Theta,z; \beta = x,z$), it is convenient to express these functions in the form

$$\Sigma_{\alpha\beta}(r,\omega) = |\Sigma_{\alpha\beta}(r,\omega)| \cdot \exp[-i\phi_{\alpha\beta}(r,\omega)] \qquad (3.2)$$

where $|\Sigma_{\alpha\beta}|$ represents the amplitude and $\phi_{\alpha\beta}(r,\omega)$ the phase angle. The typical effects of epicentral distance on the amplitudes of the Green's functions are illustrated in Figs. 3.2a and 3.2b for a frequency of 10 Hz. In Fig. 3.2a the amplitudes $|\Sigma_{\Theta x}(r,\omega)|$, $|\Sigma_{\Theta z}(r,\omega)|$ and $|\Sigma_{zx}(r,\omega)|$ are plotted versus epicentral distance for a source at a depth $z_s = 5.5$ km in a typical geologic structure. The behavior of the amplitudes $|\Sigma_{\Theta x}(r,\omega)|$ and $|\Sigma_{\Theta z}(r,\omega)|$ for a source at a depth $z_s = 1.0$ km is shown in Fig. 3.2b. The results shown in Fig. 3.2 indicate a general reduction in amplitude with epicentral distance which results from

geometrical spreading and material attenuation. In addition, significant amplitude fluctuations can be observed. These fluctuations associated with the interference of the different types of waves contributing to the total amplitude are particularly strong for shallow sources. For deeper sources and lower frequencies the fluctuations are not as pronounced and, as a first approximation, it is possible to assume that the amplitudes of the Green's functions will remain constant for variations of the epicentral distance of the order of a few tens of meters.

The variation of the phase angles $\phi_{\alpha\beta}(r,\omega)$ with epicentral distance can be described by calculating the equivalent phase velocities $c_{\alpha\beta}(r,\omega)$ defined by

$$c_{\alpha\beta}(r,\omega) = \omega\left(\frac{d\phi_{\alpha\beta}}{dr}\right)^{-1} \tag{3.3}$$

The variations of the equivalent phase velocities $c_{\theta x}(r,\omega)$, $c_{rx}(r,\omega)$ and $c_{zx}(r,\omega)$ versus epicentral distance are presented in Fig. 3.3. In this figure, the reciprocals of the phase velocities are plotted versus epicentral distance for frequencies of 1., 5.5 and 10 Hz. The calculations are based on a typical geologic structure and on a source buried at a depth of 5.5 km. The results presented in Fig. 3.3 indicate that for epicentral distances less than the source depth, the phase velocities are high and essentially independent of frequency. This result is in agreement with the expectation of a dominant direct ray in this region. For epicentral distances in the range from 5 to 12 km the phase velocities exhibit a dependence on both frequency and epicentral distance. In this range of epicentral distances, the phase velocity $c_{\theta x}$ oscillates about a value of the order of 3.5 km/sec, while c_{rx} and c_{zx} oscillate about a value of the order of 5.0 km/sec. In spite of the fluctuations with epicentral distance, it is still possible to assume, as a first approximation, that the phase velocities will remain constant for variations of the epicentral distance of a few tens of meters.

Based on these observations, it is possible to write

$$\Sigma_{\alpha\beta}(r,\omega) \approx \Sigma_{\alpha\beta}(r_o,\omega)\exp\left[-i\omega(r-r_o)/c_{\alpha\beta}(r_o,\omega)\right] \tag{3.4}$$

for $|r-r_o|$ less than a few tens of meters. Eqs. (3.1) and (3.4) indicate that the free-field motion in the vicinity of a point $(r_o,\Theta_o,0)$ can be approximated by six plane dispersive waves. A further simplification is obtained by noting that

$$c_{\theta x}(r,\omega) \approx c_{\theta z}(r,\omega) = c_H(r,\omega)$$

and (3.5)

$$c_{rx}(r,\omega) \approx c_{rz}(r,\omega) \approx c_{zx}(r,\omega) \approx c_{zz}(r,\omega) = c_V(r,\omega)$$

From Eqs. (3.1), (3.4) and (3.5) it can be shown that

$$U_\theta(r,\Theta,\omega) \approx U_\theta(r_o,\Theta_o,\omega)\exp[-i\omega(r-r_o)/c_H(r_o,\omega)] \tag{3.6}$$

and

$$U_r(r,\Theta,\omega) \approx U_r(r_o,\Theta_o,\omega)\exp[-i\omega(r-r_o)/c_V(r_o,\omega)]$$

$$U_z(r,\Theta,\omega) \approx U_z(r_o,\Theta_o,\omega)\exp[-i\omega(r-r_o)/c_V(r_o,\omega)] \tag{3.7}$$

for $|r-r_o| \ll 1$ km and $|\Theta-\Theta_o| < 1°$. Eqs. (3.6) and (3.7) indicate that the free-field motion in the vicinity of a point of coordinates $(r_o, \Theta_o, 0)$ can be obtained if the motion (U_r, U_θ, U_z) at the control point and the equivalent phase velocities c_H and c_V are known. The tangential motion would be defined by the amplitude $U_\theta(r_o, \Theta_o, \omega)$ on the ground surface and by the equivalent phase velocity $c_H(r_o,\omega)$. The

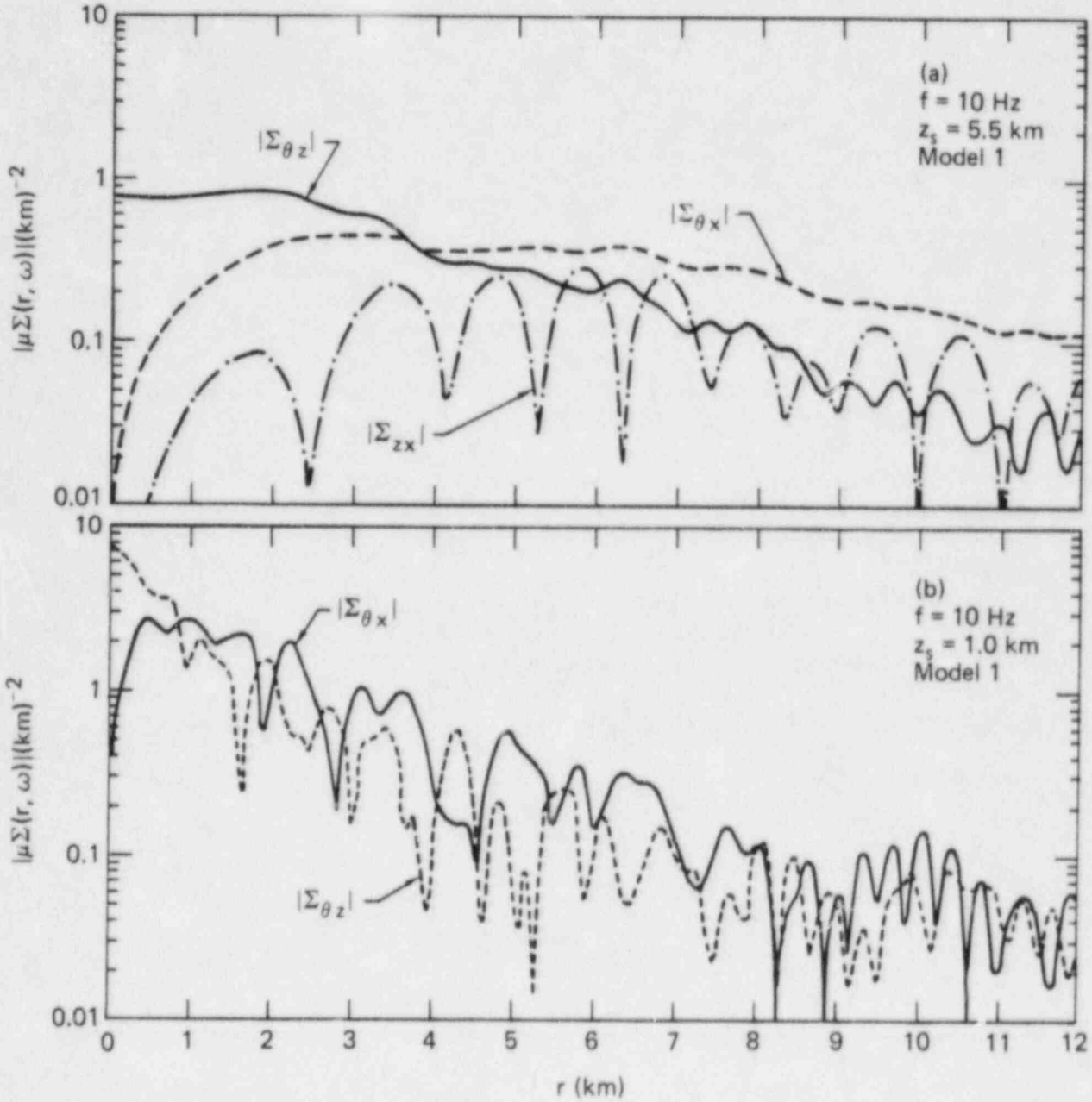

FIG. 3.2. Dependence of the amplitudes of the Green's functions on epicentral distance for a frequency of 10 Hz: (a) source depth 5.5 km, (b) source depth 1.0 km (μ = shear modulus at source depth) (Luco and Sotiropoulos, 1980).

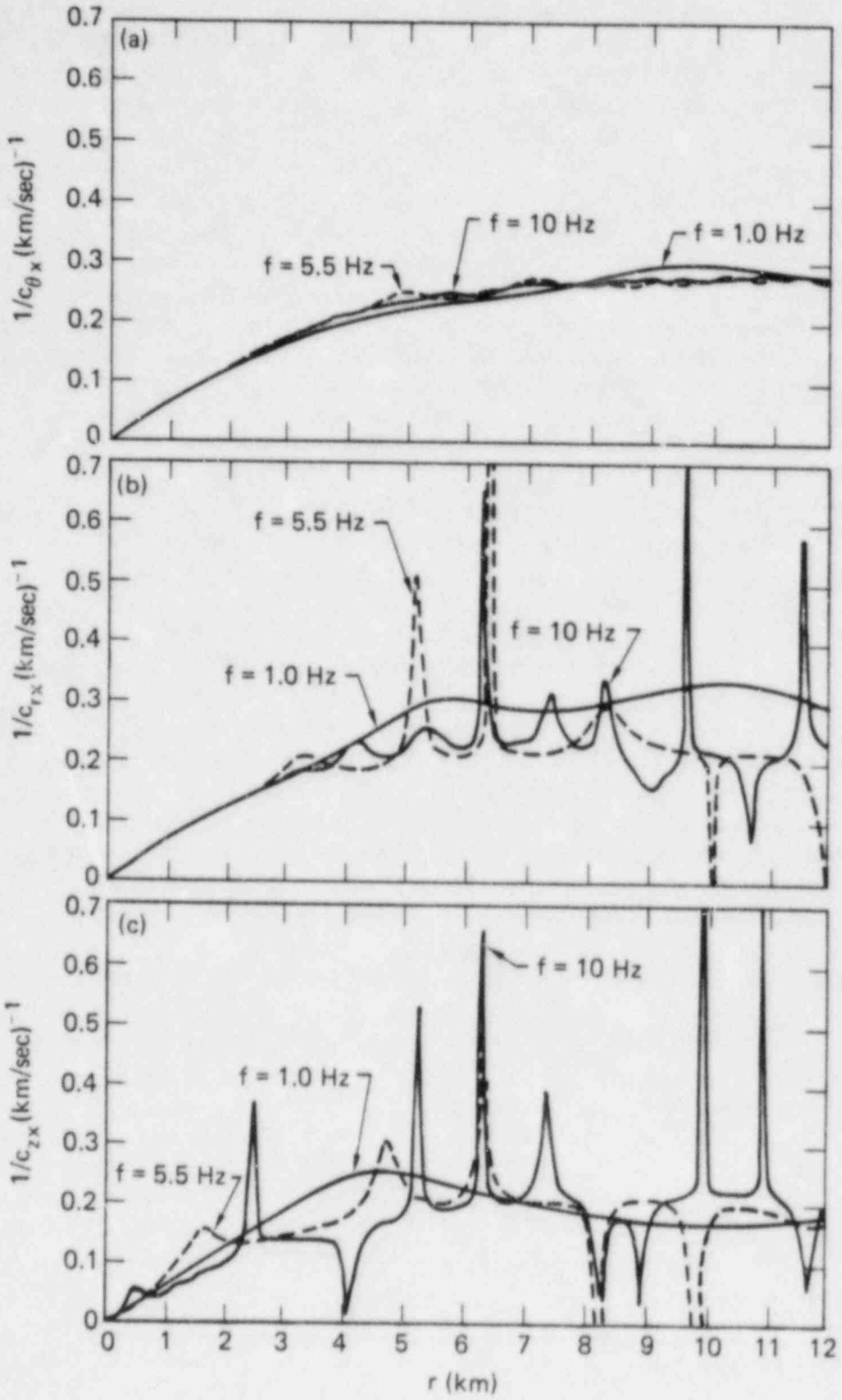

FIG. 3.3. Dependence of the equivalent phase velocities $c_{\Theta x}$, c_{rx} and c_{zx} on epicentral distance for frequencies of 1.0, 5.5, and 10 Hz. The source is at a depth of 5.5 km. (Luco and Sotiropoulos, 1980).

tangential motion at depth can be calculated by considering a nonvertically incident plane SH-wave with the given phase velocity $c_H(r_o,\omega)$. The radial and vertical components of motion would be defined by the amplitudes $U_r(r_o,\Theta_o,\omega)$ and $U_z(r_o,\Theta_o,\omega)$ and by the phase velocity $c_V(r_o,\omega)$. The radial and tangential motion at depth can be calculated by using a combination of a plane nonvertically incident SV-wave and a P-wave, both with the same phase velocity $c_V(r_o,\omega)$.

It is interesting to point out that Hadjian (1978), in a study of the correlation between recorded horizontal and vertical components of motion, has found that in the direction in which the correlation between two horizontal components is zero, the correlation between one horizontal component and the vertical component is maximum. It is tempting to interpret these results to indicate that the radial and vertical components of motion are related while the tangential component is independent from the other two components. The independence would result from the fact that the tangential component is dominated by SH and Love waves while the radial and vertical components are dominated by P, SV and Rayleigh waves.

Compared with the conventional assumption of vertically incident waves, the model described by Eqs. (3.6) and (3.7) introduces two new parameters corresponding to the equivalent phase velocities $c_H(r,\omega)$ and $c_V(r,\omega)$. If the geologic structure and the location of the source are known, estimates of these functions can be obtained as described above. For a typical geologic structure, Luco and Sotiropoulos (1980) have obtained $c_H \approx 3.5$ km/sec and $c_V \approx 5.0$ km/sec ($z_s = 5.5$ km, $r = 5\text{-}12$ km). A physical feeling for these values can be obtained by considering that for a frequency of 20 Hz the tangential motion at two points separated by a distance of 88 m would be 180 degrees out of phase. For a shear wave velocity on the top layer of 500 m/sec, a value of $c_H \approx 3.5$ km/sec implies an angle of incidence of 8 degrees with respect to the vertical. Significantly lower phase velocities can be obtained for shallower sources and shorter epicentral distances.

The theoretical estimates for the phase velocities described above are within the range of observed values reported by Tamura et al (1977) and Tsuchida et al. (1977). Based on recordings on five seismometers separated by distances of 100 m and disposed on a T-shaped array, Tamura et al. (1977) have calculated a value for phase velocity of 2.9 km/sec for an earthquake located at an epicentral distance of 30 km (focal depth of 80 km). The same authors, based on a linear array of six accelerometers separated by distances of 100 m, obtained a phase velocity of 2.6 km/sec for an earthquake located at an epicentral distance of 52 km (focal depth of 52 km). Tsuchida et al. (1977) based on recordings at two seismometers separated by a distance of 2.5 km have reported values of the phase velocity of 2.6 km/sec and 4.4 km/sec for earthquakes at epicentral distances of 161 and 54 km (focal depth 40 and 50 km), respectively. For a third earthquake (epicentral distance 140 km, focal depth 10 km) Tsuchida et al. report a phase velocity of -5.3 km/sec. In this case, due to variation in local soil conditions, the seismic excitation seems to have arrived first at the station farthest from the epicenter.

In regards to the variation of the amplitude of the free-field motion over short distances, Tsuchida et al. present some interesting results. Peak accelerations recorded on 2.5 km linear array of six seismometers separated by distances of 500 m show a standard deviation of the order of 20 percent of the mean peak acceleration. This standard deviation reflects the variation of peak acceleration over distances ranging from 500 m to 2500 m. Considerably lower variations can be expected over distances of a few tens of meters.

REFERENCES (3)

Crouse, C. B. (1973). *Engineering Studies of the San Fernando Earthquake,* Report EERL 73-04, Earthquake Engineering Research Laboratory, California Institute of Technology, Pasadena, California.

Duke, C. M., J. E. Luco, A. R. Carriveau, P. J. Hradilek, R. Lastrico and D. Ostrom (1971). Strong Earthquake Motion and Site Conditions: Hollywood, *Bull. Seism. Soc. Am., 60,* 4, 1271-1289.

Hadjian, A. H. (1978). On the Correlation of the Components of Strong Ground Motion. *Proc., Second International Conference on Microzonation,* San Francisco, California.

Housner, G. W. (1957). Interaction of Building and Ground During an Earthquake, *Bull. Seism. Soc. Am., 47,* 3, 179-186.

Luco, J. E. and D. A. Sotiropoulos (1980). Local Characterization of Free-Field Ground Motion and Effects of Wave Passage, *Bull. Seism. Soc. Am.* (in press).

Tamura, G., T. Noguchi and K. Kato (1977). Earthquake Observation along Measuring Lines on the Surface of Alluvial Soft Ground, *Proc. 6th World Conf. on Earthq. Engrg.,* New Delhi, India, *2,* 2-63 to 2-68.

Tsuchida, H., E. Kurata and S. Hayashi (1977). Observation of Earthquake Response of Ground with Horizontal and Vertical Seismometers Arrays, *Proc. 6th World Conf. on Earthq. Engrg.,* New Delhi, India, *2,* 2-173 to 2-178.

Trifunac, M. D. (1971). Response Envelope Spectrum and Interpretation of Strong Earthquake Ground Motion, *Bull. Seism. Soc. Am., 61,* 343-356.

Yamahara, H. (1970). Ground Motions During Earthquakes and the Input Loss of Earthquake Power to an Excitation of Buildings, *Soils and Foundations,* X, Japan Soc. of Soil Mechs. and Foundation Engrg.

4. FOUNDATION INPUT MOTION

The second step in the solution of the complete soil-structure interaction problem corresponds to the evaluation of the foundation input motion. For rigid foundations, the foundation input motion corresponds to the response of the rigid foundation to the seismic environment described by the free-field motion in absence of the superstructure. In this step, the foundation is assumed massless. The effects of the inertia of the foundation are incorporated at a later stage. The response of the rigid massless foundation to the seismic excitation can be described by the six-component vector

$$\{U_o^*\} = (\Delta_x^*, \Theta_y^*, \Delta_y^*, \Theta_x^*, \Delta_z^*, \Theta_z^*)^T \tag{4.1}$$

in which Δ_x^*, Δ_y^* and Δ_z^* represent the translational components of the response at a point of reference, while Θ_x^*, Θ_y^* and Θ_z^* represent the rotational components of the response. In general, the foundation input motion $\{U_o^*\}$ depends on the geometry of the foundations, on the characteristics of the soil deposit and on the nature of the seismic excitation.

Before proceeding with the discussion of the methods available to evaluate the foundation input motion it is convenient to describe some of its characteristics for different foundations and types of seismic excitations. In the first place, for flat foundations subjected to vertically-incident shear or compressional waves the response of the foundation includes only translational components with amplitudes equal to those of the free-field motion on the ground surface. Thus, in the case of flat foundations and vertically incident shear or compressional waves the evaluation of the foundation input motion is trivial. For flat foundations subjected to nonvertically incident seismic waves, the foundation input motion includes translational and rotational components and the amplitude of the translational response differs from the amplitude of the free-field motion on the ground surface.

As a first example, consider a flat, rigid square foundation of total width 2a supported on a uniform half-space and subjected to nonvertically incident SH waves as shown in Fig. 4.1. The free-field motion on the ground surface for SH waves propagating in the yz-plane ($\Theta_H = 0$ in Fig. 4.1) can be written in the form

$$\begin{Bmatrix} u_x^g(x,y,0) \\ u_y^g(x,y,0) \\ u_z^g(x,y,0) \end{Bmatrix} \exp(i\omega t) = \begin{Bmatrix} U_{gx}(\omega) \\ 0 \\ 0 \end{Bmatrix} \exp\left[i\omega\left(t - \frac{y}{c}\right)\right] \tag{4.2}$$

where $U_{gx}(\omega)$ corresponds to the amplitude of the free-field motion on the ground surface and $c = \beta/\cos\Theta_v$ to the apparent horizontal velocity of propagation (phase velocity), in which β is the shear wave velocity in the half-space and Θ_v is the vertical angle of incidence ($\Theta_v = 90°$ for vertical incidence). The components of the foundation input motion, in this case, can be expressed in the form

$$\begin{aligned} \Delta_x^* &= S_{xx}(a_o, \beta/c, 0)U_{gx} \\ a\Theta_z^* &= R_{zx}(a_o, \beta/c, 0)U_{gx} \\ a\Theta_y^* &= R_{yz}(a_o, \beta/c, 0)U_{gx} \\ \Delta_y^* &= \Delta_z^* = a\Theta_x^* = 0 \end{aligned} \tag{4.3}$$

where S_{xx}, R_{zx} and R_{yz} are complex functions of the dimensionless frequency $a_o = \omega a/\beta$ and of the ratio β/c. The numerical values for the real and imaginary parts of these functions, as obtained by Wong and Luco (1978a), for a half-space with a Poisson's ratio $\nu = 1/3$ are shown in Fig. 4.1 for different angles of incidence Θ_v. In this case, the response of the massless foundation consists of translation along the x-axis and torsion about the vertical z-axis. A small rocking component about the y-axis is also obtained. Equation (4.3) indicates that S_{xx} corresponds to the ratio of the translational response at the center

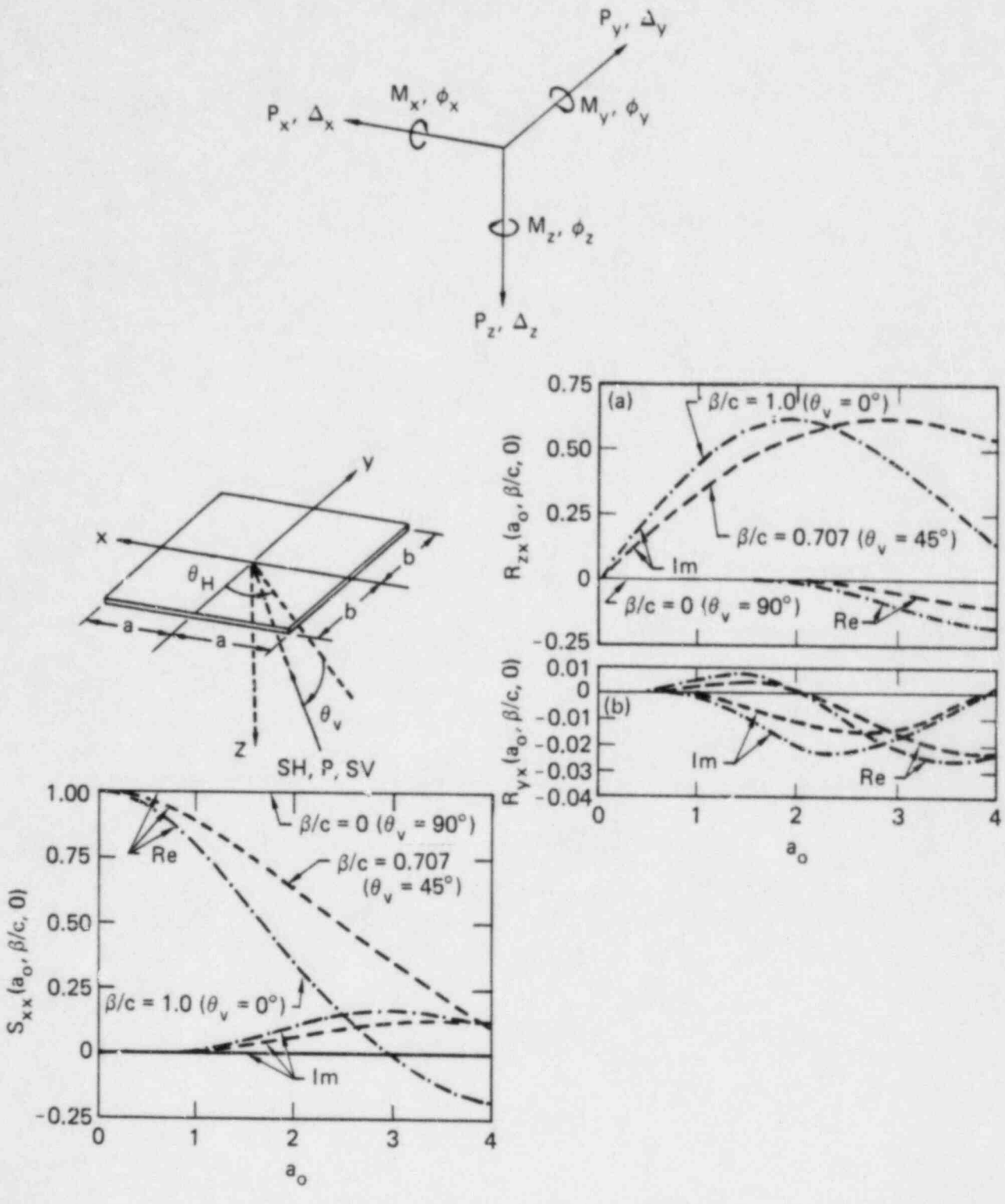

FIG. 4.1. Response of a square rigid foundation to nonvertically incident SH waves ($\Theta_H = 0$) (Wong and Luco, 1978a).

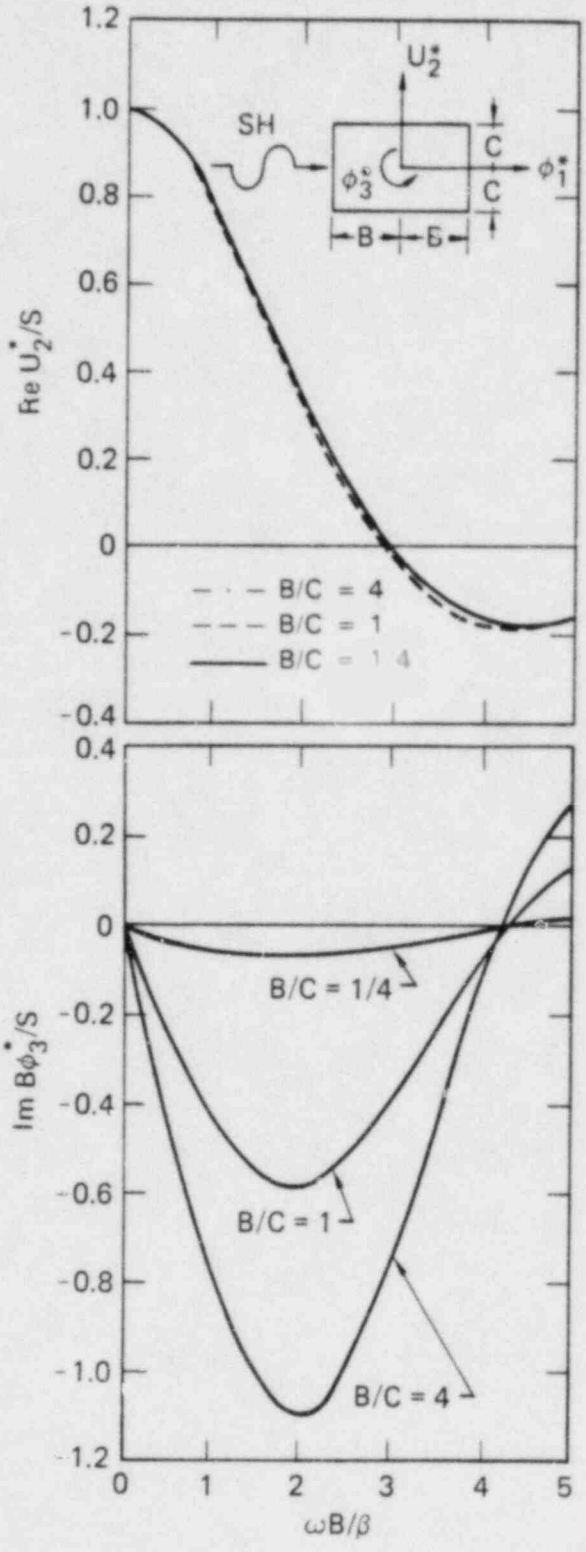

FIG. 4.2. Effect of aspect ratio B/C on the foundation input motion for SH waves ($\xi = 0$, $\nu = 0.33$, $\Theta = 0°$) (Wong and Luco, 1978b).

of the foundation to the amplitude of the free-field motion. The results in Fig. 4.1 indicate that the real part of S_{xx} is dominant implying that at low frequencies the translational response is essentially in phase with the free-field motion at the center of the foundation. For vertical incidence ($\Theta_v = 90°$), $S_{xx} = 1$ for all frequencies. For other angles of incidence S_{xx} exhibits a marked decrease with frequency; the reduction in translational response being largest for horizontally propagating waves ($\Theta_v = 0°$).

The torsional response of the foundation is defined by the function R_{zx}. In particular, R_{zx} corresponds to the ratio of the tangential displacement $a\Theta_z^*$ induced by torsion at the points of coordinates $(\pm a,0,0)$ and $(0,\pm a,0)$ on the foundation to the amplitude of the free-field motion. The results presented in Fig. 4.1 indicate that the imaginary part of R_{zx} is dominant implying that the torsional response is 90° out of phase with the free-field motion at the center of the foundation. The torsional response is zero for vertically incident waves ($\Theta_v = 90°$) and it reaches its highest values for horizontally incident waves ($\Theta_v = 0°$). In particular, for $a_0 \approx 2.0$ the amplitude of the tangential motion $a\Theta_z^*$ can be as high as 60 percent of the free-field motion amplitude.

The rocking response of the foundation is defined by R_{yx}. As shown in Fig. 4.1, the rocking response is very small and can be neglected for most practical purposes.

The effects of aspect ratio on the response of a flat rectangular foundation subjected to horizontally propagating SH waves are illustrated in Fig. 4.2. These results indicate that the translational response is essentially independent of the aspect ratio while the torsional response increases as the width of the foundation (in a direction normal to the direction of propagation of the seismic wave) decreases.

As a second example consider a flat rigid foundation of total width 2a supported on a uniform half-space and subjected to nonvertically incident P or SV waves as shown in Fig. 4.3. The free-field motion on the ground surface for waves propagating in the yz-plane ($\Theta_H = 0$ in Fig. 4.1) can be written in the form

$$\begin{Bmatrix} u_x^g(x,y,0) \\ u_y^g(x,y,0) \\ u_z^g(x,y,0) \end{Bmatrix} \exp(i\omega t) = \begin{Bmatrix} 0 \\ U_{gy}(\omega) \\ U_{gz}(\omega) \end{Bmatrix} \exp\left[i\omega\left(t - \frac{y}{c}\right)\right] \tag{4.4}$$

where U_{gy} and U_{gz} correspond to the amplitudes of the horizontal and vertical components of the free-field motion on the ground surface. The apparent horizontal velocity c takes the form $c = \alpha/\cos\Theta_v$ or $\beta/\cos\Theta_v$, where α and β are the compressional and shear velocities in the half-space, depending on whether the incident waves are P or SV waves. The components of the free-field motion U_{gy} and U_{gz} are not independent of each other. For a given type of seismic excitation the ratio U_{gy}/U_{gz} depends on the angle of incidence (Θ_v) and on the value of the Poisson's ratio.

The response of the massless foundation for this type of excitation can be written in the form

$$\begin{aligned} \Delta_y^* &= S_{yy}U_{gy} + S_{yz}U_{gz} \\ \Delta_z^* &= S_{zy}U_{gy} + S_{zz}U_{gz} \\ a\Theta_x^* &= R_{xy}U_{gy} + R_{xz}U_{gz} \\ \Delta_x^* &= a\Theta_y^* = a\Theta_z^* = 0 \end{aligned} \tag{4.5}$$

The functions S_{yy}, S_{yz}, S_{zy}, S_{zz}, R_{xy} and R_{xz} depend on the dimensionless frequency $a_0 = \omega a/\beta$, on the ratio β/c and on the value of the Poisson's ratio υ. Numerical values for the real and imaginary parts of these functions, as obtained by Wong and Luco (1978a), are shown in Fig. 4.3. Inspection of these results reveals that the functions S_{yz}, S_{zy} and R_{xy} have amplitudes significantly lower than those of the functions S_{yy}, S_{zz} and R_{xz}. For most practical applications Eqs. (4.5) can then be simplified to

$$\Delta_y^* = S_{yy}U_{gy} \quad , \quad \Delta_z^* = S_{zz}U_{gz} \quad , \quad a\Theta_x^* = R_{xz}U_{gz} \tag{4.6}$$

The results shown in Fig. 4.3 indicate that the translational response of the foundation for nonvertically incident P or SV waves can be significantly lower than the motion in the free-field. The reduction in response is more pronounced at high frequencies and for shallow angles of incidence (larger values of β/c). The rocking response of the foundation about the x-axis is determined by the function R_{xz}. The imaginary part of this function is dominant indicating that the rocking response is 90° out of phase with the vertical component of motion on the free-field. The values obtained for the function R_{xz} indicate that the vertical motion $a\Theta_x^*$, induced by rocking of the foundation can have an amplitude similar to the amplitude of the vertical component in the free-field.

The response of a rigid rectangular foundation supported on an elastic half-space and subjected to a Rayleigh wave is described in Fig. 4.4. For Rayleigh waves propagating in the x-direction ($\Theta = 0$ in Fig. 4.4) the response of the foundation involves horizontal translation U_1^*, vertical translation U_3^* and rocking ϕ_2^* about the x_2-axis. The ratios U_1^*/R_H, U_3^*/R_H and $a\phi_2^*/R_H$, where R_H represents the amplitude of the horizontal component of the Rayleigh wave on the free-field, are shown in Fig. 4.4 versus the dimensionless frequency $a_o = \omega a/\beta$ for aspect ratios $b/a = 0.5$ and 1.0. The results presented in this figure indicate that the translational response of the foundation at intermediate and high frequencies is significantly lower than the motion in the free-field. (The vertical component in the free-field, R_V, is equal to $1.565R_H$ for $\upsilon = 1/3$). As shown in Fig. 4.4, Rayleigh waves induce a large rocking response. Another interesting result is that the aspect ratio of the foundation has no marked effect on the response; the important parameter being the length of the foundation in the direction of propagation of the incident wave.

The results presented above indicate that the translational response of flat, rigid foundations subjected to nonvertically incident waves may have amplitudes significantly lower than the amplitude of motion on the free-field. On the other hand, nonvertically incident SH waves may induce a significant torsional response while nonvertically incident P, SV and Rayleigh waves induce a marked rocking response of the foundation.

The characteristics of the foundation input motion for embedded foundations are examined next. The response of rigid symmetric foundations embedded in the ground and subjected to vertically incident shear waves includes translational and rocking components. The amplitudes $|\Delta_H^*|$ and $|\phi_M^*|$ of the translational and rocking components of the response of rigid cylindrical foundations of radius a embedded to a depth h on a uniform elastic half-space ($\nu = 1/4$) and subjected to vertically incident shear waves are illustrated in Fig. 4.5 (after Day, 1977). The results presented in this figure for embedment ratios $h/a = .5$, 1.0 and 2.0 are referred to the center of the bottom of the foundation and are normalized by the amplitude of the free-field motion on the ground surface denoted by $|U_o|$. The results shown in the lower portion of Fig. 4.5 indicate that the amplitude of the translational response of the foundation at intermediate and high frequencies is significantly lower than the amplitude of the free-field motion on the ground surface. At low frequencies, the reduction in translational response increases with embedment ratio h/a. This behavior can be contrasted with the case of flat foundations ($h/a = 0$) subjected to vertically incident shear waves in which the translational response of the foundation has the same amplitude as the free-field motion. (As the frequency tends to zero the ratio Δ_H^*/U_o should tend to one. The slight deviations from this limiting value appearing in Fig. 4.5 result from limitations of the finite element model used.)

The results shown in the upper portion of Fig. 4.5 indicate that the response of the foundation includes a significant rocking component. At low frequencies, the rocking response increases with embedment ratio h/a. The rocking response for $h/a = 1$ is such that amplitude of the vertical motion on the perimeter of the foundation, $a\phi_M^*$, can be as high as 40 percent of the amplitude of the free-field motion. Again, this behavior must be contrasted with the case of a flat foundation subjected to vertically incident shear waves in which no rocking response is obtained.

The components of the foundation input motion for cylindrical foundations embedded in an elastic half-space and subjected to horizontally incident shear waves are illustrated in Fig. 4.6 (after Day, 1977). In this case, the response of the foundation includes a translational component Δ_H^*, a torsional component ϕ_T^* and a rocking component ϕ_M^*. As shown in the upper portion of Fig. 4.6, the rocking

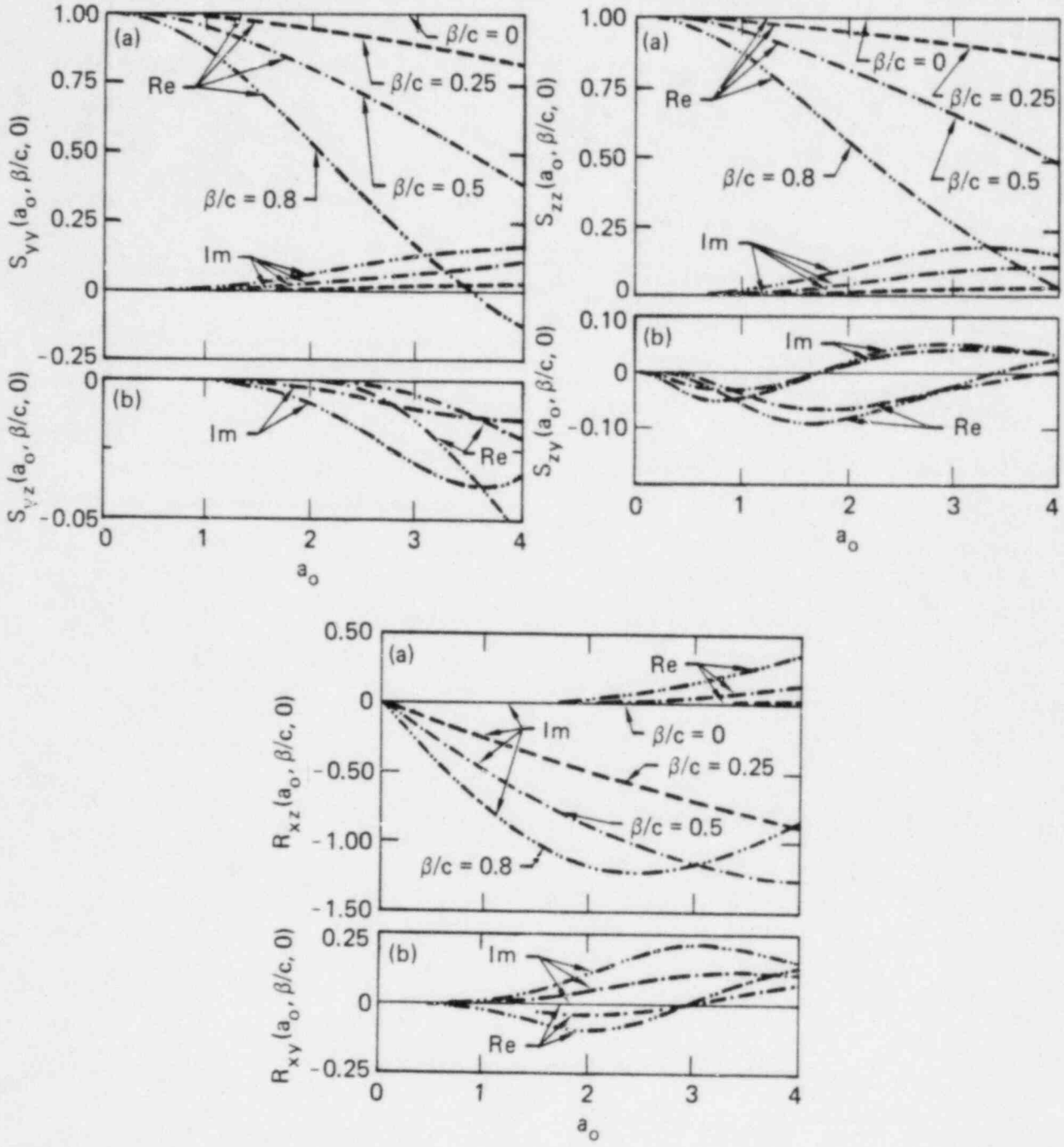

FIG. 4.3. Response of a square rigid foundation to nonvertically incident P and SV waves ($\Theta_H = 0$) (Wong and Luco, 1978a).

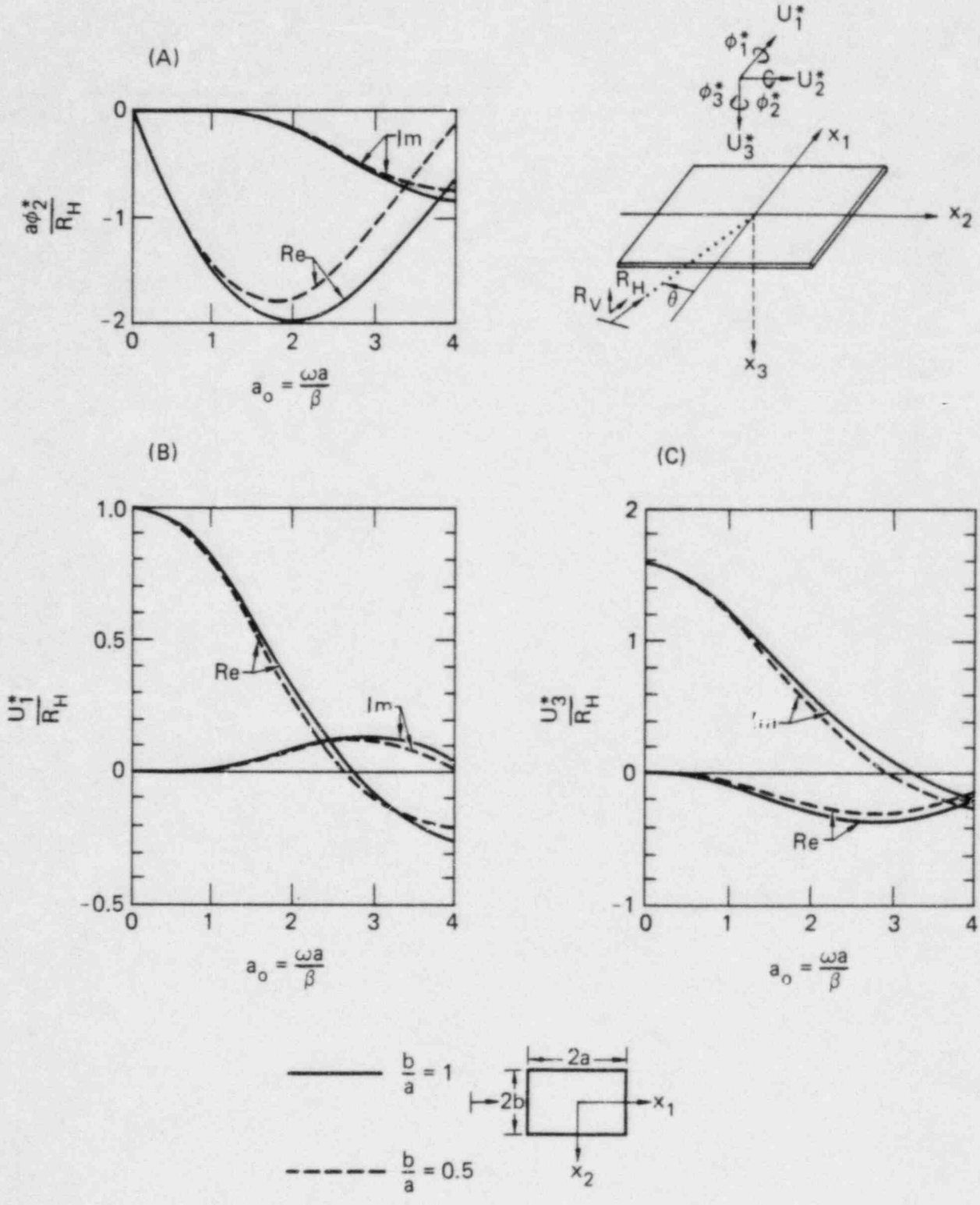

FIG. 4.4. Response of a rigid rectangular foundation to a Rayleigh wave propagating in the x_1 direction ($\Theta = 0$, $\nu = 1/3$) (Luco and Wong, 1977).

response increases with embedment ratio h/a but is generally small, and, except for deeply embedded foundations, can be neglected for most practical purposes. The translational response, shown in the central portion of the figure, exhibits a marked reduction at intermediate and high frequencies. This reduction for embedment ratios larger than 0.5 is not significantly affected by the embedment depth. Finally, the results shown in the lower part of Fig. 4.6 indicate that a significant torsional response is obtained. The torsional response is such that the tangential motion $a\phi_T^*$ on the perimeter of the foundation can reach an amplitude of the order of 40 percent of the amplitude of motion on the ground surface. It is interesting to notice that the torsional response for embedment ratios larger than 0.5 is essentially independent of embedment depth.

In summary, the response of rigid embedded foundations subjected to horizontally incident waves is not significantly different from the response of flat foundations to the same type of excitation. The main features of the response correspond to the marked filtering of the high frequency components of the translational response and to the large torsional motion induced. For foundations with embedment ratios lower than 0.5 the filtering of the translational response for horizontally incident shear waves is more pronounced than the filtering for vertically incident waves. For deeply embedded foundations (h/a $>$ 0.5) the opposite occurs.

The previous description indicates that the characteristics of the foundation input motion depend on the geometry of the foundation, on the composition of the free-field motion in terms of the different types of waves, on the frequency content of these waves and on their angles of incidence or phase velocities. As discussed in the previous chapter, the composition of the free-field motion and the characteristic phase velocities involved depend on the type of seismic source, on the location of the site relative to the source and on the geologic structure along the path from the source to the site. In general, the phase velocities will be larger than the shear wave velocities in the upper layers and consequently the results described for horizontally incident shear waves tend to exaggerate the torsional response as well as the filtering of the translational components of the response. Also, the presence of stiffer layers at depth tends to reduce the ratio of the vertical component of Rayleigh waves to the corresponding horizontal components. As a result the rocking response associated with Rayleigh waves may be less pronounced than that shown in Fig. 4.4.

The problem of determining the response of rigid foundations of various geometries subjected to different types of seismic waves has been addressed by several researchers and a number of results are available. In particular, two-dimensional antiplane models have received considerable attention. The response of an infinitely long foundation with circular cross-section subjected to SH-waves with particle motion in the direction of the long axis of the foundation (antiplane shear), has been obtained by Luco (1969) and Trifunac (1972). Results for the case of semi-elliptical cross-sections have been presented by Wong (1975), Wong and Trifunac (1974) and Luco et al. (1975). An integral equation approach for foundations of arbitrary cross-section and numerical results for the partial case of rectangular cross-sections have been presented by Wong (1975). Thau and Umek (1973) and Dravinski and Thau (1976a) have presented a transient solution for foundations with rectangular cross-sections subjected to SH-waves. Two-dimensional plane-strain models have also been studied. Oien (1971) obtained the response of a flat strip foundation subjected to Rayleigh waves, while Thau and Umek (1974) and Dravinski and Thau (1976b) studied the transient response of rigid foundations of rectangular cross-section excited by plane waves.

The translational and torsional response of a circular foundation supported on an elastic half-space and subjected to plane non-vertically incident SH waves has been studied by Kobori et al. (1976 a,b). The torsional response of a circular foundation to nonvertically incident SH waves has also been studied by Luco (1976a). Tani et al. (1973), Iguchi (1973) and Scanlan (1976) have obtained approximate values for the response of rectangular foundations subjected to nonvertically incident waves. The response of a rigid square foundation to SH, P and SV waves has been determined by Wong and Luco (1978a). The response of rectangular foundations to Rayleigh waves has been described by Luco and Wong (1977). Tables of foundation input motions for rectangular foundations with different

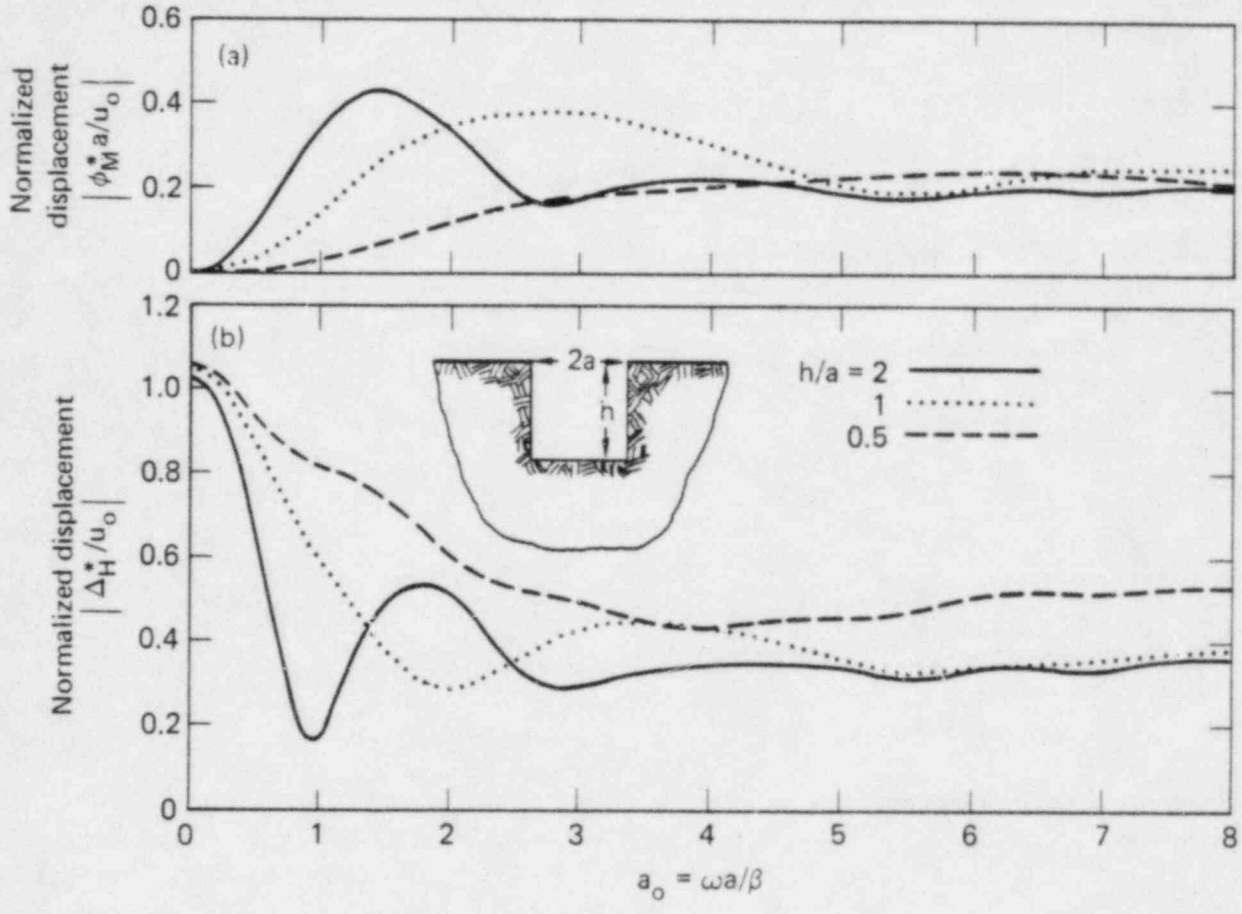

FIG. 4.5. Input motion amplitudes for cylindrical foundations subjected to vertically incident, plane S waves: (a) rocking; and (b) horizontal translation. h/a is the ratio of depth to radius of the cylinder (Day, 1977).

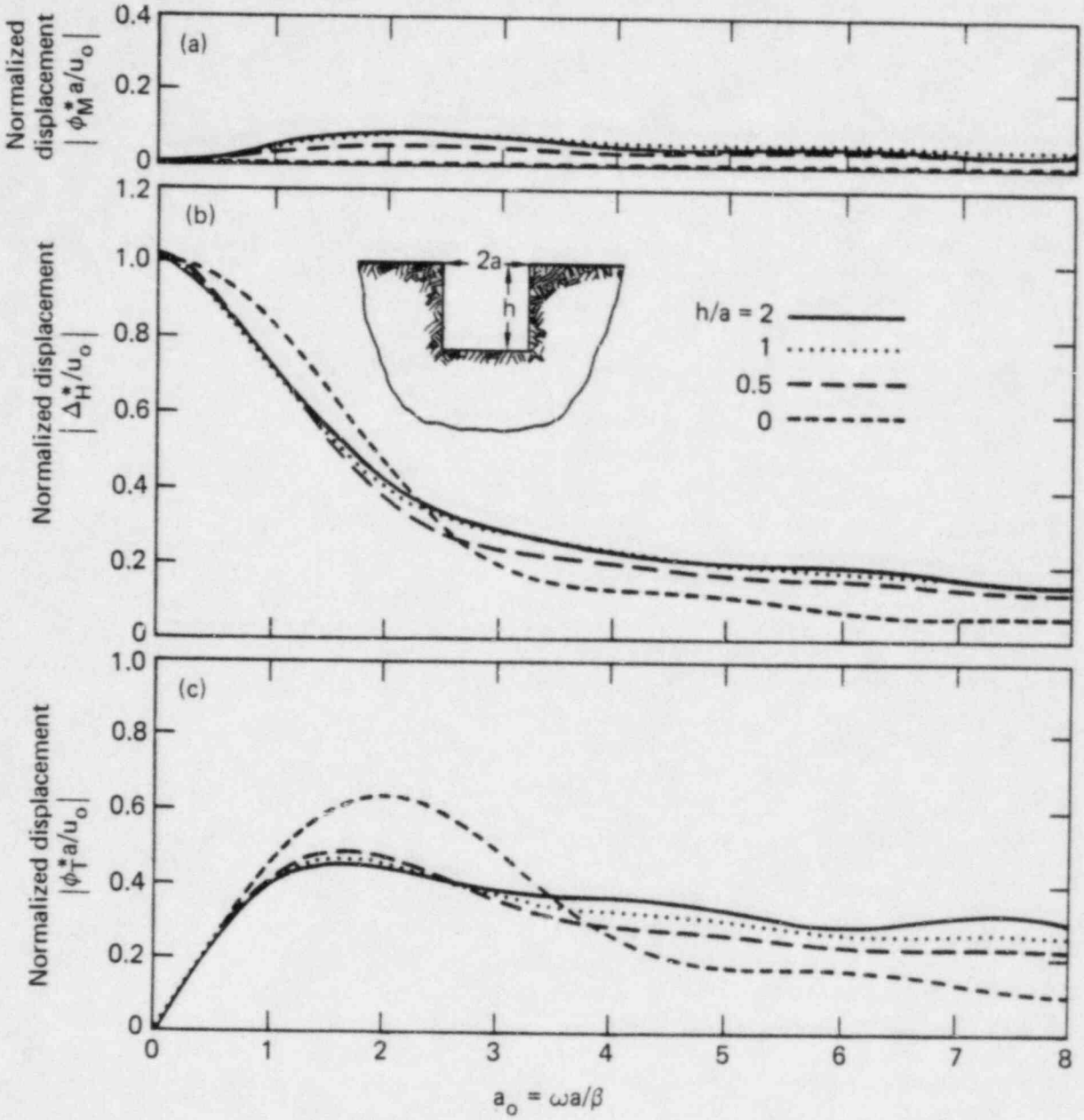

FIG. 4.6. Input motion amplitudes for cylindrical foundations subjected to horizontally incident, plane SH waves: (a) rocking; (b) horizontal translation; and (c) torsion. h/a is the ratio of depth to radius of the cylinder (Day, 1977).

aspect ratios subjected to horizontally incident SH and Rayleigh waves have been presented by Wong and Luco (1978b).

The torsional response of a rigid hemispherical foundation subjected to nonvertically incident SH waves has been obtained by Luco (1976b). The complete response of hemispherical foundations subjected to different types of waves has been studied by Day (1977), Day and Frazier (1979) and Lee (1979). Apsel and Luco (1976) have obtained the torsional response of semi-ellipsoidal foundations embedded in uniform half-space and subjected to nonvertically incident SH waves. The response of cylindrical foundations to different types of seismic excitation has been obtained by Day (1977, 1978). Finally, Dominguez (1978) has obtained the response of rigid foundations of rectangular shape embedded in a uniform half-space.

The problem of determining the response of a rigid massless foundation subjected to seismic waves corresponds to a mixed boundary-value problem in elastodynamics. On the free surface of the ground the condition of zero tractions is imposed, while at the interface between the foundation and the soil, displacement conditions are prescribed. The displacement on the interface must correspond to a rigid-body motion of the foundation. In addition, the resultant force and moment of the tractions that the soil exerts on the foundation must be zero. Also, as the distance to the foundation tends to infinity the total displacement field must tend to the free-field motion. A somewhat more convenient formulation can be obtained by introducing the concept of driving forces. Referring to Eqs. (2.3) and (2.4), the total response $\{U_o\}$ of a rigid massless foundation subjected to seismic excitation and to external forces $\{F_s\}$ is given by

$$\{U_o\} = \{U_o^*\} + [C(\omega)]\{F_s\} \tag{4.7}$$

Where $\{U_o^*\}$ is the foundation input motion and $[C(\omega)]$ is the compliance matrix for the foundation, Eq. (4.7) can also be written in the form

$$\{U_o\} = [C(\omega)](\{F_s\} + \{F_s^*\}) \tag{4.8}$$

where the driving force vector $\{F_s^*\}$ is such that

$$\{U_o^*\} = [C(\omega)]\{F_s^*\} \tag{4.9}$$

The physical meaning of the driving force vector $\{F_s^*\}$ can be obtained by inspection of Eq. (4.8). In particular, if the foundation is held fixed under the action of the seismic excitation, then $\{U_o\} = 0$ and $\{F_s\} = -\{F_s^*\}$, i.e. the external forces required to keep the foundation fixed are of equal amplitude and opposite direction to the driving forces. The driving force vector corresponds, then, to the forces that the soil exerts on the foundation when the foundation is held fixed while subjected to the seismic excitation. If the driving force vector and the compliance matrix for the foundation are known, then, the foundation input motion can be easily calculated by use of Eq. (4.9).

The problem of determining the driving force vector corresponds to a problem of scattering of seismic waves by a rigid fixed intrusion (foundation) in an elastic half-space. The solution of this problem can be obtained by superposition of the free-field motion (in absence of the cavity for the foundation) with a displacement field which exactly cancels the free-field along the interface between the foundation and the ground. The evaluation of this latter displacement field corresponds to a radiation problem of the same type as that involved in the evaluation of the compliance matrix for the foundation. The same methods of solution can then be used to evaluate both the compliance matrix and the driving force. For this reason, the discussion of the analytical methods used to evaluate the foundation input motion is not presented here but in the chapter dealing with the compliance function.

It is interesting to point out an additional connection between the problem of determining the foundation input motion and the problem of determining the compliance functions for the foundation. Let

$\{U_g(\vec{x})\}$ and $\{\overset{\nu}{T}_g(\vec{x})\}$ denote the free-field displacement and traction vectors at every point $\vec{x}$ along the interface S between the foundation and the ground. Also, define the 3 × 6 matrix $[\alpha(\vec{x})]$ by

$$[\alpha(\vec{x})] = \begin{bmatrix} 1 & z & 0 & 0 & 0 & -y \\ 0 & 0 & 1 & -z & 0 & x \\ 0 & -x & 0 & y & 1 & 0 \end{bmatrix} \tag{4.10}$$

which defines the displacement at a point $\vec{x}(x,y,z)$ on the interface S for unit rigid-body motions of the foundation in the order $(\Delta_x, \Theta_y, \Delta_y, \Theta_x, \Delta_z, \Theta_z)$. Finally, let the 3 × 6 matrix $[\overset{\nu}{T}(\vec{x})]$ represent the traction vector at a point $\vec{x}$ on the interface S between the ground and the foundation for unit rigid-body motions of the foundation also in the order $(\Delta_x, \Theta_y, \Delta_y, \Theta_x, \Delta_z, \Theta_z)$. With this notation, it can be shown that

$$[C(\omega)]^{-1} = \int_S [\overset{\nu}{T}(\vec{x})]^T [\alpha(\vec{x})] dS \tag{4.11}$$

and

$$\{U_o^*\} = [C] \int_S [\overset{\nu}{T}(\vec{x})]^T \{U_g(\vec{x})\}\, dS - [C] \int_S [\alpha(\vec{x})]^T \{\overset{\nu}{T}_g(\vec{x})\} dS \tag{4.12}$$

Equation (4.11) reveals that the evaluation of the compliance matrix reduces to the evaluation of the matrix $[\overset{\nu}{T}(\vec{x})]$. Equation (4.12) indicates that the foundation input motion $\{U_o^*\}$ can be easily calculated once the matrix $[\overset{\nu}{T}(\vec{x})]$ and the free-field displacement $\{U_g(\vec{x})\}$ and traction $\{\overset{\nu}{T}_g(\vec{x})\}$ are known. It is clear, then, that the compliance matrix and the foundation input motion vector can be obtained simultaneously.

In the particular case of flat foundations $\{\overset{\nu}{T}_g(\vec{x})\} = 0$ and Eq. (4.12) reduces to

$$\{U_o^*\} = [C] \int_S [\overset{\nu}{T}(\vec{x})]^T \{U_g(\vec{x})\} dS \tag{4.13}$$

which indicates that the free-field motion corresponds to a weighted average of the free-field motion along the contact area between the foundation and the soil. The weights in this case are associated with the elements of the traction matrix $[\overset{\nu}{T}(\vec{x})]$. This result explains the success of the method used by Tani et al. (1973), Iguchi (1973) and Scanlan (1976) to obtain estimates of the foundation input motion by use of weighted averages of the free-field motion. Equation (4.12) reveals that this approximate method cannot be used, in the same fashion, for embedded foundations.

REFERENCES (4)

Apsel, R. J. and J. E. Luco (1976). Torsional Response of a Rigid Embedded Foundation. *J. Engrg. Mech. Div., ASCE, 102,* EM6, 957-970.

Day, S. M. (1977). *Finite Element Analysis of Seismic Scattering Problems,* Ph.D. dissertation, University of California, San Diego, La Jolla, California.

Day, S. M. (1978). Seismic Response of Embedded Foundations. *Preprint 3450, ASCE Convention,* Oct. 1978, Chicago.

Day, S. M. and G. A. Frazier (1979). Seismic Response of Hemispherical Foundation, *J. Engrg. Mech. Div., ASCE, 105,* 29-41.

Dominguez J. (1978). *Response of Embedded Foundations to Travelling Waves.* Publication R78-24, Dept. of Civil Engineering, Massachusetts Institute of Technology, Cambridge, Mass.

Dravinski, M. and S. A. Thau (1976a). Multiple Diffractions of Elastic Shear Waves by a Rigid Rectangular Foundation Embedded in an Elastic Half-Space. *J. Applied Mechanics, ASME, 43,* 295-299.

Dravinski, M. and S. A. Thau (1976b). Multiple Diffractions of Elastic Waves by a Rigid Rectangular Foundation: Plane-strain Model. *J. Applied Mechanics,* ASME, *43,* 291-294.

Iguchi, M. (1973). Seismic Response with Consideraton of Both Phase Differences of Ground Motion and Soil-Structure Interaction. *Proc. Japan Earthquake Engineering Symposium,* Tokyo.

Kobori, T., R. Minai and Y. Shinozaki (1976a). Vibration of a Rigid Circular Disk on an Elastic Half-Space Subjected to Plane Waves. *Theoretical and Applied Mechanics, 21,* 109-119, Univ. of Tokyo Press.

Kobori, T., R. Minai and Y. Shinozaki (1976b). Vibration of a Rigid Circular Disk on an Elastic Half-Space Subjected to Plane Waves (Part 2). *Theoretical and Applied Mechanics, 24,* 153-167, Univ. of Tokyo Press.

Lee, V. W-S. (1979). *Investigation of Three-Dimensional Soil-Structure Interaction,* Report CE-79-11, Dept. of Civil Engrg., Univ. of Southern California, Los Angeles, California.

Luco, J. E. (1969). Dynamic Interaction of a Shear Wall with the Soil. *J. Engrg. Mech. Div., ASCE, 95,* 333-346.

Luco, J. E., H. L. Wong and M. D. Trifunac (1975). A Note on the Dynamic Response of Rigid Embedded Foundations, *Earthquake Engrg. and Structural Dynamics, 4,* 119-127.

Luco, J. E. (1976a). Torsional Response of Structures for Obliquely Incident Seismic Waves. *Earthquake Engineering and Struct. Dynamics, 4,* 207-219.

Luco, J. E. (1976b). Torsional Response of Structures for SH Waves: The Case of Hemispherical Foundations. *Bull. Seism. Soc. Am., 66,* 1, 109-123.

Luco, J. E. and H. L. Wong (1977). Dynamic Response of Rectangular Foundations for Rayleigh Wave Excitation, *Proc. 6th World Conf. Earthquake Engrg.,* New Delhi, India.

Oien, M. A. (1971). Steady Motion of a Rigid Strip Bonded to an Elastic Half-Space. *J. Applied Mechanics, ASME, 38,* 328-344.

Scanlan, R. H. (1976). Seismic Wave Effects on Soil-Structure Interaction, *Earthq. Engrg. and Struct. Dynamics, 4,* 379-388.

Tani, S., J. Sakurai and M. Iguchi (1973). The Effect of Plane Shape and Size of Buildings on the Input Earthquake Motion, *Proc. 5th World Conf. on Earthq. Engrg.*, Rome.

Thau, S. A. and A. Umek (1973). Transient Response of a Buried Foundation to Antiplane Shear Waves. *J. Applied Mechanics,* ASME, *40,* 1041-1066.

Thau, S. A. and A. Umek (1974). Coupled Rocking and Translating Vibrations of Buried Foundation. *J. Appl. Mech., ASME, 41,* 697-702.

Trifunac, M. D. (1972). Interaction of a Shear Wall with the Soil for Incident Plane SH Waves. *Bull. Seism. Soc. Am., 62,* 63-83.

Wong, H. L. (1975). *Dynamic Soil-Structure Interaction,* Report EERL-75-01, Earthq. Engrg. Research Lab., California Institute of Technology, Pasadena, California.

Wong, H. L. and J. E. Luco (1978a). Dynamic Response of Rectangular Foundations to Obliquely Incident Seismic Waves, *Earthq. Engrg. and Struct. Dynamics, 6,* 3-16.

Wong, H. L. and J. E. Luco (1978b). *Tables of Impedance Functions and Input Motions for Rectangular Foundations,* Report CE 78-15, Dept. of Civil Engrg., Univ. of Southern California, Los Angeles.

Wong, H. L. and M. D. Trifunac (1974). Interaction of a Shear Wall with the Soil for Incident Plane SH Waves: Elliptical Rigid Foundation. *Bull. Seism. Soc. Am., 64,* 1825-1842.

5. COMPLIANCE AND IMPEDANCE FUNCTIONS FOR RIGID FOUNDATIONS

One of the key elements entering into the formulation of the soil structure interaction problem is the compliance matrix $[C(\omega)]$ for the foundation. For rigid foundations the 6×6 compliance matrix relates the generalized force $\{F_s\} = (F_{xs}, M_{ys}, F_{ys}, M_{xs}, F_{zs}, M_{zs})^T$ that the foundation exerts on the soil with the generalized displacement $\{U_s\} = (\Delta_{xs}, \Theta_{ys}, \Delta_{ys}, \Theta_{xs}, \Delta_{zs}, \Theta_{zs})$ of the foundation as indicated by Eq. (2.4). For reasons to be described shortly, it is sometimes convenient to refer to the impedance matrix or dynamic stiffness matrix $[K(\omega)]$ defined as the inverse of the compliance matrix. The compliance and impedance matrices depend on the geometry of the foundation, on the characteristics of the soil deposit, on the nature of the contact between the foundation and the soil, and, on the frequency of the excitation.

Before proceeding with the discussion of the methods available to evaluate the compliances and impedance matrices it is convenient to describe some of their characteristics. For rigid foundations with two vertical planes of symmetry (xz-and yz-planes) the impedance matrix can be written in the form

$$[K(\omega)] = Ga \begin{bmatrix} K^{xz}_{HH} & aK^{xz}_{HM} & 0 & 0 & 0 & 0 \\ aK^{xz}_{MH} & a^2K^{xz}_{MM} & 0 & 0 & 0 & 0 \\ 0 & 0 & K^{yz}_{HH} & -aK^{yz}_{HM} & 0 & 0 \\ 0 & 0 & -aK^{yz}_{MH} & a^2K^{yz}_{MM} & 0 & 0 \\ 0 & 0 & 0 & 0 & K^{zz}_{VV} & 0 \\ 0 & 0 & 0 & 0 & 0 & a^2K^{zz}_{TT} \end{bmatrix} \tag{5.1}$$

where G is a shear modulus of reference and a is a length of reference. Each one of the elements appearing in the impedance matrix can be written in turn in the form $K = k + ia_o c$, where k and c are designated normalized stiffness and damping coefficients. In Eq. (5.1), $a_o = \omega a/\beta$ represents a dimensionless frequency in which β is a shear wave velocity of reference. The coupling impedances are such that $K^{xz}_{MH} = K^{xz}_{HM}$ and $K^{yz}_{MH} = K^{yz}_{HM}$. The normalized stiffness and damping coefficients can be thought of as frequency-dependent spring and dashpot constants, respectively. In the case of arbitrarily shaped foundations the impedance matrix is fully populated.

The normalized stiffness and damping coefficients for a flat square foundation of width 2a supported on a uniform half-space (Poisson's ratio $\nu = .33$, hysteric damping constant $\xi = .05$) are illustrated in Fig. 5.1. The results presented in this figure indicate that the stiffness and damping coefficients are clearly dependent on frequency and that the coupling impedance functions for flat foundations are significantly smaller than the diagonal terms. For soils with Poisson's ratios close to 0.5 the frequency dependence of the vertical, k_{VV}, and rocking, k_{MM}, stiffness coefficients is more pronounced than that shown in Fig. 5.1.

The effects of material damping on the impedance functions are illustrated in Fig. 5.2. In this figure the normalized torsional stiffness (solid lines) and damping (segmented lines) coefficients for a square foundation supported on a uniform half-space are shown for different values of the hysteric damping constants. Material damping in the soil leads to reductions in the stiffness coefficients at high frequencies while increasing the damping coefficients at low frequencies. (The results shown in Fig. 5.2 have been normalized by a length of reference corresponding to the radius of a circular foundation of area equal to that of the square foundation).

The effects of the aspect ratio of rectangular foundations on the impedance functions are illustrated in Fig. 5.3. In this figure the normalized horizontal stiffness (solid lines) and damping (segmented lines) coefficients for a flat rectangular foundation of dimensions $2B \times 2C$ are shown for different values of the aspect ratio B/C. The impedance functions are normalized by a length of reference corresponding to the radius of a circular foundation of area equal to that of the rectangular foundation. The results presented in Fig. 5.3 indicate that the horizontal impedances for elongated foundations may be significantly different in two orthogonal directions (the horizontal impedances are

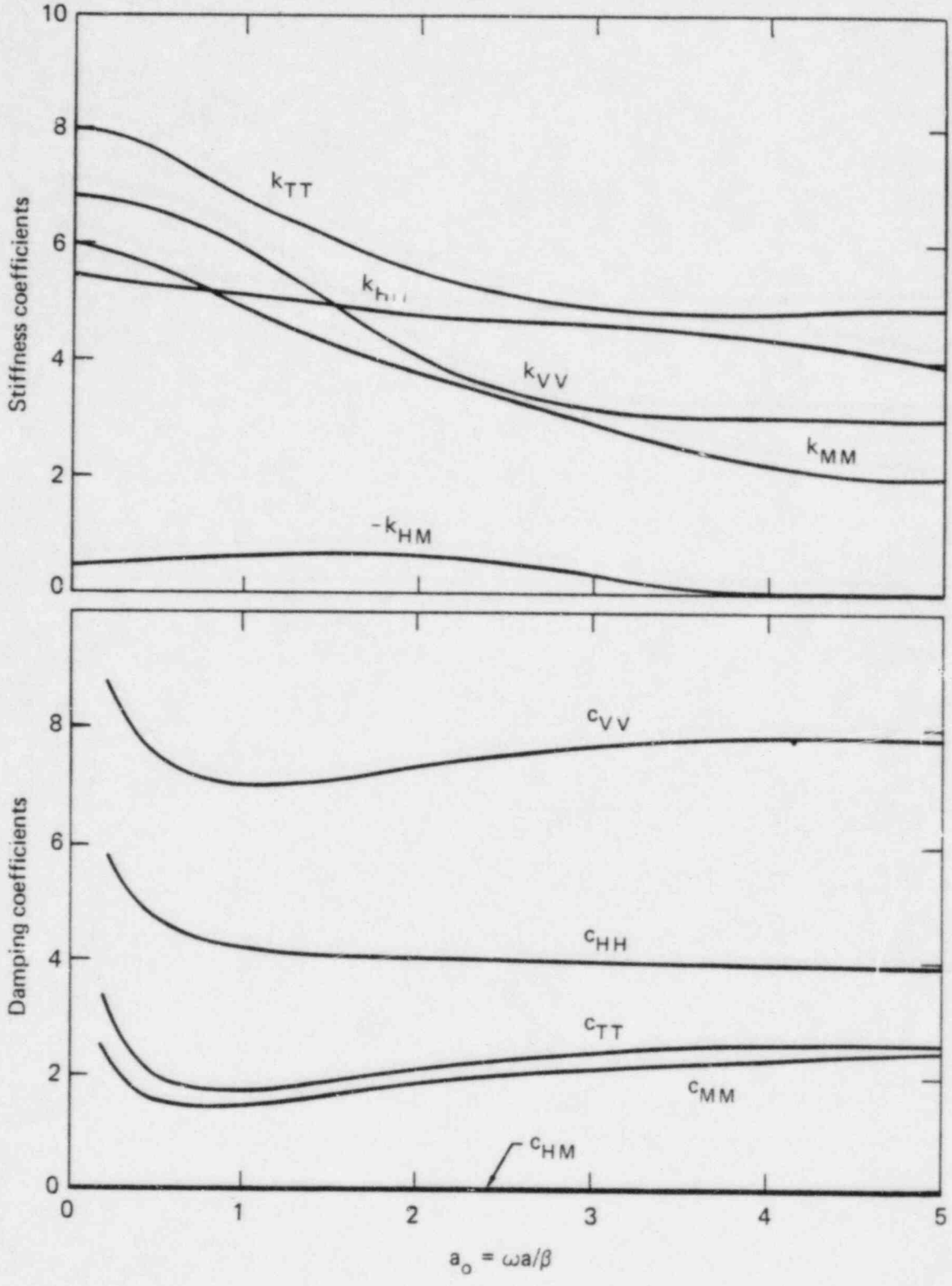

FIG. 5.1. Dynamic stiffness and damping coefficients for a square foundation ($\nu = 0.33$, $\xi = 0.05$) (Luco and Wong, 1978).

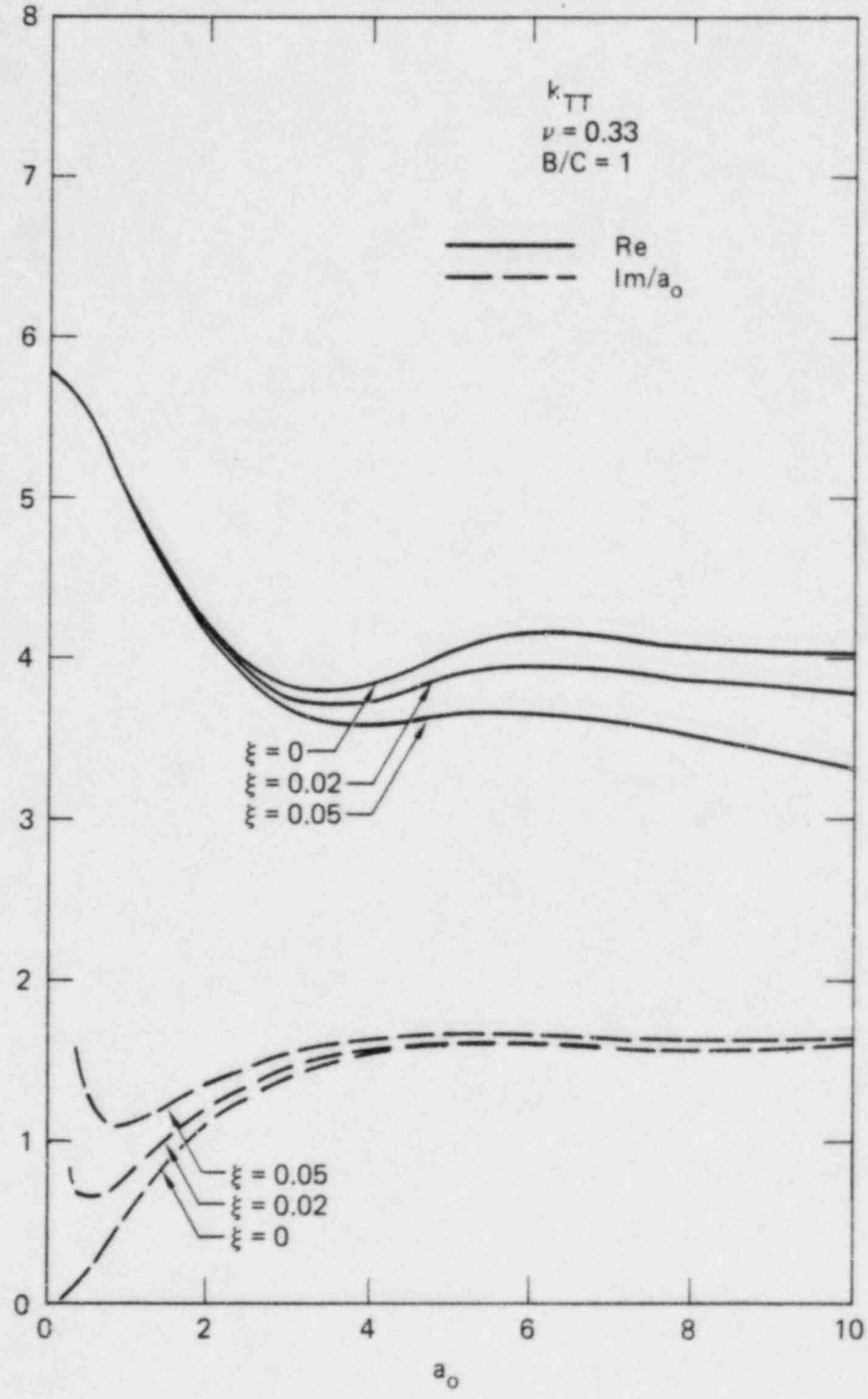

FIG. 5.2. Effect of material damping on the torsional impedance function K_{TT} (B/C = 1, ν = 0.33) (Wong and Luco, 1978).

lower in the long direction of the foundation). Internal holes in the foundation do not significantly affect the impedance functions provided that the foundation can be assumed to remain rigid (Wong, 1975; Wong and Luco, 1976).

Layering of the soil deposit may have an important effect on the impedance functions. The nature of these effects is illustrated in Fig. 5.4 in which the normalized rocking impedance functions for a flat circular foundation supported on an elastic layer resting on an elastic half-space are presented for different values of the ratio of the thickness of the layer to the radius of the foundation. The results presented in Fig. 5.4 are normalized by the static stiffness coefficient for a circular foundation on an elastic half-space with the properties of the top layer. The velocity contrast between the layer and the half-space (shear wave velocity of the layer = 0.4 of the shear wave velocity in the half-space) introduces a very strong frequency dependence, increases the stiffness at low frequencies and leads to a very marked reduction in the damping coefficients at low frequencies. In general, the effects of layering are more pronounced on the vertical and horizontal impedance functions than on the rocking and torsional impedance functions.

For deeply embedded foundations the reaction of the soil adjacent to the foundation may have an important effect on the impedance functions. These effects are illustrated in Fig. 5.5 (after Day, 1977) in which the torsional stiffness and damping coefficients for a circular foundation of basal radius a embedded to a depth h in a uniform half-space ($\nu = 0.25$, $\xi = 0.0$) are presented for different values of the embedment ratio h/a (h/a = 0, 0.5, 1. and 2.). The results presented in Fig. 5.5 for the case of the welded contact between the foundation and the soil indicate marked increases in both the stiffness and damping coefficients as embedment increases. The coupling impedance functions, $K_{HM} = K_{MH}$, which are small for flat foundations become significant for deeply embedded foundations (impedance functions referred to the bottom of the foundation). The results presented in Fig. 5.5, while giving an idea of the effects of embedment, may not be realistic in the sense that perfect contact between the foundation and the soil has been assumed and that the variation of rigidity of the soil with depth has not been considered.

The effects of partial loss of contact between the foundation and the soil along the lateral perimeter of an embedded foundation are illustrated in Fig. 5.6. In this case a cylindrical foundation of radius a embedded to a depth h = 2a on a uniform half-space is considered ($\nu = 0.25$, $\xi = 0.01$). Loss of contact along the upper portion of the lateral perimeter is considered. The results presented indicate that the loss of contact leads to a pronounced reduction in both the stiffness and damping coefficient. In this situation, a first approximation can be obtained by considering an "effective" embedment corresponding to the depth of foundation over which actual contact exists. The effects of possible lateral separation as well as the fact that the rigidity of the soil increases with depth leads to embedment effects less pronounced than those shown in Fig. 5.5.

As exemplified by the previous discussion, a considerable amount of information about the compliance or impedance functions is readily available. In particular, impedance or compliance functions for circular foundations supported on a uniform elastic half-space have been presented by Veletsos and Wei (1971) and Luco and Westmann (1971). The case of a circular foundation on a viscoelastic half-space has been studied by Veletsos and Verbic (1973) and Luco (1976a). Tables of impedance functions for rectangular foundations with different aspect ratios supported on a uniform viscoelastic half-space have been presented by Wong and Luco (1978). Impedance and compliance functions for strip foundations have been obtained by Karasudhi et al. (1968) and Luco and Westmann (1972) for the case of vibrations normal to the axis of the strip (plane-strain) and by Hradilek (1970) for the case of vibrations along the axis of the strip foundation (longitudinal shear). The longitudinal impedances for infinitely long embedded foundations have been obtained by Luco (1969) for the case of semi-circular cross sections and by Wong and Trifunac (1974) and Luco et al. (1975) for the case of semi-elliptical cross sections. Torsional impedance functions for hemispherical and semi-ellipsoidal foundations embedded in a uniform half-space have been presented by Luco (1976b) and Apsel and Luco (1976), respectively. Day (1977), Day and Frazier (1979) and Lee (1979) have obtained the impedance functions for hemispherical foundations embedded in a uniform half-space. Impedance functions for cylin-

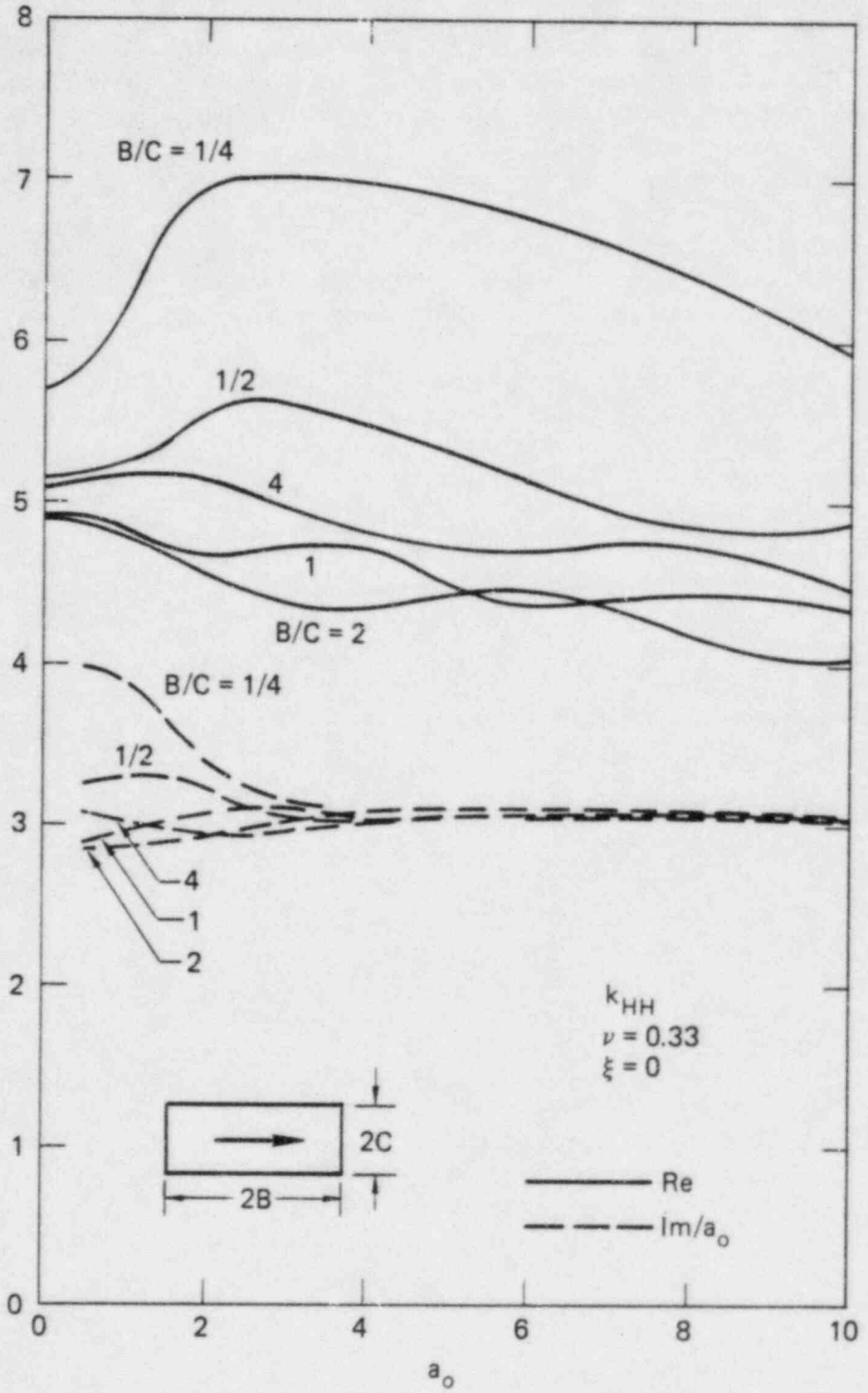

FIG. 5.3. Effect of aspect ratio B/C on the impedance function K_{HH} ($\nu = 0.33$, $\xi = 0$) (Wong and Luco, 1978).

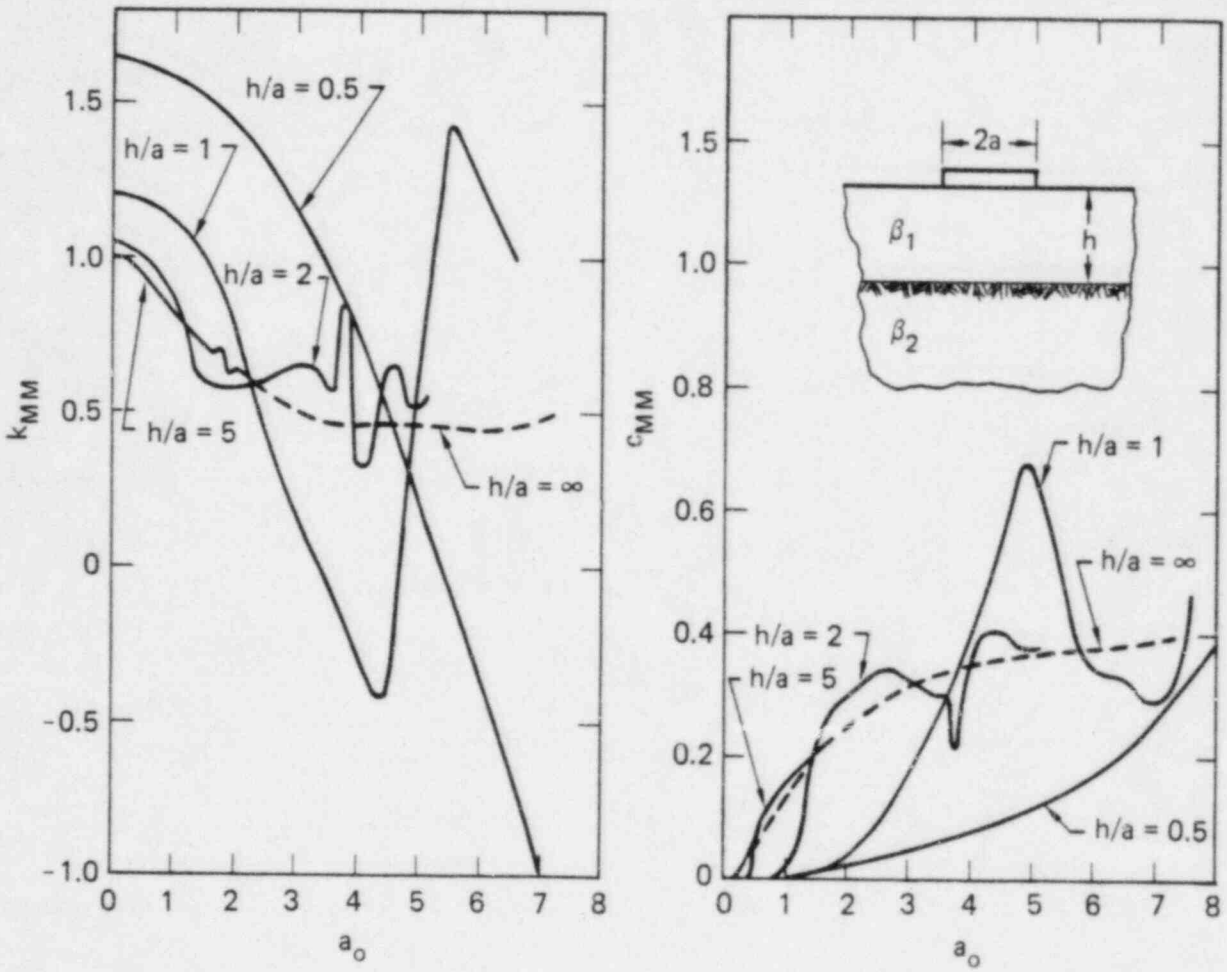

FIG. 5.4. Effect of layering on the rocking impedance functions ($\beta_1\beta_2 = 0.4$) (Luco, 1974).

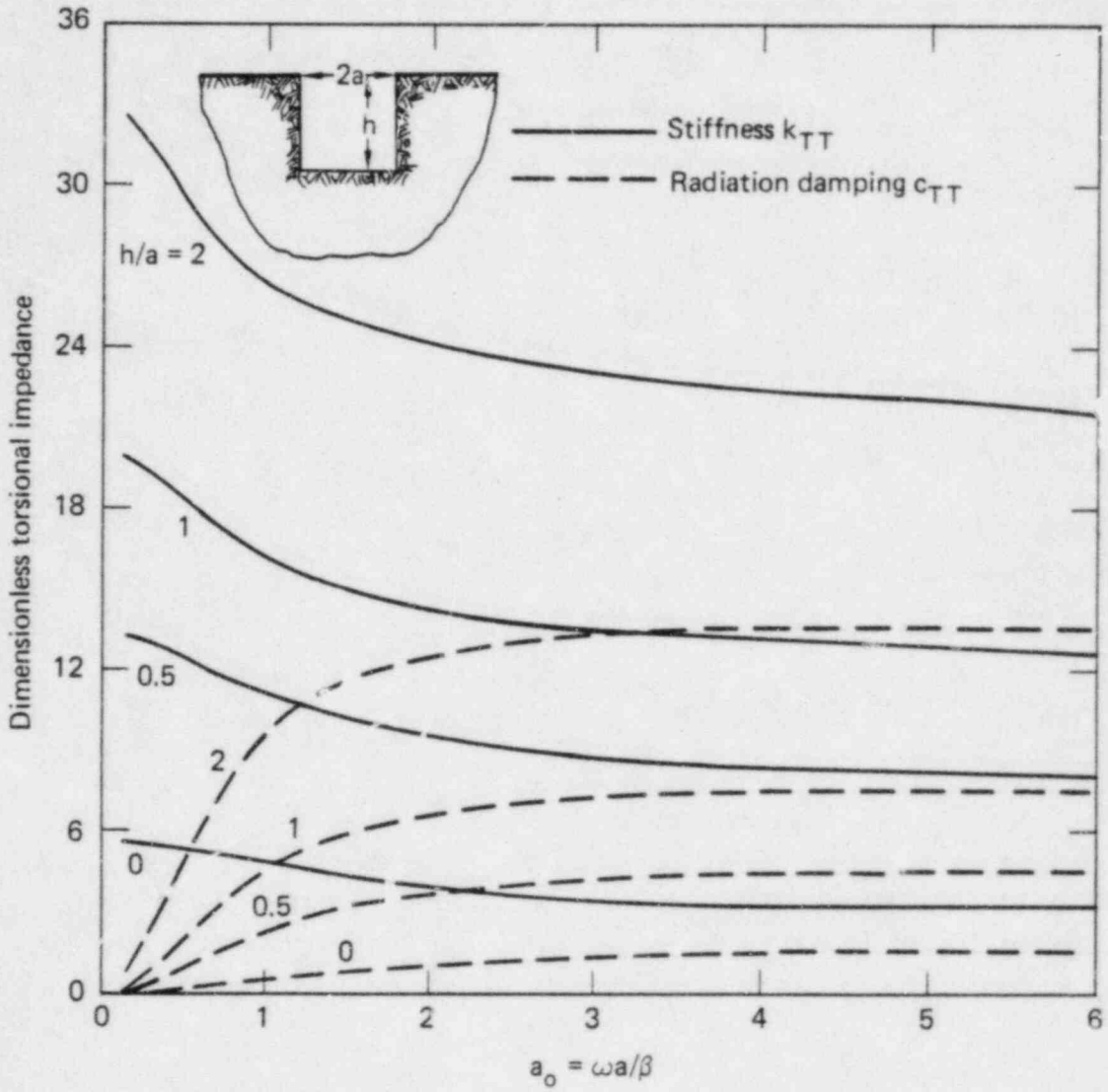

FIG. 5.5. Torsional stiffness and radiation damping for embedded cylinders. The parameter h/a corresponds to the ratio depth-to-radius of the cylinder (Day, 1977).

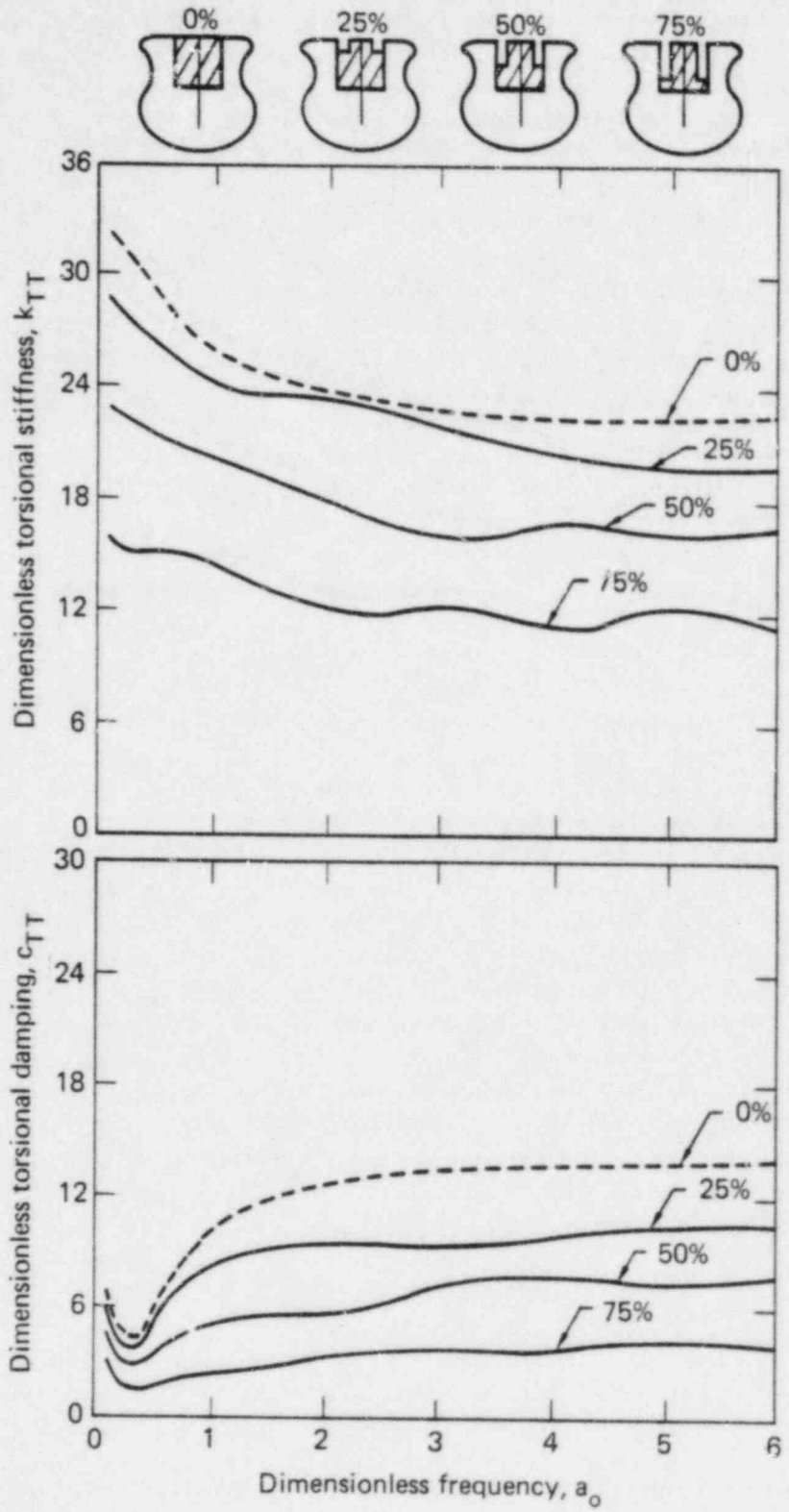

FIG. 5.6. Effects of contact conditions on the torsional stiffness and damping coefficients. The parameter is the percentage of separation of the lateral boundary of the cylinder (Apsel, 1979).

drical foundations embedded in a uniform half-space have been presented by Day (1977, 1978) and Apsel (1979). Finally, Dominguez (1978) has obtained the impedance functions for rectangular foundations embedded in a uniform half-space. The information contained in these studies is sufficient to solve a variety of practical interaction problems involving simple foundation geometries and reasonably uniform soil deposits. In more complex situations specific calculations employing one of the methods described below need to be performed.

The evaluation of the impedance functions for rigid foundations entails the solution of a mixed boundary-value problem in elastodynamics in which displacements are prescribed along the contact between the foundation and the soil while tractions are prescribed on the soil surface not covered by the foundation. Although some of the methods available to obtain the impedance functions for embedded foundations are also applicable to the case of flat foundations it is convenient to discuss these two cases separately.

The evaluation of the impedance or compliance functions for flat rigid circular foundations and two-dimensional strip footings resting on a uniform half-space has been the subject of numerous investigations in the last 40 years. A complete list of references up to 1975 may be found in the work of Wong (1975). In the case of circular and strip foundations the resulting mixed boundary-value problem may be reduced by standard techniques to the solution of Fredholm integral equations of the second kind [e.g., Karasudhi et al (1968), Luco and Westmann (1971)]. For more complex foundation geometries the problem has been approximately solved by defining an equivalent circular base, or by assuming a certain stress distribution on the contact between the foundation and the soil. This last approach has been used, among others, by Thomson and Kobori (1963) to obtain the compliance functions for rectangular foundations.

In recent years, Wong (1975) and Wong and Luco (1976) have developed a method to evaluate the impedance or compliance functions for flat rigid foundations of arbitrary shape placed on the surface of an elastic half-space. The method is based on dividing the contact area between the foundation and the soil into a number of sub-regions and in assuming that the contact tractions within each area are uniform but of unknown amplitude. Evaluating the displacements generated by the uniform tractions in each of the sub-regions and invoking the displacement boundary conditions leads to a discrete variational problem in terms of the unknown tractions. Once the contact tractions have been obtained by solving the variational problem, the total forces and moments acting on the foundation may be computed, leading to the desired impedance matrix for the foundation. This approach corresponds to an extension of the works of Lysmer (1965), in which the vertical compliance for a rigid circular foundation was evaluated by considering several uniformly loaded concentric rings, and of Elorduy et al (1967), where the contact tractions within each sub-region were replaced by concentrated loads.

The method of reduction to Fredholm integral equation of the second kind has been used by Kashio (1970), Wei (1971) and Luco (1974) to obtain the impedance functions for flat circular foundations supported on an elastic layer resting on an elastic half-space. This technique has also been used by Luco (1976a) to obtain the impedance functions for circular foundations resting on a multilayered viscoelastic half-space. The method of assuming a distribution of contact tractions has been employed by Kobori and Suzuki (1970) to obtain the impedance functions for rectangular foundations supported on a multilayered viscoelastic medium. In the studies mentioned above involving multilayered soil models the Haskell-Thomson technique has been used to incorporate the layering effects. This technique becomes numerically unstable at certain frequencies. With the recent development of an efficient and stable technique to evaluate the dynamic Green's functions for layered viscoelastic media [Apsel (1979), Luco and Apsel (1980a)] it has become possible to use the method of subdivision of the contact area to obtain the impedance functions for arbitrarily shaped flat foundations resting on a multilayered viscoelastic half-space (Wong and Luco, 1980).

The problem of determining the impedance functions for rigid embedded foundations is considerably more complex than that for flat foundations. Simple analytical solutions can be obtained only for special geometries and types of excitation. For instance, Luco (1976b) and Apsel and Luco (1976) obtained, respectively, the torsional response of rigid hemispherical and semi-ellipsoidal foundations

embedded in a uniform half-space by use of the method of separation of variables. The complete impedance matrix for a rigid hemispherical foundation was obtained by Lee (1979) by expanding spherical wave functions into power series.

Given the difficulty of obtaining exact analytical solutions, several approximate analytical methods have been proposed. One of the best known approximate methods is the Baranov-Novak approach in which it is assumed that the soil reactions at the base of the foundation are equal to those of a foundation placed on the soil surface, while the lateral soil reactions are evaluated independently. Baranov (1967) proposed that the lateral reactions may be evaluated by considering an independent layer surrounding the foundation. This layer in turn is represented by a series of infinitesimally thin independent layers. Compatability between layers and the underlying half-space is satisfied only at the foundation and at infinity. This approach has been used by Novak and Beredugo (1972), Beredugo and Novak (1972), Berdugo (1971), and Novak and Sachs (1973) to obtain the dynamic response of a rigid cylindrical foundation embedded in an elastic half-space.

The finite element method has been used to determine the impedance functions of cylindrical foundations embedded in an elastic half-space. Kuhlemeyer (1969) and Lysmer and Kuhlemeyer (1971) have studied the vertical response; Kaldjian (1969), and Waas (1972) have considered the torsional response; while Urlich and Kuhlemeyer (1973) and Kausel, et al. (1975 a,b) have studied the coupled rocking and lateral vibrations of embedded foundations. In these studies, the solutions were obtained in the frequency domain and special nonreflecting boundaries were used along the lateral boundary of the model to avoid some of the problems associated with the finite size of a finite element model. If the lower boundary of the finite element model does not coincide with soil region in which a high velocity contrast exists, the calculated radiation dampings at low frequencies can be significantly underestimated. In addition, spurious oscillations of the impedance function can be obtained.

A different type of finite element analysis has been proposed by Day (1977). In this method the transient response of a finite element model to an impulsive motion of the rigid foundation is obtained. Taking advantage of the fact that the forces acting on the foundation tend to the static limit after a short time it is possible to terminate the calculations before the arrival of reflections from the overall boundaries of the model. This approach has been used successfully by Day (1977, 1978) and Day and Frazier (1979) to obtain the impedance functions for hemispherical and cylindrical foundations embedded in a uniform half-space. One of the limitations of this method is that it is difficult to incorporate the effects of frequency-independent hysteretic damping.

In the two types of axisymmetric finite element analyses mentioned above it is possible to model the backfill by a conical region surrounding the foundation. Parallel layers can be easily modelled. The use of finite element models in the general three-dimensional case is hampered by the high cost, and, in the case of analysis in the frequency domain, by the lack of standard non-reflecting boundaries.

A hybrid method which combines the continuum and the finite element approaches has been proposed by Dasgupta (1980). In this method, the region of soil to be occupied by the embedded foundation is discretized by a finite element mesh. The forces acting at nodal points on the boundary of this region can be written in the form

$$\begin{Bmatrix} F_1 \\ \hline F_2 \end{Bmatrix} = \left[\begin{array}{c:c} K_{11}^f & K_{12}^f \\ \hdashline K_{21}^f & K_{22}^f \end{array}\right] \begin{Bmatrix} U_1 \\ \hline U_2 \end{Bmatrix} \tag{5.2}$$

where subscript 1 refers to nodes on the soil surface while subscript 2 refers to nodes along the embedded area where contact between the foundation and the soil will exist. In Eq. (5.2) the matrices K_{ij}^f correspond to condensed dynamic stiffness matrices ($K - \omega^2 M + i\omega C$) after the displacements of the internal nodes have been eliminated from the equations of motion. Considering the half space before the soil has been excavated it is possible to write

$$F_1 = K_{11}^h U_1 \tag{5.3}$$

where K_{11}^h is a dynamic stiffness matrix relating the forces and displacements on the surface of the half-space. This matrix would be obtained by the continuum approach. From Eqs. (5.2) and (5.3) it is possible to obtain

$$F_2 = \left(K_{21}^f \left(K_{11}^h - K_{11}^f\right)^{-1} K_{12}^f + K_{22}^f\right) U_2 \tag{5.4}$$

from where the dynamic stiffness matrix K_{22}^e for the semi-infinite region outside the foundations is given by

$$K_{22}^e = -K_{21}^f \left(K_{11}^h - K_{11}^f\right)^{-1} K_{12}^f - K_{12}^f \tag{5.5}$$

The impedance matrix [K] for a rigid foundation can be easily obtained from the matrix $[K_{22}^e]$ by

$$[K] = [\alpha]^T [K_{22}^e] [\alpha] \tag{5.6}$$

where $[\alpha]$ is the matrix connecting the displacement vector $\{U_2\}$ with the rigid body motion $\{U_o\}$ of the foundation.

This technique combines the finite element method applied to a finite region (the portion of soil to be occupied by the foundation) with the continuum approach for a half-space. This technique, which has been used by Dasgupta to obtain the impedance function for two-dimensional foundations, could also be used in the three-dimensional case. This method appears to be promising for foundations with shallow embedment. For deeply embedded foundations the method could become unstable since the number of nodes on region 1 could be considerably less than in region 2. In addition, the process of condensing the dynamic stiffness for the finite element region could become costly. In the application of this method, it is important that the matrix K_{11}^h appearing in Eq. (5.3) be calculated as the inverse of a dynamic flexibility matrix [Dasgupta and Chopra (1979)].

To obtain analytical solutions to the mixed boundary-value problem for the case of rigid foundations of arbitrary shape embedded in a layered medium it is necessary to resort to an integral equation formulation. To describe the different integral equation methods of solution, it is convenient to consider the general case of an intrusion occupying the volume V' embedded in a layered viscoelastic half-space occupying the volume V (Fig. 5.7). The interface between the intrusion and the surrounding medium is represented by the surface S.

Assuming harmonic time dependence of the type $e^{i\omega t}$, the Knopoff-de Hoop representation theorem applied to volume V leads to

$$\varepsilon(\vec{x})u_i(\vec{x}) = \int_S [G_{ji}(\vec{y}, \vec{x})T_j^u(\vec{y}) - H_{ji}^u(\vec{y}, \vec{x})u_j(\vec{y})]dS(\vec{y}) \quad (i, j = 1, 2, 3), \tag{5.7}$$

in which

$$\varepsilon(\vec{x}) = \begin{cases} 0 & \vec{x}\varepsilon V' \\ \frac{1}{2} & \vec{x}\varepsilon S \\ 1 & \vec{x}\varepsilon V \end{cases} \tag{5.8}$$

In Eq. (5.7), $u_j(\vec{y})$ and $T_j^u(\vec{y})$ represent the displacement and traction components on S ($\vec{y}\varepsilon S$), $G_{ji}(\vec{y}, \vec{x})$ represents the jth component of the displacement vector at point $\vec{y}\varepsilon S$ due to a concentrated point load

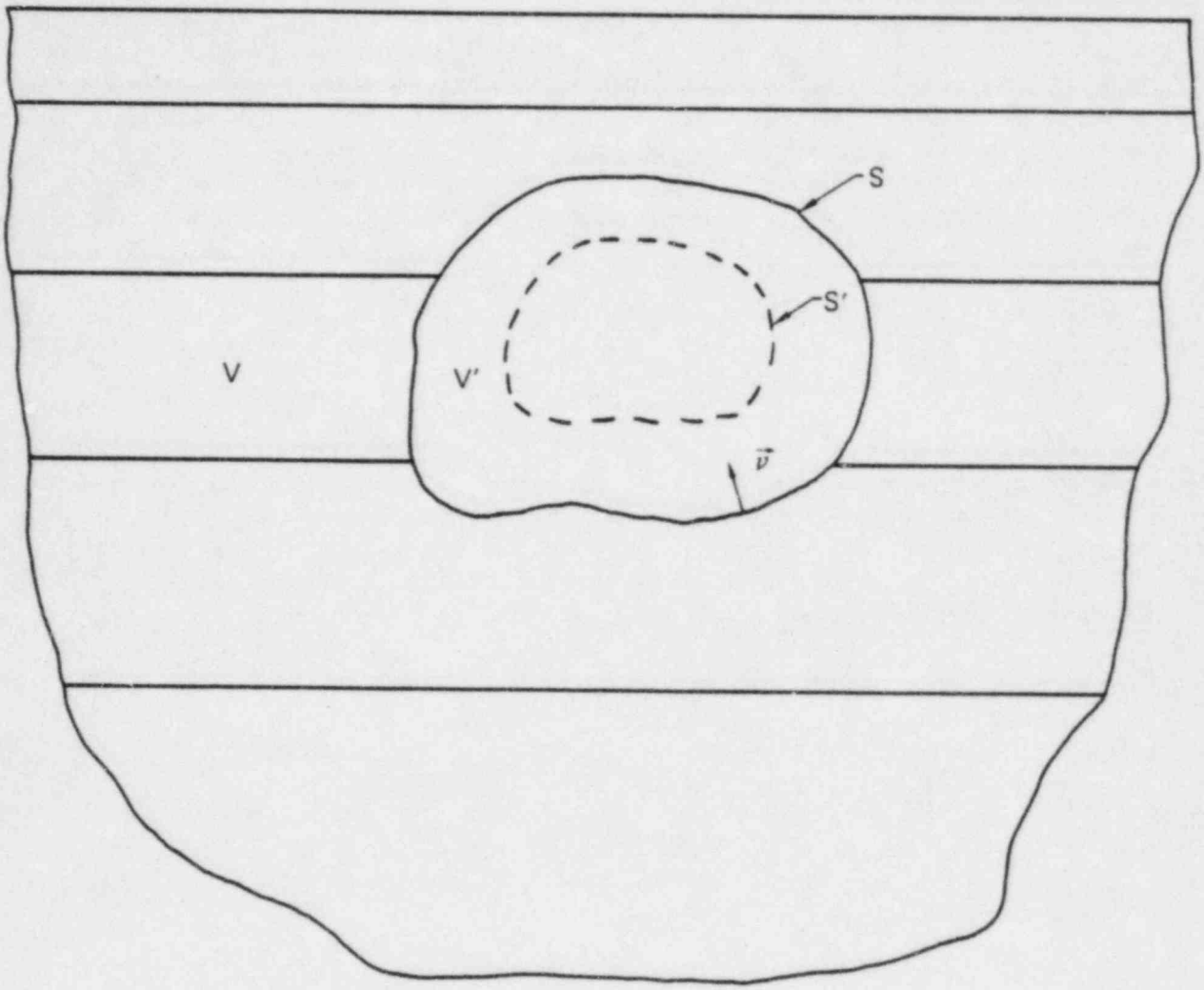

FIG. 5.7. Description of the system and notation for the integral equation method.

at $\vec{x}$ acting in the i-direction, while $H^{\upsilon}_{ji}(\vec{y}, \vec{x})$ denotes the corresponding jth component of the traction vector at $\vec{y}\varepsilon S$ due to a concentrated point load at $\vec{x}$ acting in the i-direction. The normal υ to the surface S is taken positive pointing into V'. In Eq. (5.7) and in the sequel, the summation convention over repeated indices is adopted.

A first integral equation approach results from selecting the point $\vec{x}$ on the surface S. Assuming that the displacement vector $u_j(\vec{y})$ is known for $\vec{y}\varepsilon S$ (welded contact problem) then Eq. (5.7) becomes an integral equation for the unknown traction vector, $T^{\upsilon}_j(\vec{y})$ on S. The kernel $G_{ji}(\vec{y}, \vec{x})$ of this integral equation is singular when $\vec{x}$ approaches $\vec{y}$. Once the tractions $T^{\upsilon}_j(\vec{y})$ on the surface S have been obtained by solving the integral equation, the impedance function for the foundation can be readily calculated by integration. This approach has been used by Dominguez (1978) to obtain the impedance functions for rectangular foundations embedded in a uniform elastic half-space. In Dominguez's work, the Green's functions for a full space were used making it necessary to extend the surface S to cover the surface of the half-space. This is not necessary if the Green's functions for a half-space are used. The main complication of this approach arises from the singularity of the kernel.

A second integral equation approach results from selecting the point $\vec{x}$ to be on a surface S' internal to S. Assuming again that the displacement vector $u_j(\vec{y})$ is known on the surface S (welded contact problem), Eq. (5.7) leads to

$$\int_S G_{ji}(\vec{y}, \vec{x}) T^{\upsilon}_j(\vec{y}) dS(\vec{y}) = \int_S H^{\upsilon}_{ji}(\vec{y}, \vec{x}) u_j(\vec{y}) dS(\vec{y}) \quad (\vec{x}\varepsilon V', \vec{y}\varepsilon S) \tag{5.9}$$

which corresponds to a Fredholm integral equation of the first kind for the unknown traction $T^{\upsilon}_j(\vec{y})$ on S. This approach suggested by Kupratze (1963) has the advantage that the kernel $G_{ji}(\vec{y}, \vec{x})$ is not singular. The disadvantage is that the accuracy of the numerical solution of the integral Eq. (5.9) depends on the location of the surface S'. In addition, the kernel is not symmetric.

A third approach has been proposed by Luco and Apsel (1980a). It consists in representing the unknown tractions $T^{\upsilon}_j(\vec{y})$ appearing in Eq. (5.9) by

$$T^{\upsilon}_j(y) = \int_{S'} H^{\upsilon}_{jk}(\vec{y}, \vec{x}') F_k(\vec{x}') dS'(x') \tag{5.10}$$

where $F_k(\vec{x}')$ corresponds to an unknown distribution of forces on a surface S' internal to S. Substitution from Eq. (5.10) into Eq. (5.9) leads to the following integral equation for $F_k(\vec{x}')$

$$\int_{S'} \hat{G}_{ij}(\vec{x}, \vec{x}') F_j(\vec{x}') dS'(\vec{x}') = \int_S H^{\upsilon}_{ji}(\vec{y}, \vec{x}) u_j(\vec{y}) dS(\vec{y}) \qquad (\vec{x}\varepsilon S') \tag{5.11}$$

where

$$\hat{G}_{ij}(\vec{x}, \vec{x}') = \int_{S'} G_{ki}(\vec{y}, \vec{x}) H^{\upsilon}_{kj}(\vec{y}, \vec{x}') dS(\vec{y}) \tag{5.12}$$

It is easily proven that the kernel $\hat{G}_{ij}(\vec{x}, \vec{x}')$ is symmetric, i.e.,

$$\hat{G}_{ij}(\vec{x}, \vec{x}') = \hat{G}_{ji}(\vec{x}', \vec{x}) \tag{5.13}$$

Equation (5.11) constitutes, then, a non-singular integral equation with symmetric kernel in the unknown distribution of forces $F_j(\vec{x}')$, $\vec{x}'\varepsilon S'$. Once this equation is solved, the tractions on the surface S may be obtained by use of Eq. (5.10).

One advantage of this formulation over that of Kupratze is that the kernel is symmetric. In addition, it can be shown that Eq. (5.11) corresponds to the Euler's equation for a functional which has as extreme value the work of the unknown tractions on the given displacements.

If $[F(\vec{x}')]$ is a 3 × 6 matrix denoting the solution of Eq. (5.11) for each one of the six degrees of freedom of the foundation, it can be shown that the impedence matrix [K] for the foundation can be written in the form

$$[K] = \int_S \int_{S'} [\alpha(\vec{y})]^T [H^v(\vec{y},\vec{x}')] [F(\vec{x}')] dS'(\vec{x}') dS(\vec{y}) \tag{5.14}$$

where $[\alpha(\vec{y})]$ is a 3 × 6 matrix relating the three components of displacement at $\vec{y}\varepsilon S$ with the each of the six degrees of freedom of the rigid foundation. The 3 × 3 matrix $[H^v(\vec{y},\vec{x}')]$ has for elements $H^v_{ij}(\vec{y},\vec{x})$.

The foundation input motion $\{U_o^*\}$ for a given seismic excitation can be obtained from

$$\{U_o^*\} = [K]^{-1} \int_{S'} [F(\vec{x}')]^T \{U_g(\vec{x}')\} dS'(\vec{x}') \tag{5.15}$$

where the 3 × 1 vector $\{U_g(\vec{x}')\}$ represents the components of the free-field motion on the internal surface S'. Equations (5.14) and (5.15) indicate that both the impedance matrix and the foundation input motion vector can be readily obtained once Eq. (5.11) has been solved. This technique has been used by Apsel (1979) to obtain the impedance functions for cylindrical foundations embedded in uniform and layered viscoelastic half-spaces.

Finally, it is possible to replace the foundation by a set of unknown forces $F_k(\vec{x}')$ distributed over a surface S' internal to S and require that

$$\int_{S'} G_{jk}(\vec{y},\vec{x}') F_k(\vec{x}') dS'(\vec{x}') = U_j(\vec{y}) \qquad (\vec{y}\varepsilon S') \tag{5.16}$$

This equation can be solved in a least square sense leading to

$$\int_{S'} \hat{\tilde{G}}_{ik}(\vec{x},\vec{x}') F_k(\vec{x}') dS(\vec{x}') = \int_S \tilde{G}_{ij}(\vec{x},\vec{y}) U_j(\vec{y}) dS(\vec{y}) \tag{5.17}$$

where

$$\hat{\tilde{G}}_{ik}(\vec{x},\vec{x}') = \int_S \tilde{G}_{ij}(\vec{x},\vec{y}) G_{jk}(\vec{y},\vec{x}') dS(\vec{y}) \tag{5.18}$$

In Eq. (5.18) the tilde denotes complex conjugate. The integral Eq. (5.17) has a Hermitian non-singular kernel. Once the unknown forces $F_k(\vec{x}')$ have been obtained from Eq. (5.17), the tractions are calculated from Eq. (5.10). This approach has been used by Ohsaki (1970) to obtain the static response of a rigid rectangular foundation embedded in a uniform elastic half-space.

As indicated above several alternatives are available. With the recent development of an efficient method to calculate Green's functions for layered viscoelastic media [Apsel (1979), Luco and Apsel (1980a)] it has become possible to use any of the integral equation methods just described to evaluate impedance functions for three-dimensional foundations embedded in a layered viscoelastic media. These methods are also applicable to the evaluation of the foundation input motion for a prescribed free-field motion, and, in practice, both the impedance functions and the foundation input motion can be obtained as a result of the same set of calculations as indicated by Eqs. (5.14) and (5.15).

REFERENCES (5)

Apsel, R. J. (1979). *Dynamic Green's Functions for Layered Media and Applications to Boundary-Value Problems.* Ph.D dissertation, Univ. of California, San Diego, La Jolla, California.

Apsel, R.J. and J.E. Luco (1976). Torsional Response of a Rigid Embedded Foundation, *J. Engrg. Mech. Div.*, ASCE, *102*, EM6, 957-970.

Baranov, V.A. (1967). On the Calculation of Excited Vibrations of an Embedded Foundation, (in Russian), *Voprosy Dynamiki: Prochnocti,* No. 14, Polytechnical Institute of Riga, 195-209.

Beredugo, Y.O. (1971). *Vibrations of Embedded Symmetric Footings,* Ph.D. Dissertation, University of Western Ontario, London, Canada, 247 pp.

Beredugo, Y.O. and Novak, M.(1972). Coupled Horizontal and Rocking Vibration of Embedded Footings, *Canadian Geotechnical J., 9,* 4.

Dasgupta, G. (1980). Foundation Impedance Matrices Substructure Deletion, *J. of the Engrg. Mech. Div.*, ASCE, *103,* 517,523.

Dasgupta, G. and A. K. Chopra (1979). Dynamic Stiffness Matrices for Viscoelastic Half Planes. *J. Engrg. Mech. Div., ASCE,* 105, 729-746.

Day, S. M. (1977). *Finite Element Analysis of Seismic Scattering Problems,* Ph.D. dissertation, Univ. of California, San Diego, La Jolla, California.

Day, S. M. (1978). Seismic Response of Embedded Foundations, *Preprint 3450, ASCE Convention, Oct. 1978,* Chicago.

Day, S. M. and G. A. Frazier (1979). Seismic Response of Hemispherical Foundation. *J. Engrg. Mech. Div., ASCE,* 105, 29-41.

Dominguez, J. (1978). *Dynamic Stiffness of Rectangular Foundations.* Report R78-20, Dept. of Civil Engrg., Massachusetts Institute of Technology, Cambridge, Mass.

Elorduy, J., J. A. Nieto and E. M. Szekely (1967). Dynamic Vertical Loading. *Proc. Int. Symp. on Wave Propagation and Dynamic Properties of Earth Materials.*

Hradilek, P. J. (1970). *Dynamic Soil-Structure Interaction,* M.S. Thesis, School of Engineering and Applied Science, Univ. of California, Los Angeles, California.

Kaldjian, M.J. (1969). Torsional Stiffness of Embedded Footings, *Soil Mech. Found. Div.,* ASCE, *95,* No. SM1, 969-980.

Karasudhi, P., Keer, L.M. and Lee, S.L. (1968). Vibratory Motion of a Body on an Elastic Half-Space, *J. Applied Mechanics, ASME, 35,* 697-705.

Kashio, J. (1970). *Steady State Response of a Circular Disk Resting on a Layered Medium.* Ph.D. dissertation, Rice University.

Kausel, E., J.M. Roesset and G. Waas (1975a). Dynamic Analysis of Footings on Layered Media, *J. of the Engrg. Mech. Div., ASCE, 101,* No. EM5, 679-693.

Kausel, E., and J.M. Roesset (1975b). Dynamic Stiffness of Circular Foundations, *J. of Engrg. Mech. Div., ASCE, 101,* No. EM6, 771-785.

Kobori, T. and T. Suzuki (1970). Foundation Vibrations on a Viscoelastic Multilayered Medium. Proc. Third Japan Earthq. Engrg. Symposium, Tokyo, 493-499.

Kuhlemeyer, R.L. (1969). *Vertical Vibrations of Footings Embedded in Layered Media,* Ph.D. Dissertation, Univ. of California, Berkeley, 253 pp.

Kupratze, V.D. (1963). Dynamical Problems in Elasticity, *Progress in Solid Mechanics,* III, North-Holland Publishing Co., Amsterdam, Holland.

Lee, V. W-S. (1979). *Investigation of Three-Dimensional Soil-Structure Interaction,* Report CE 79-11, Dept. of Civil Engrg., Univ. of Southern California, Los Angeles, California.

Luco, J. E. (1969). Dynamic Interaction of a Shear Wall with the Soil. *J. Engrg. Mecn. Div.,* ASCE, *95,* 333-346.

Luco, J. E. (1974). Impedance Functions for a Rigid Foundation on a Layered Medium. *Nuclear Engrg. and Design., 31,* 204-217.

Luco, J. E. (1976a). Vibrations of a Rigid Disc on a Layered Viscoelastic Medium. *Nuclear Engineering and Design, 36,* 325-340.

Luco, J.E. (1976b). Torsional Response of Structures for SH Waves: the case of Hemispherical Foundations, *Bull. Seism. Soc. Am., 66,* 1, 109-124.

Luco, J. E. and R. J. Apsel (1980a). On the Green's Functions for Layered Media: Part I. (submitted for publication).

Luco, J. E. and R. J. Apsel (1980b). An Integral Equation Approach to Some Mixed Boundary-Value Problems in Elastodynamics (in preparation).

Luco, J. E., H. L. Wong and M. D. Trifunac (1975). A Note on the Dynamic Response of Rigid Embedded Foundations. *Earthq. Engrg. and Struct. Dynamics, 4,* 2, 119-128.

Luco, J.E. and R.A. Westmann (1971). Dynamic Response of Circular Footings, *J. Engineering Mechanics Division, ASCE, 97,* 1381-1395.

Luco, J.E. and R.A. Westmann (1972). Dynamic Response of a Rigid Footing Bonded to an Elastic Half-Space, *J. Applied Mechanics, ASME, 39,* 527-534.

Lysmer, J. (1965). *Vertical Motion of Rigid Footings,* Report No. 3-115, Dept. of Civil Engineering, University of Michigan, Ann Arbor, Michigan.

Lysmer, J. and R.L. Kuhlemeyer (1969). Finite Dynamic Model for Infinite Media, *J. Engrg. Mech. Div.,* ASCE, *95,* No. EM4, 859-877, Closure to Discussions, February 1971, 129-131.

Novak, M. and Y.O. Beredugo (1972). Vertical Vibration of Embedded Footings, *Soil Mech. Found. Div., ASCE, 98,* 1291-1310.

Novak, M. and K. Sachs (1973). Torsional and Coupled Vibrations of Embedded Footings, *Int. Jour. Earthq. Engrg. Struct. Dyn., 2,* 1, 11-33.

Ohsaki, Y. (1973). On Movements of a Rigid Body in Semi-infinite Elastic Medium, *Proc. Japan Earthquake Engrg. Symp.,* B-21, August-Sept. 1973, Tokyo, 245-252.

Thomson, W.T. and T. Kobori (1963). Dynamical Compliance of Rectangular Foundations on an Elastic Half-Space, *J. Applied Mechanics, ASME, 30,* 579-584.

Urlich, C.M. and R.L. Kuhlemeyer (1973). Coupled Rocking and Lateral Vibrations of Embedded Footings, *Can. Geotech., 10,* 2, 145-160.

Veletsos, A.S. and Y.T. Wei (1971). Lateral and Rocking Vibrations of Footings, *J. Soil Mechanics and Foundations Division, ASCE, 97,* 1227-1248.

Veletsos, A. S. and B. Verbic (1973). *Vibration of viscoelastic foundations.* Report 73-18, Dept. of Civil Engrg., Rice University, Houston, Texas.

Waas, G. (1972). *Earthquake Vibration Effects and Abatement for Military Facilities,* Tech. Report, S-71-14, U.S. Army Engineer WES, Vicksburg, Miss., 182 pp.

Wei, Y. (1971). *Steady State Response of Certain Foundation Systems,* Ph.D. dissertation, Rice University, Houston, Texas.

Wong, H. L. and M. D. Trifunac (1974). Interaction of a Shear Wall with the Soil for Incident Plane SH Waves: Elliptical Rigid Foundation. *Bull. Seism. Soc. Am., 64,* 1825-1842.

Wong, H.L. (1975). *Dynamic Soil-Structure Interaction,* Report EERL-75-01, Earthquake Engineering Research Lab., California Institute of Technology, Pasadena, California.

Wong, H.L. and J.E. Luco (1976). Dynamic Response of Rigid Foundations of Arbitrary Shape, *Earthquake Engineering and Structural Dynamics, 4,* 579-587.

Wong, H. L. and J.E. Luco (1978). *Tables of Impedance Functions and Input Motions for Rectangular Foundations.* Report CE 78-15, Dept. of Civil Engrg., Univ. of Southern California, Los Angeles, California.

Wong, H.L. and J.E. Luco (1980). *Soil Structure Interaction: A Linear Continuum Mechanics Approach (CLASSI)*, Report CE, Dept. of Civil Engineering, Univ. of Southern California, Los Angeles, California.

6. EQUIVALENT MASS MATRIX FOR THE SUPERSTRUCTURE

To evaluate the equivalent mass matrix $[M_b(\omega)]$ appearing in Eqs. (2.6) and (2.7), it is convenient to consider a model of the superstructure consisting of N rigid bodies interconnected by elastic members. In general, the relative motion of the j-th rigid body with respect to a frame of reference attached to the moving rigid foundation can be described by six generalized coordinates $(U_{xj}, U_{yj}, U_{zj}, \Theta_{xj}, \Theta_{yj}, \Theta_{zj})$ corresponding to the components of the relative displacement of the center of mass and to the components of the relative rotation vector. The generalized relative displacement vector for the superstructure $\{U\}$ is defined by the $6N \times 1$ vector

$$\{U\} = (U_{x1},\ldots,U_{xN},\Theta_{y1},\ldots,\Theta_{yN},U_{y1},\ldots,U_{yN},\Theta_{x1},\ldots,\Theta_{xN},U_{z1},\ldots,U_{zN},\Theta_{z1},\ldots,\Theta_{zN})^T \tag{6.1}$$

The generalized total displacement vector $\{U_t\}$ is defined similarly except that the translational and rotational components are referred to a fixed frame of reference.

For small vibrations, the total displacement vector $\{U_t\}$ is given by

$$\{U_t\} = [\alpha]\{U_o\} + \{U\} \tag{6.2}$$

where $\{U_o\} = (\Delta_x, \Theta_y, \Delta_y, \Theta_x, \Delta_z, \Theta_z)^T$ is the total foundation motion and $[\alpha]$ is the $6N \times 6$ rigid displacement matrix

$$[\alpha] = \begin{bmatrix} \{1\} & \{z\} & 0 & 0 & 0 & -\{y\} \\ 0 & \{1\} & 0 & 0 & 0 & 0 \\ 0 & 0 & \{1\} & -\{z\} & 0 & \{x\} \\ 0 & 0 & 0 & \{1\} & 0 & 0 \\ 0 & -\{x\} & 0 & \{y\} & \{1\} & 0 \\ 0 & 0 & 0 & 0 & 0 & \{1\} \end{bmatrix} \tag{6.3}$$

in which

$$\{1\} = (1,\ldots,1)^T$$
$$\{x\} = (x_1,\ldots,x_N)^T, \qquad \{y\} = (y_1,\ldots,y_N)^T, \qquad \{z\} = (z_1,\ldots,z_N)^T \tag{6.4}$$

where (x_j, y_j, z_j) correspond to the coordinates of the j-th rigid body.

By writing the equations of motion for the superstructure and using the fixed base modes of vibration, it can be shown that

$$\{U\} = [\phi][D(\omega)][\beta]^T\{U_o\} \tag{6.5}$$

where $[\phi]$ is the $6N \times 6N$ fixed-base modal matrix for the superstructure normalized with respect to the mass matrix of the superstructure, i.e.,

$$[\phi]^T[M][\phi] = [I]. \tag{6.6}$$

The $6 \times 6N$ matrix $[\beta]$ appearing in Eq. (6.5) corresponds to the modal participation matrix

$$[\beta] = [\alpha]^T[M][\phi] \tag{6.7}$$

and $[D(\omega)]$ is a diagonal $6N \times 6N$ modal amplification matrix having for elements

$$D_r(\omega) = \frac{(\omega/\omega_r)^2}{1 - (\omega/\omega_r)^2 + 2i\zeta_r(\omega/\omega_r)} \qquad ,(r = 1,6N) \tag{6.8}$$

in which ω_r and ζ_r correspond to the r-th fixed-base natural frequency and modal damping ratio, respectively.

From Eqs. (6.2) and (6.5), it is found that the total displacement $\{U_t\}$ is given by

$$\{U_t\} = ([\alpha] + [\phi]\,[D(\omega)]\,[\beta]^T)\,\{U_o\} \tag{6.9}$$

from which the total displacement $\{U_t\}$ can be calculated once the total motion of the foundation $\{U_o\}$ is known.

The generalized force $\{F_b\} = (F_{xb}, M_{yb}, F_{yb}, M_{xb}, F_{zb}, M_{zb})^T$ that the superstructure exerts on the foundation (referred to the point of reference in the foundation) may be obtained by considering the total linear and angular momenta. For small vibrations,

$$\{F_b\} = \omega^2\,[\alpha]^T[M]\,\{U_t\} \qquad . \tag{6.10}$$

By substitution from Eq. (6.9) into Eq. (6.10), it is found that $\{F_b\}$ can be written in the form

$$\{F_b\} = \omega^2[M_b(\omega)]\{U_o\} \tag{6.11}$$

where the equivalent mass matrix $[M_b(\omega)]$ is given by

$$[M_b(\omega)] = [M_{bo}] + [\beta]\,[D(\omega)]\,[\beta]^T \tag{6.12}$$

in which

$$[M_{bo}] = [\alpha]^T[M][\alpha] \tag{6.13}$$

corresponds to the 6×6 mass matrix of the superstructure for rigid translations and rotations about the point of reference on the foundation.

The three-dimensional formulation described above has been presented by Lee and Wesley (1971). An earlier two-dimensional formulation has been presented by Tajimi (1967).

It is of interest to discuss the behavior of the equivalent mass matrix $[M_b(\omega)]$ as the frequency ω tends to infinity. From Eq. (6.8), it can be seen that $[D(\omega)] \rightarrow -[I]$ as $\omega \rightarrow \infty$. Eq. (6.12) indicates, then, that

$$[M_b(\omega)] \rightarrow [M_{bo}] - [\beta]\,[\beta]^T \text{ as } \omega \rightarrow \infty \tag{6.14}$$

If the set of fixed-base modes is complete, it can be shown that

$$[\alpha] = [\phi][\beta]^T \tag{6.15}$$

and

$$[M_{bo}] = [\beta][\beta]^T \tag{6.16}$$

Eqs. (6.14) and (6.16) reveal that if the set of fixed base modes is complete, $[M_b(\omega)] \to 0$ as $\omega \to \infty$. Referring to Eq. (2.7), it may be seen that at sufficiently high frequencies, the total reponse of the foundation $\{U_o\}$ becomes essentially independent of the properties of the superstructure.

If the set of modes is not complete, $[M_b(\omega)]$ will not tend to zero as $\omega \to \infty$, but to a residual mass matrix which represents the contribution to the base forces and moments of the modes excluded.

For most practical applications, not all fixed base modes need to be considered. If the first $\bar{N}$ modes of vibration are included, then the matrices $[\phi]$, $[\beta]$ and $[D(\omega)]$ will have dimensions $6N \times \bar{N}$, $6 \times \bar{N}$ and $\bar{N} \times \bar{N}$, respectively. One of the advantages of the formulation is that for frequencies lower than the fixed-base natural frequencies of the modes excluded, the contributions of these modes to the base forces and moments are still approximately represented in the equivalent mass matrix $[M_b(\omega)]$ through the matrix $[M_{bo}]$.

Another advantage of the procedure described to obtain the equivalent mass matrix is that the fixed-base mode shapes, natural frequencies, modal damping ratios and participation factors can be obtained by the method most appropriate to the particular structure being analyzed. For complex structures, these quantities may be obtained by use of a finite element model; in other cases, simplified lumped mass or continuous representations may be adequate.

If the superstructure does not admit a decomposition into classical normal modes, the relative displacement vector $\{U\}$ can be written in the form

$$\{U\} = \omega^2(-\omega^2[M] + i\omega[C] + [K])^{-1}[M][\alpha]\{U_o\} \tag{6.17}$$

in which [M], [C], and [K] represent, respectively, the fixed-base mass, damping and stiffness matrices for the superstructure. From Eqs. (6.10), (6.2), (6.17) and (2.6), it can be shown that the equivalent mass matrix $[M_b(\omega)]$ is given in this case by

$$[M_b(\omega)] = [M_{bo}] + \omega^2[\alpha]^T[M](-\omega^2[M] + i\omega[C] + [K])^{-1}[M][\alpha] \tag{6.18}$$

where $[M_{bo}]$ is given by Eq. (6.13).

REFERENCES (6)

Lee, T.H., and D.A. Wesley (1971). Soil-Foundation Interaction of Reactor Structures Subjected to Seismic Excitation, *Proc. 1st Int. Conf. Struct. Mech. in Reactor Technology*, Berlin, Paper K3/5.

Tajimi, H. (1967). Discussion: Building-Foundation Interaction Effects, Proc. Paper 5200, *Jour. of the Engrg. Mech. Div.*, ASCE, *93*, 294-298.

Wong, H.L., and J.E. Luco (1977). The Application of Standard Finite Element Programs in the Analysis of Soil-Structure Interaction, *Proc. 2nd SAP User's Conf.*, Univ. of Southern California, Los Angeles.

7. RESPONSE OF STRUCTURES TO NONVERTICALLY INCIDENT SEISMIC WAVES

The first objective of this chapter is to discuss the characteristics of the response of structures subjected to nonvertically incident seismic waves. The second objective is to illustrate the use of the formulation described in the previous chapters to obtain the response of the complete soil-structure system.

The conventional methods of analysis to evaluate the seismic response of structures including soil-structure interaction effects are based on the assumption that the seismic excitation can be represented by plane vertically incident compressional or shear waves. As a result of such assumption, the foundation input motion for flat foundations is considered to be equal for all points along the base of the foundation and would consist of a pure vertical or horizontal translation. In terms of the structural response, the implications of the assumption of vertically incident waves are that the torsional response will occur only if the superstructure or foundation are not symmetric and that the rocking response will be associated to a large degree with the mass distribution of the structure in height.

As discussed in Chapter 4, the foundation input motion for nonvertically incident seismic waves may be significantly different from the free-field motion on the ground surface. In particular it was found that: (i) Love and nonvertically incident SH waves induce a torsional component of response even in the case of symmetric structures and foundations; (ii) Rayleigh waves and nonvertically incident P and SV waves induce additional contributions to the rocking response, and (iii) nonvertically incident seismic waves may lead to reductions of the high-frequency components of the translational response at foundation level. The importance of these effects depends on the phase velocity of the free-field motion. The lower the phase velocity the more important these effects will become. To analyze the effects of nonvertically incident waves it is convenient to consider separately the cases of nonvertically incident SH waves and of Rayleigh-P-SV waves.

In a pioneering study, Newmark (1969) found that nonvertically incident SH waves may induce a significant torsional response even in the case of symmetric structures. In Newmark's work, the torsional input for oblique SH waves was evaluated approximately and the soil-structure interaction effects were not included. The approximation used for the torsional input motion was

$$\Theta_z^*(t) = \frac{\partial U_y(x - c_H t)}{\partial x} = -\frac{1}{c_H}\frac{\partial U_y}{\partial t} \tag{7.1}$$

in which $U_y(x - c_H t)$ represents the free-field motion for a plane SH wave propagating with phase velocity c_H in the direction of the x-axis. In this study, Newmark proposes the introduction of an accidental eccentricity which would simulate the effects of nonvertically incident SH waves when used in conjunction with conventional analyses involving only translational input motion at foundation level. For a building in which lateral resistance is distributed along the perimeter, the accidental eccentricity e_x can be written in the form

$$\frac{e_x}{2a} = \alpha\left(1 + \frac{b}{a}\right)\left(\frac{2f_y a}{c_H}\right) \tag{7.2}$$

in which the coefficient α is a numerical coefficient taking values $\alpha = 1.25$ for $0.3 < f_y < 1$ and $\alpha = 0.75$ for $1.5 < f_y < 5$. In Eq. (7.2), 2a denotes the length of the foundation in the direction of propagation (x-direction), 2b corresponds to the width of the foundation and f_y to the fundamental frequency of the structure (in Hz) in the direction of the particle motion (y-axis). In a recent study, Luco and Sotiropoulos (1980) have used a better approximation to the torsional input motion and have modified Eq. (7.2) to read

$$\frac{e_x}{2a} = \alpha \left[\frac{1 + \frac{b}{a}}{1 + \left(\frac{b}{a}\right)^2} \right] \left(\frac{2 f_y a}{c_H} \right) \tag{7.3}$$

The accidental eccentricity given by Eq. (7.3) coincides with that given by Eq. (7.2) when $a >> b$ but leads to values half as large when $a = b$. For a structure with a square foundation of dimension $2a \times 2b = 40 \times 40$m and fundamental frequency $f_y = 5$Hz, Eq. (7.3) leads to a value of $e_x/2a = 0.05$ for a phase velocity $c_H = 3000$ m/sec. For $c_H = 300$ m/sec, the accidental eccentricity ratio would take the value $e_x/2a = 0.50$. It should be noted that the ratio of the basal shear stress induced by torsion to the shear stress induced by the lateral loads is of the order of $e_x/2a$. These results emphasize the importance of employing realistic values for the phase velocity c_H. The theoretical and experimental evidence described in Chapter 3 indicates that c_H lies in the range of 2.5 km/sec to 4.5 km/sec. Under these conditions, the minimum requirement of the Uniform Building Code of an accidental eccentricity of 5 percent of the longer plan dimension seems reasonable.

The use of an accidental eccentricity to simulate the torsional effects introduced by nonvertically incident waves, although convenient in static analyses, introduces some undesirable effects in dynamic analyses. In particular, additional coupling of the translational and torsional response and modifications of the natural frequencies of the superstructure are produced. A more convenient approach in the case of dynamic analyses is to consider directly the torsional input as an additional excitation.

The response of a one-story structure supported on a rigid foundation mat and subjected to nonvertically incident SH waves has been studied by Iguchi (1973). In Iguchi's work the effects of soil-structure interaction were included and an approximation to the torsional input motion was used. Lee and Wesley (1975) considered the response of a non-axisymmetric reactor structure subjected to a horizontally incident SH wave. In this study, which includes the effects of soil-structure interaction, Newmark's estimate of the torsional input motion was used. The effects of scattering on the translational input motion were not considered. It was found that the torsional response of the reactor structure induced by horizontally incident SH waves is larger than the response associated with a 5 percent eccentricity. Kobori and Shinozaki (1975) have analyzed the torsional response of a one-story structure subjected to obliquely incident SH waves. In this work, the exact torsional input for a circular rigid foundation was used. The torsional response of continuous elastic and symmetrical structures supported on a flat circular foundation and an embedded hemisperical foundation have been studied by Luco (1975a, b). Veletsos et al. (1975) and Matsushima (1977) have studied the effects of nonvertically incident waves on the response of one-story structures supported on several columns resting on individual footings. Abdel-Ghaffar and Trifunac (1977) and Werner, Lee, Wong and Trifunac (1977) have analyzed the response of bridge spans supported on piers when subjected to nonvertically incident waves.

To illustrate the effects of nonvertically incident SH waves on the response of structures, Luco and Wong (1979) considered two symmetric elastic structures with the properties listed in Table 7-1. The first structure (Model 1) corresponds approximately to a ten-story reinforced concrete building with a height of 40 m and a square floor plan of 20 × 20 m. The structure is assumed to have significantly different stiffness in the x and y directions. The 20 × 20 m square foundation is assumed to be rigid and resting on a uniform soil characterized by a shear wave velocity of 400 m/sec. The second structure considered (Model 2) corresponds to an idealized model of a containment building in a nuclear power plant. The model, in this case, has the same stiffness in the x and y directions. The foundation is represented by an equivalent rigid 40 × 40 m square mat resting on a uniform soil with a shear wave velocity of 600 m/sec. For simplicity, the fixed-base natural frequencies were assumed to be in the ratios 1:3:5:7 ..., and the mode shapes and participation factors for horizontal vibrations were taken equal to those for a uniform shear wall. The mode shapes and modal participation factors for vertical and torsional vibrations were taken equal to those for a uniform bar. Modal damping coefficients of 2

TABLE 7-1

Properties of the models considered (Luco and Wong, 1979).

	Model 1	Model 2
H (m)	40	60
ℓ (m)	10	20
M'_b (kg)	10^7	3×10^7
$S_{bx}/HM'_b = S_{by}/HM'_b$	0.50	0.50
$I_{bx}/H^2M'_b = I_{by}/H^2M'_b$	0.33	0.38
$I_{bz}/H^2M'_b$	0.04	0.10
M'_o/M'_b	0.15	0.45
$S_{ox}/HM'_b = S_{oy}/HM'_b$	0.000	0.000
$I_{ox}/H^2M'_b = I_{oy}/H^2M'_b$	0.003	0.017
$I_{oz}/H^2M'_b$	0.006	0.034
Fixed-base natural frequencies (Hz):		
vibrations in xz-plane	1, 3, 5, 7, 9	5, 15, 25
vibrations yz-plane	2, 6, 10, 14, 18	5, 15, 25
vertical vibrations	3, 9, 15, 21, 27	6, 18, 30
torsional vibrations	3, 9, 15, 21, 27	8, 24, 40
Modal damping coefficients (all modes)	0.02	0.02
Shear wave velocity in soil (m/sec)	400	600
Shear modulus in soil (N/m^2)	3×10^8	6.75×10^8
Poisson's ratio in soil	0.333	0.333
Damping coefficients in soil	0.05	0.05

percent were used for both structures and all fixed-base modes considered.

In Table 7-1, H represents the height of the structure, ℓ the half-width of the foundation, M_b' the mass of the superstructure, and I_{bx} and I_{bz} the mass moments of inertia about the x and z-axes, respectively. The terms S_{bx} and S_{by} represent the moments of the masses about x and y-axes through the foundations. The corresponding quantities for the foundation are M_o', I_{ox}, I_{oz}, S_{ox} and S_{oy}.

Calculations of the response in the time domain and of floor response spectra were obtained by setting the horizontal component of the free-field motion equal to the NS acceleration time-history recorded at El Centro for the 1940 Imperial Valley earthquake. For Model 1, calculations were performed separately for excitations impinging normal to both sides of the foundation as shown in Figure 7.1. For the symmetric Model 2, it is sufficient to consider excitation leading to response in only one direction.

The transfer functions and floor response spectra at several locations on Model 1 when excited by SH waves impinging on the foundation along the x-axis (Figure 7.1a) are shown in Figures 7.2 and 7.3, respectively, for angles of incidence $\Theta_v = 0°$ (horizontal), 45° and 90° (vertical incidence). The translational response (U_y) at the center of the base, shown in Figures 7.2a and 7.3a, illustrates the effects of soil-structure interaction in the neighborhood of the fixed-base natural frequencies (2, 6, 10, 14, 18 cps). A marked reduction of the response associated with scattering by the rigid foundation can be noticed at frequencies higher than 6 cps. Figures 7.2b and 7.3b illustrate the translational response U_y at a point at the edge of the base (location 2 in Figure 7.1a). For nonvertically incident SH waves, the contribution of the torsional response of the structure can be seen in the neighborhood of the fixed-base natural frequencies in torsion (3, 9, 15, 21 and 27 cps). In addition, due to the torsional response of the foundation, the reduction of the response at high frequencies is not as marked as at the center of the foundation.

The rocking response $\ell\Theta_x$ (ℓ = 10 m) about the x-axis at the base of the structure is shown in Figures 7.2c and 7.3c in which it can be seen that a lower response is obtained for horizontally incident waves. Figures 7.2d and 7.3d illustrate the torsional response $\ell\Theta_z$ at the base of the structure for angles of incidence $\Theta_v = 0°$ and 45° (for vertical incidence, the torsional response is zero under the assumption of a symmetric structure). The torsional response at the base shown in Figure 7.2d follows the torsional input motion $\ell\Theta_z^*$ except for oscillations near the fixed-base torsional frequencies.

The translational response at the center of the top of the structure (point 3 in Figure 7.1a) is shown in Figures 7.2e and 7.3e. The transfer function at the top shows a significant reduction at frequencies higher than 6 cps for nonvertically incident waves. The floor response spectrum at the top, however (Figure 7.3e), does not show the same behavior. The reduction at high frequencies in this case is less than 5%. The difference must be attributed to the fact that the response in the fundamental mode which is affected only slightly by scattering of waves controls the time response. Finally, Figures 7.2f and 7.3f illustrate the translational response at a point on the edge of the top (point 4 in Figure 7.1a). The effects of the torsional response can be seen clearly at 3 and 9 cps. The floor response spectrum (Figure 7.3f) shows that the response at the high frequency end of the spectrum is 20% higher for nonvertically incident waves than for vertically incident excitation.

The transfer functions and floor response spectra at several locations on Model 1 when excited by SH waves inpinging on the foundation along the y-axis (not shown) exhibit similar characteristics to those just described for excitation along the x-axis. In this case, it is more difficult to visualize the torsional effects since the fixed-base torsional frequencies (3, 9, 15, 21 and 27 cps) coincide with some of the fixed-base translational frequencies. One significant difference corresponds to the much lower rocking response for vibrations in the more flexible direction of the structure.

The response of Model 2 to SH waves with particle motion along the y-axis and with different angles of incidence is shown in Figures 7.4 and 7.5. In this case, due to the higher mass and stiffness of the superstructure, the effects of soil-structure interaction are, in general, more pronounced than for Model 1. The translational response at the center of the base presented in Figures 7.4a and 7.5a exhibits a pronounced filtering of nonvertically incident SH waves by the foundation in the frequency range from 5 to 20 cps. The translational response at the edge of the base (point 2 in Figure 7.1c) shown in Figures 7.4b and 7.5b is clearly affected by torsion of the foundation (Figures 7.4d and 7.5d) for frequencies in the vicinity of 6 and 16 cps. These torsional effects can also be seen in Figure 7.4e il-

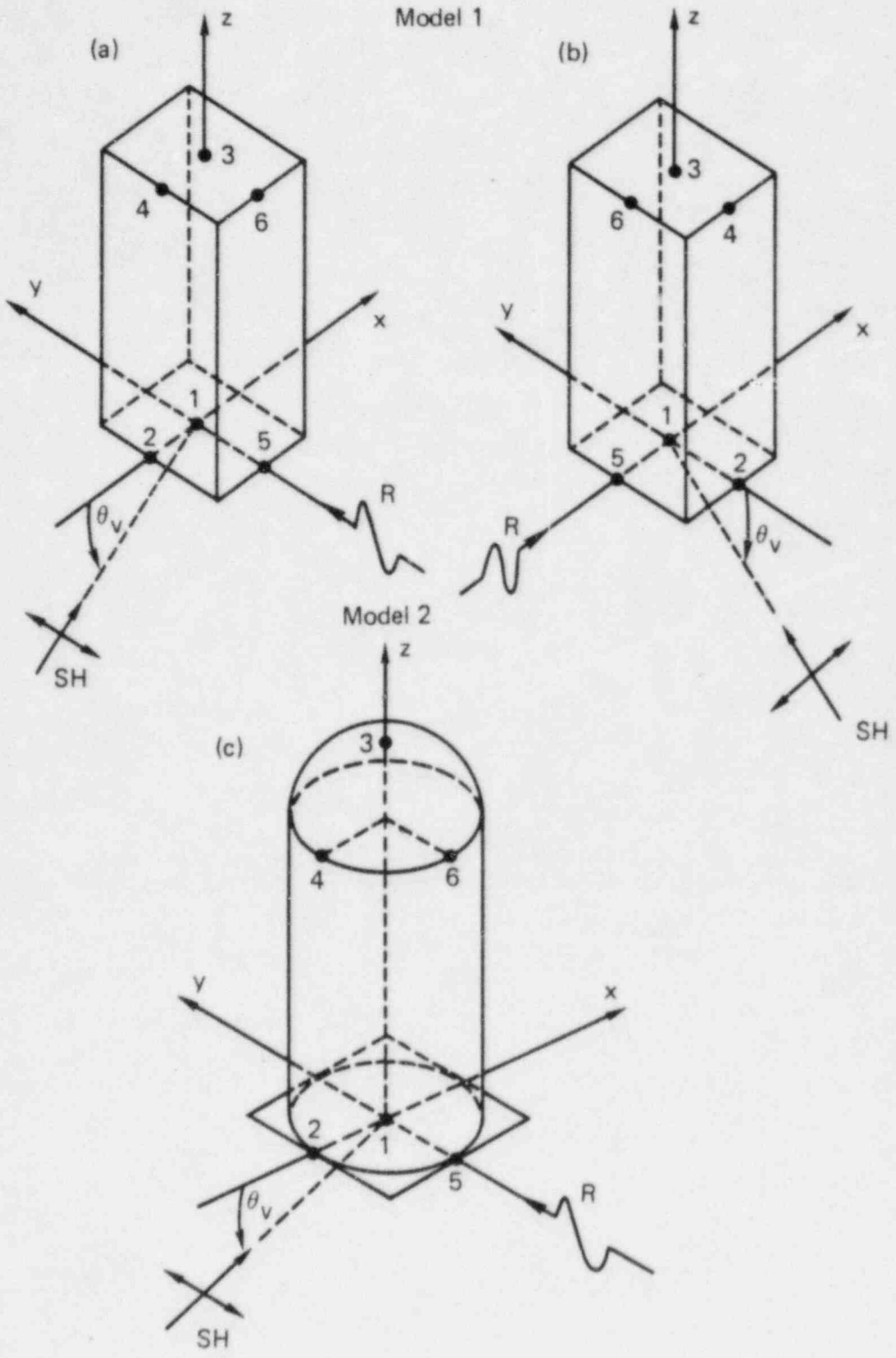

FIG. 7.1. Description of the types of seismic excitation considered and locations at which the response is calculated (Luco and Wong, 1979).

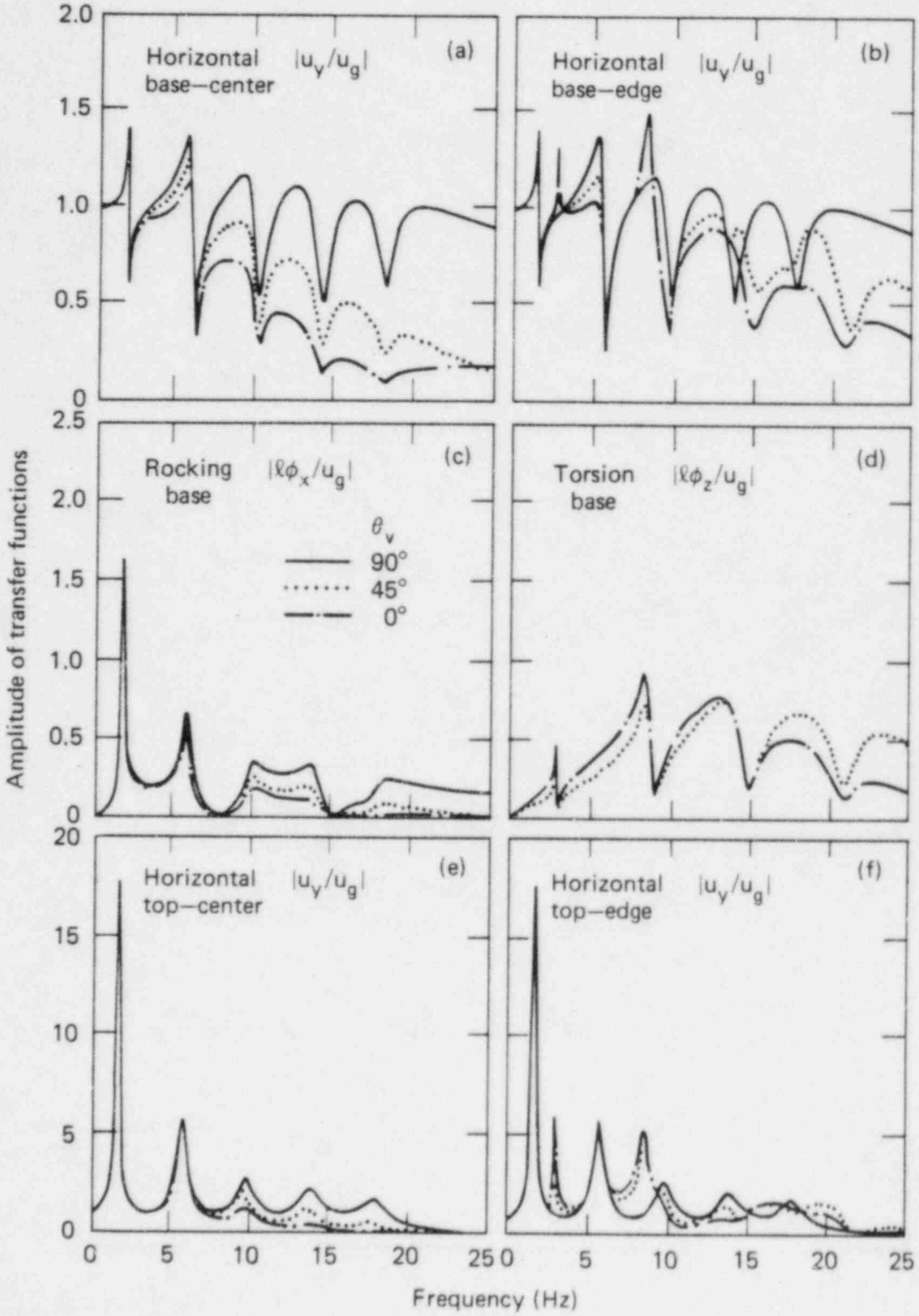

FIG. 7.2. Transfer functions for Model 1 excited by SH waves with particle motion along y-axis (Luco and Wong, 1979).

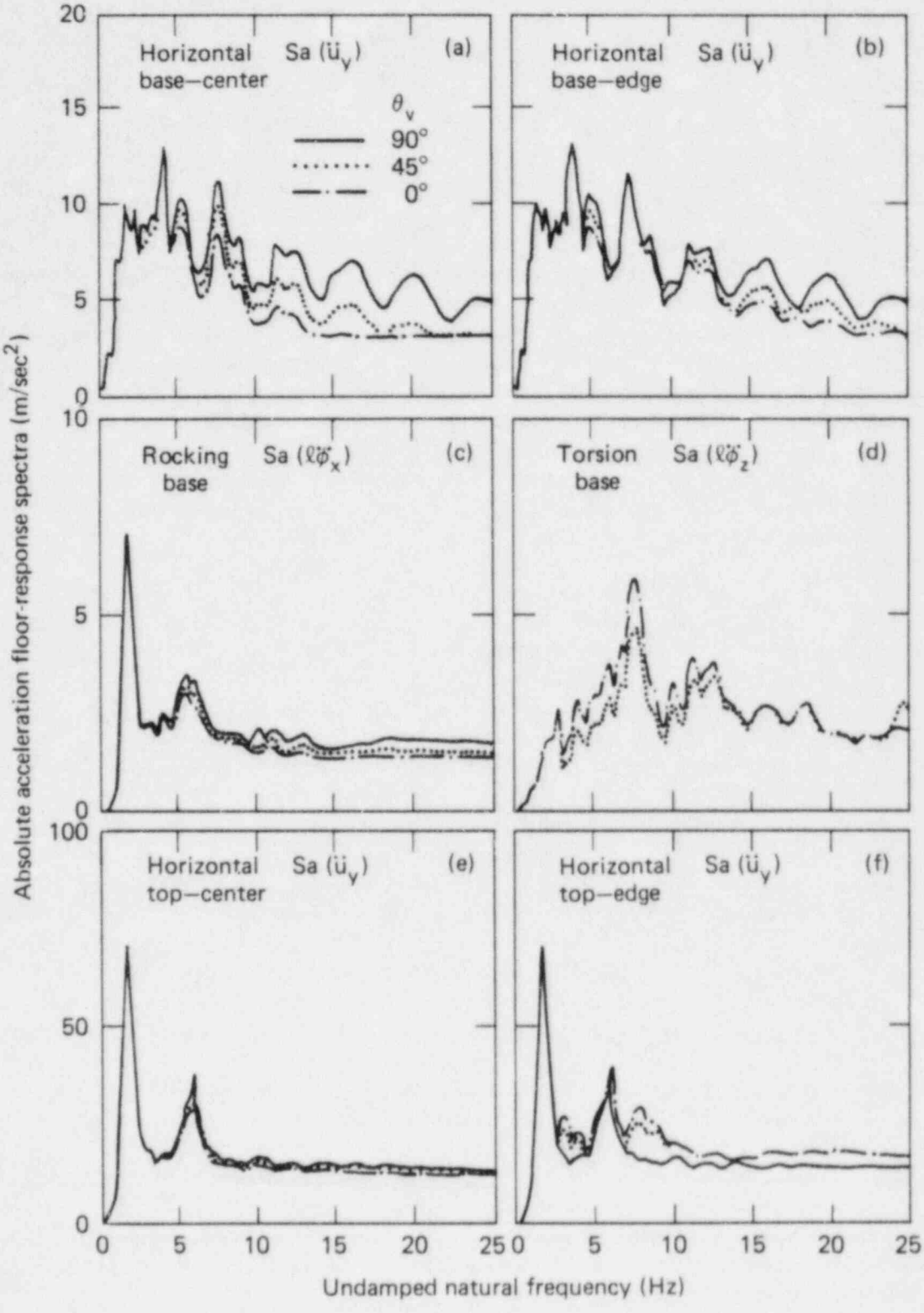

FIG. 7.3. Absolute acceleration floor response spectra for Model 1 excited by SH waves with particle motion along y-axis (2% damping) (Luco and Wong, 1979).

lustrating the transfer function for a point on the edge of the structure at elevation 40 m (point 4 in Figure 7.1c). The response at the top of Model 2 shown in Figures 7.4f and 7.5f exhibits a marked filtering effect for nonvertically incident waves. Due to the strong interaction effects, large shifts in resonant frequencies take place. The peak translational response at the top occurs at a frequency of approximately 3 cps while the fundamental fixed-base translational frequency for this model is 5 cps. Similarly, the peak torsional response occurs at 6 cps while the fundamental fixed-base torsional frequency is 8 cps.

The values of the absolute acceleration floor response spectra for a frequency of 25 Hz and for three angles of incidence ($\Theta = 90°$, vertical, $\Theta = 45°$, and $\Theta = 0°$, horizontal) are listed in Table 7-2.

In summary, Luco and Wong (1979) have studied the response to nonvertically incident SH waves of simplified models of a ten-story reinforced concrete building with different stiffness in two orthogonal directions (Model 1), and of the containment structure of a nuclear power plant (Model 2). For obliquely incident SH wave excitation, it has been found that the translational response at the center of the foundation at frequencies higher than 5 cps is significantly lower than the response for vertically incident SH waves. The response at the center of the top of the structure is also lower for nonvertically incident SH waves, but the reduction depends on the charactertistics of the structure: reductions of less than 6% were obtained for Model 1, while a reduction of 38% was obtained for Model 2 at high frequencies. Due to the contribution of the torsional components, the response at the edge of the top of the structure can be higher for nonvertically incident SH waves. The torsional response induced by nonvertically incident waves is significant as shown by the results obtained at the base of the structure.

It should be emphasized that the apparent phase velocities considered by Luco and Wong are quite low (for $\beta = 600$ m/sec and $\Theta = 45°$, the phase velocity is 849 m/sec) and, consequently, the results obtained should be interpreted as upper bounds for the effects of nonvertically incident SH waves. Luco and Sotiropoulos (1980) using phase velocities of the order of 3.5 km/sec have found that the reduction of the translational response is negligible and that the torsional response, while still of some importance, is considerably lower than that obtained for the lower phase velocities.

The study of the dynamic response of structures subjected to nonvertically incident P and SV waves and surface Rayleigh waves has also received some attention. Lee (1979) studied the response of a one-story structure supported on a rigid hemispherical foundation when subjected to nonvertically incident P and SV waves. Simpson (1978) has studied the response of a plane-strain model of a structure supported on a flat rigid foundation and excited by Rayleigh waves. The effects of Rayleigh waves on the response of simplified three-dimensional models of a ten-story reinforced concrete building and a containment-type structure have been analyzed by Luco and Wong (1979). In that study the foundation was assumed to be flat, rigid and supported in a uniform half-space. The characteristics of the systems considered are presented in Table 7-1. The seismic excitation was represented by a Rayleigh wave propagating with phase velocity $c_R = 0.933\beta$ (β corresponds to the shear wave velocity in the soil). The vertical component of motion in the free-field was taken to have an amplitude of 1.565 times the amplitude of the horizontal component and was 90 degrees out of phase with respect to the horizontal component. The horizontal component of motion was taken equal to the NS acceleration time-history recorded at El Centro for the 1940 Imperial Valley earthquake.

To illustrate the response of structures to Rayleigh waves some of the results of Luco and Wong for Model 1 (ten-story reinforced concrete building) and Model 2 (containment structure) are presented here. Transfer functions for the frequency response at locations 1, 3, 5 and 6 (Figure 7.1) are shown in Figures 7.6 and 7.8. Floor (in-structure) absolute acceleration response spectra at the same locations are shown in Figures 7.7 and 7.9.

The transfer functions and floor response spectra for Model 1 excited by a Rayleigh propagating in the direction of the y axis are shown in Figures 7.6 and 7.7, respectively. The transfer function for the horizontal response at the center of the base (Figure 7.6a) shows a very pronounced filtering for frequencies higher than 2 cps. The floor response spectrum at the same location (Figure 7.7a) is characterized by lower amplitudes than the corresponding spectrum for vertically incident SH waves

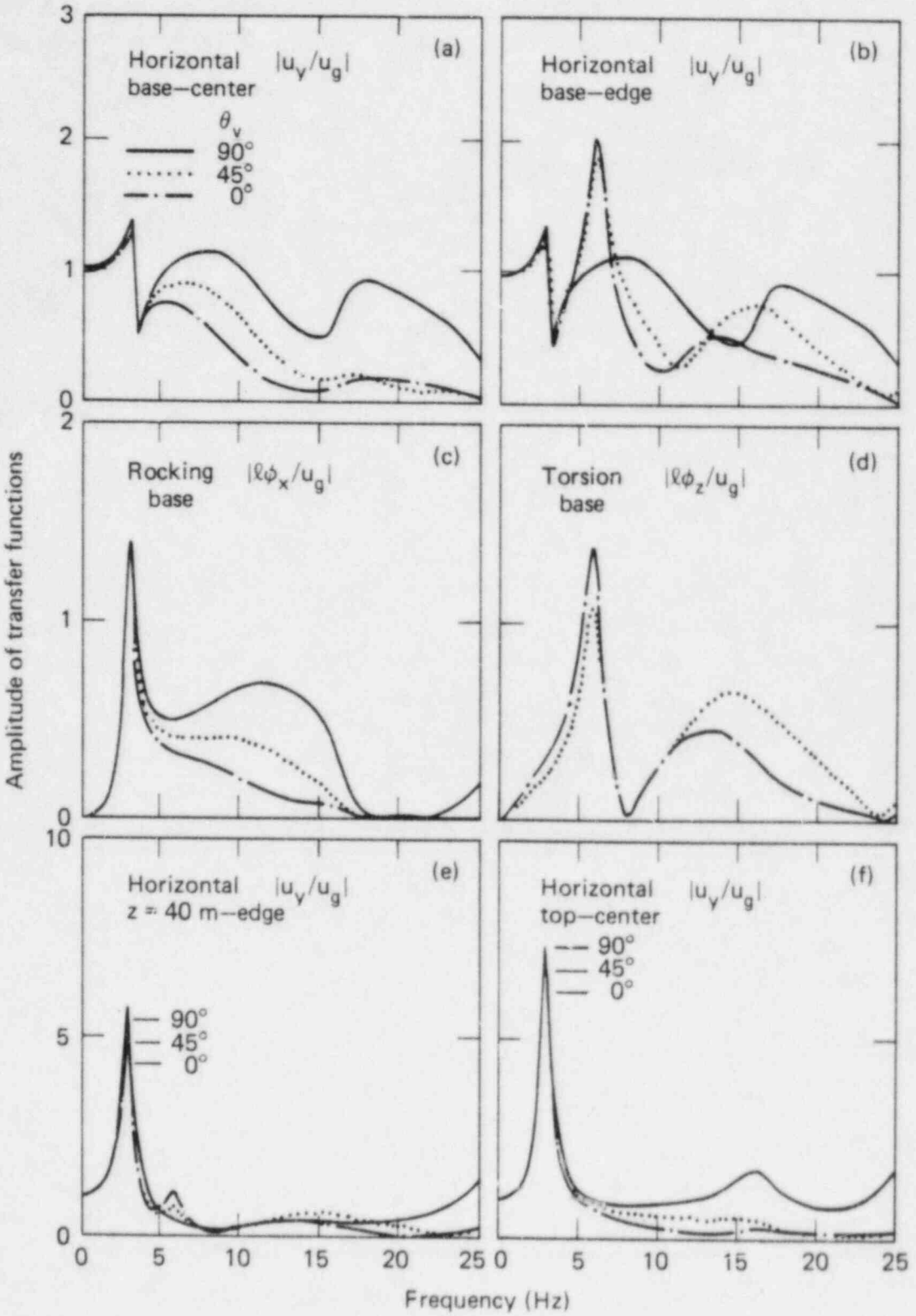

FIG. 7.4. Transfer functions for Model 2 excited by SH waves with particle motion along y-axis (Luco and Wong, 1979).

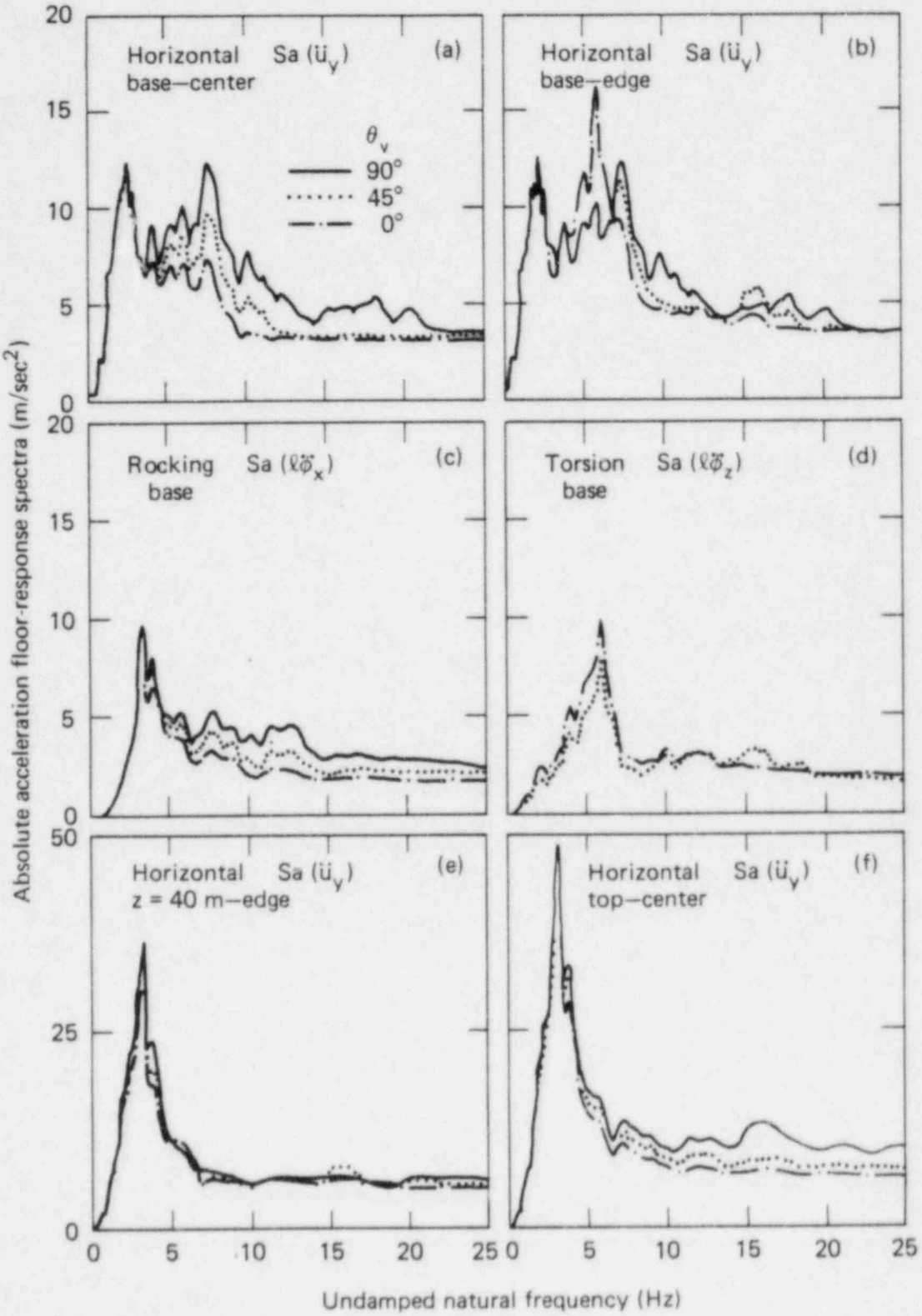

FIG. 7.5. Absolute acceleration floor response spectra for Model 2 excited by SH waves with particle motion along y-axis (2% damping) (Luco and Wong, 1979).

TABLE 7-2

Comparison of spectral amplitudes at 25 Hz (m/sec^2) (Luco and Wong, 1979).

	Station	Component	SH waves 90°	SH waves 45°	SH waves 0°	Rayleigh waves
Model 1 (motion in yz plane)	Free-field	$\ddot{u}_y$	4.07	4.07	4.07	4.07
	1	$\ddot{u}_y$	4.89	3.18	3.12	2.94
	1	$\ell\ddot{\theta}_x$	1.66	1.46	1.38	4.04
	1	$\ell\ddot{\theta}_z$	0.00	2.58	2.04	0
	1	$\ddot{u}_z$	0	0	0	6.12
	2	$\ddot{u}_y$	4.89	3.37	3.27	2.94
	5	$\ddot{u}_z$	1.66	1.46	1.38	6.20
	3	$\ddot{u}_y$	14.0	13.7	13.5	21.8
	4	$\ddot{u}_y$	14.0	16.6	16.9	21.8
	3	$\ddot{u}_z$	0	0	0	11.9
	6	$\ddot{u}_z$	–	–	–	12.0
Model 1 (motion in xz plane)	Free-field	$\ddot{u}_x$	4.07	4.07	4.07	4.07
	1	$\ddot{u}_x$	4.39	3.18	3.24	3.11
	1	$\ell\ddot{\theta}_y$	0.433	0.330	0.315	4.62
	1	$\ell\ddot{\theta}_z$	0	2.58	2.04	0
	1	$\ddot{u}_z$	0	0	0	6.12
	2	$\ddot{u}_x$	4.39	3.41	3.43	3.11
	5	$\ddot{u}_z$	0.433	0.330	0.315	8.87
	3	$\ddot{u}_x$	8.81	8.58	8.32	11.5
	4	$\ddot{u}_x$	8.81	10.1	9.98	11.5
	3	$\ddot{u}_z$	0	0	0	11.9
	6	$\ddot{u}_z$	–	–	–	13.7
Model 2	Free-field	$\ddot{u}_y$	4.07	4.07	4.07	4.07
	1	$\ddot{u}_y$	3.67	3.33	3.23	2.95
	1	$\ell\ddot{\theta}_x$	2.43	2.08	1.75	3.90
	1	$\ell\ddot{\theta}_z$	0	1.61	1.88	0
	1	$\ddot{u}_z$	0	0	0	5.36
	2	$\ddot{u}_y$	3.67	3.59	3.50	2.95
	5	$\ddot{u}_z$	2.43	2.08	1.75	4.89
	3	$\ddot{u}_y$	10.6	7.36	6.55	19.5
	4	$\ddot{u}_y$	6.31	5.87	5.61	–
	3	$\ddot{u}_z$	0	0	0	9.42
	6	$\ddot{u}_z$	–	–	–	9.24

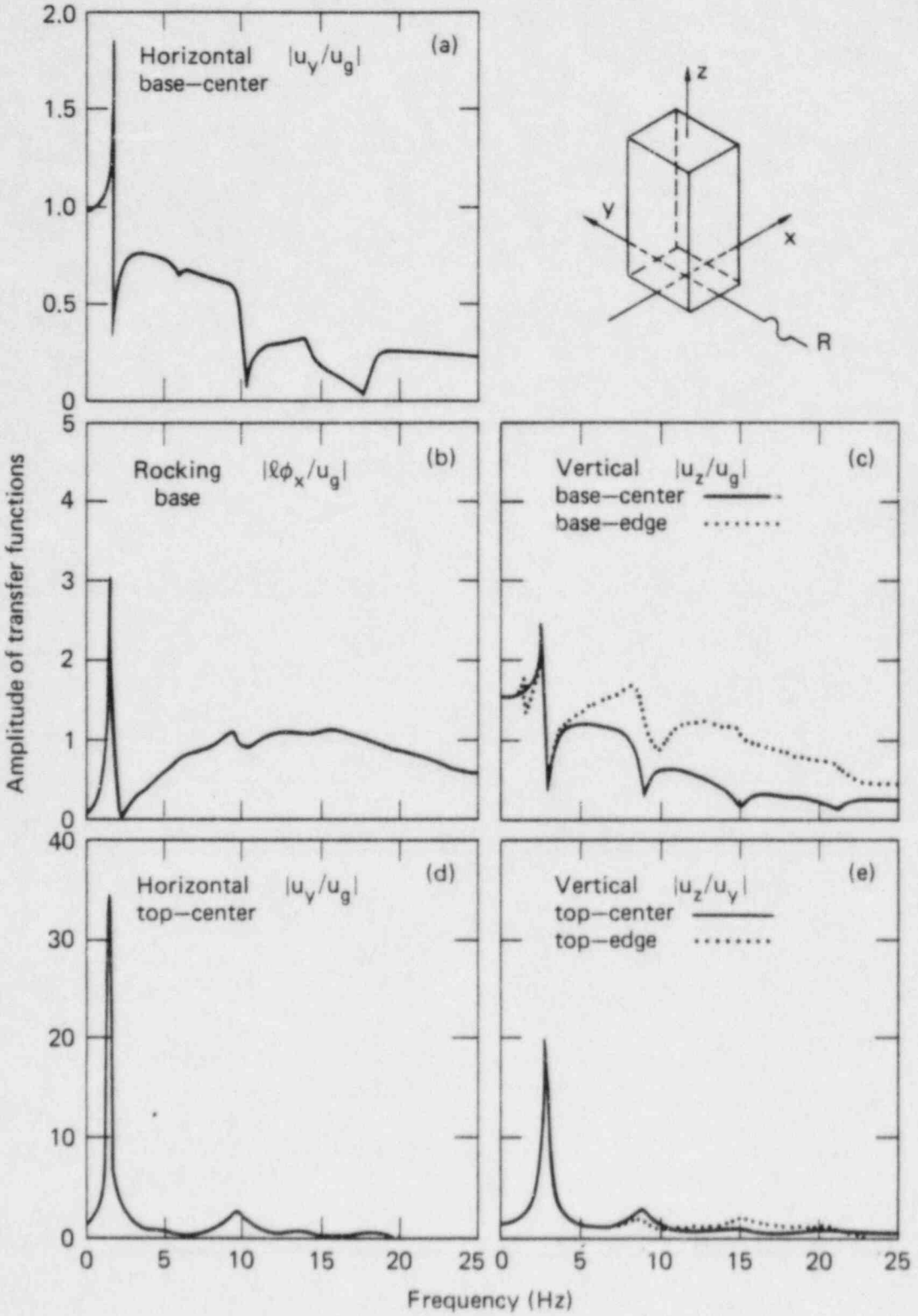

FIG. 7.6. Transfer functions for Model 1 excited by Rayleigh waves propagating along the y-axis (Luco and Wong, 1979).

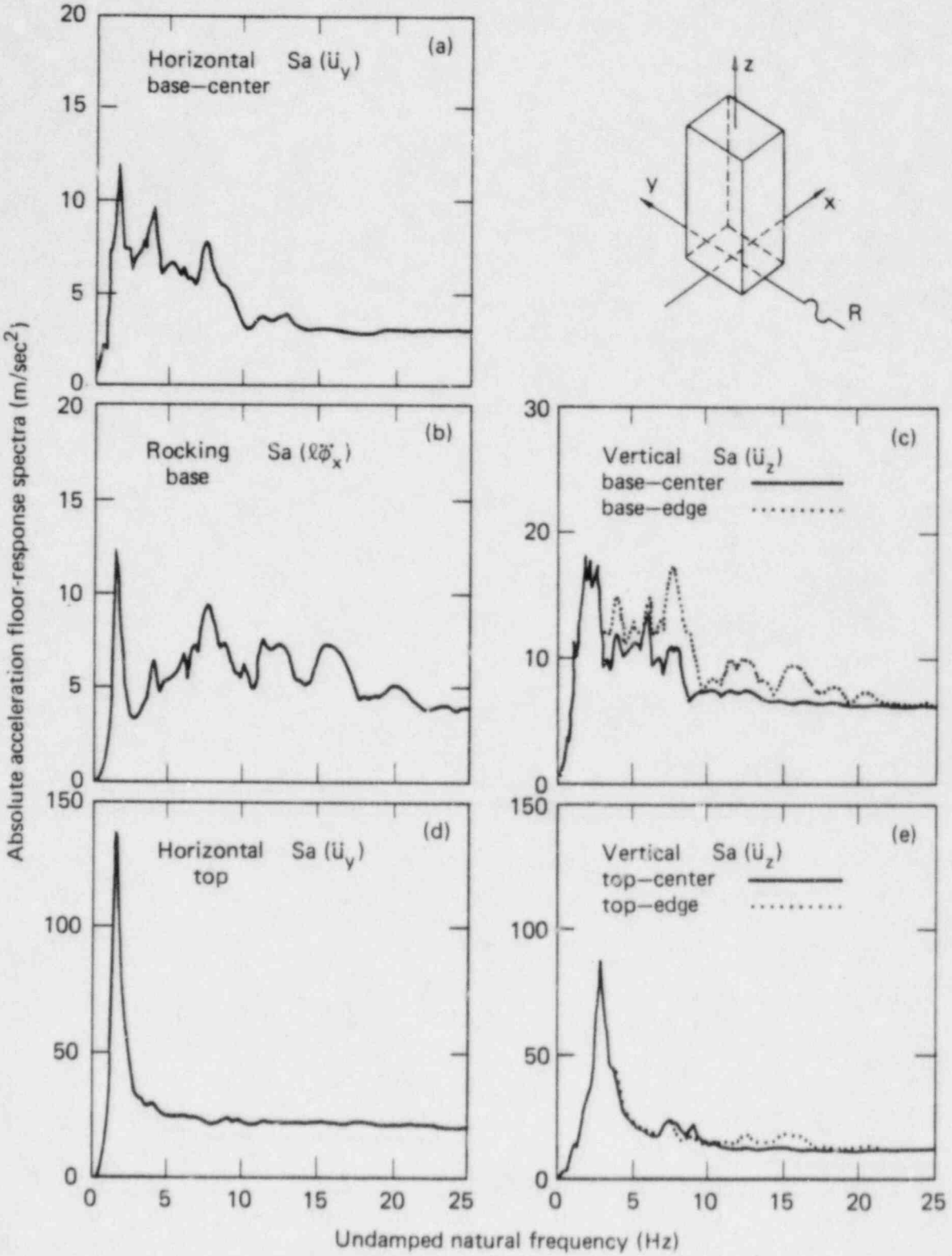

FIG. 7.7. Absolute acceleration floor response spectra for Model 1 excited by Rayleigh waves propagating along the y-axis (2% damping) (Luco and Wong, 1979).

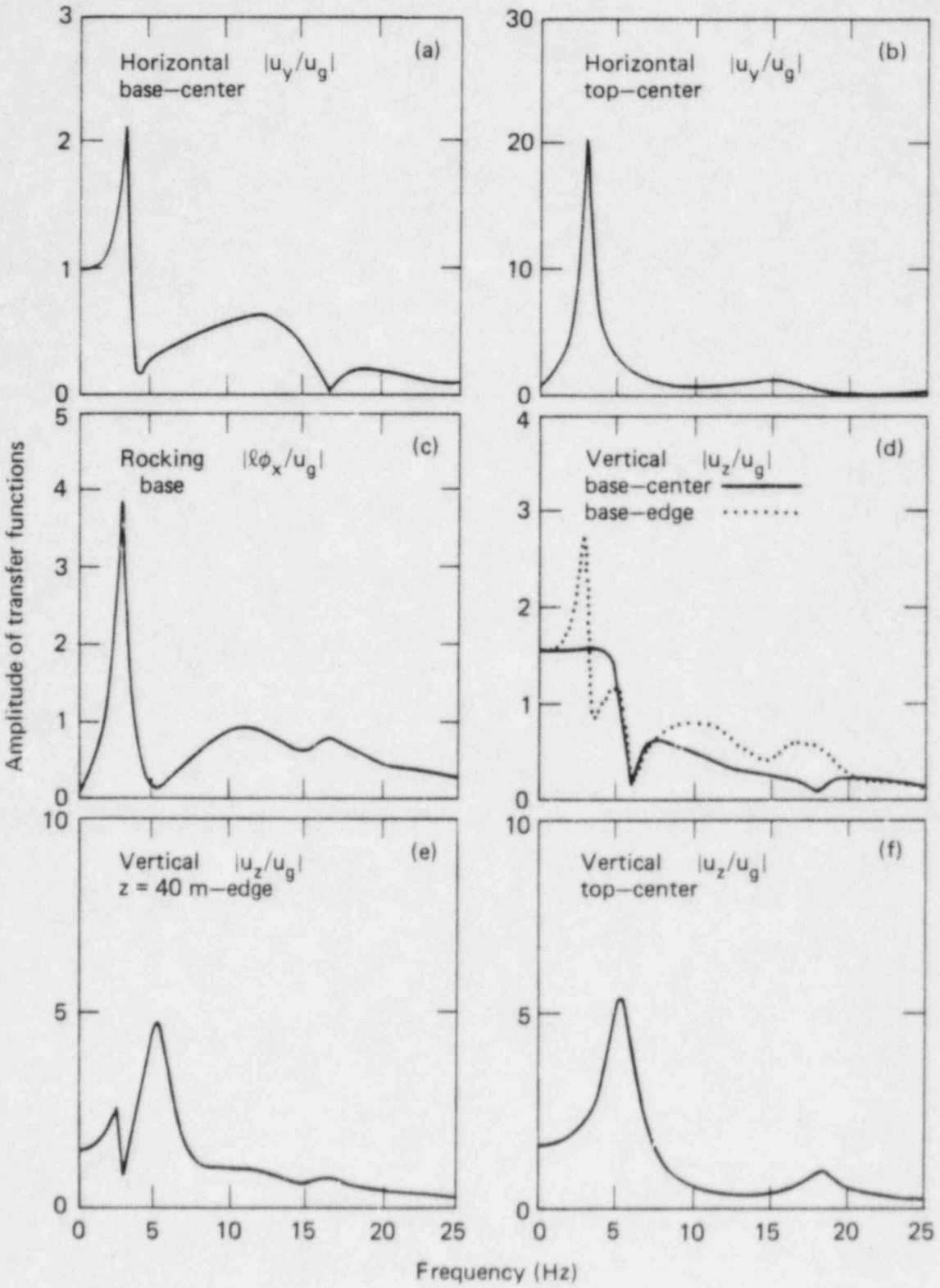

FIG. 7.8. Transfer functions for Model 2 excited by Rayleigh waves propagating along the y-axis (Luco and Wong, 1979).

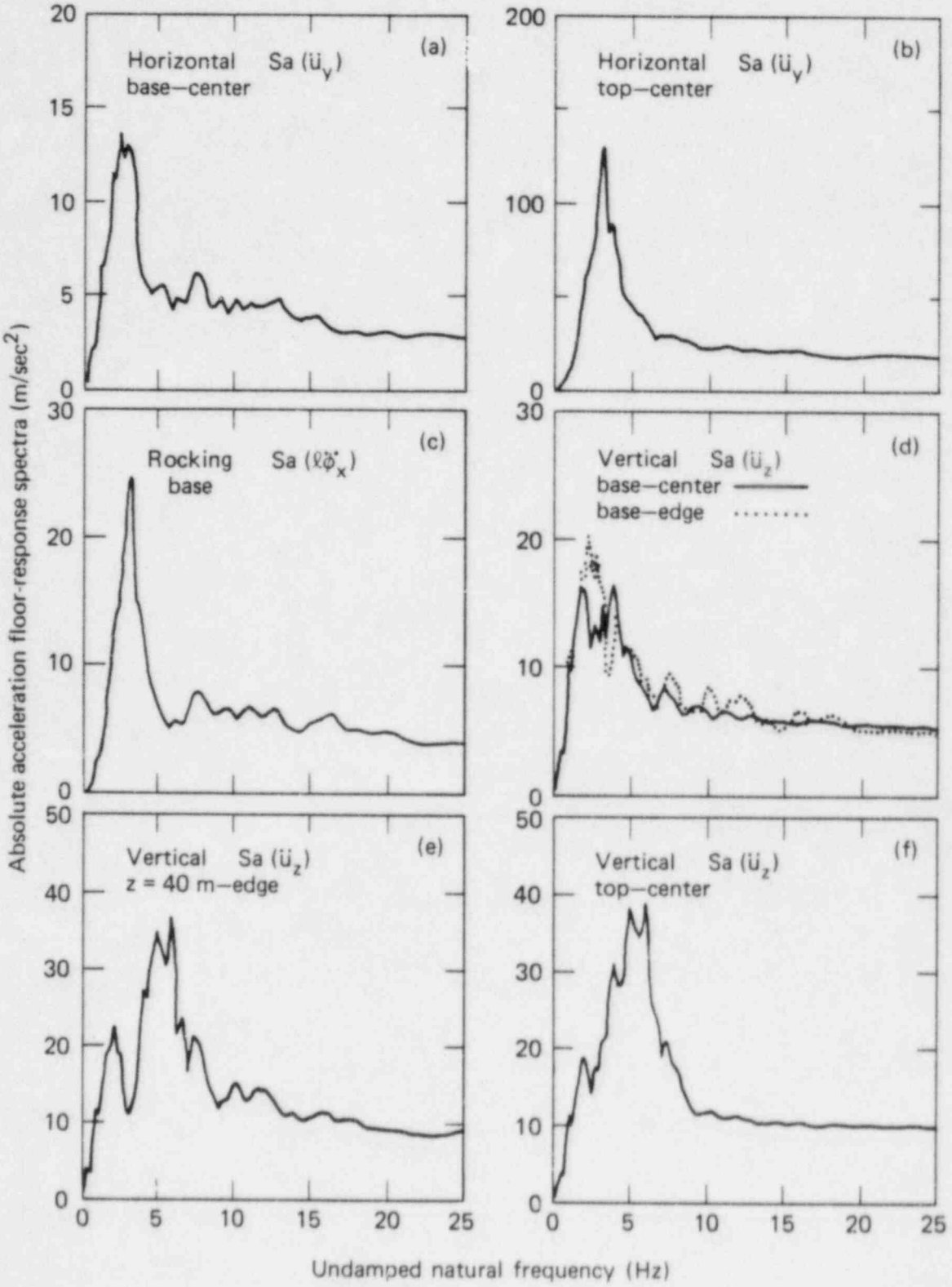

FIG. 7.9. Absolute acceleration floor response spectra for Model 2 excited by Rayleigh waves propagating along the y-axis (2% damping) (Luco and Wong, 1979).

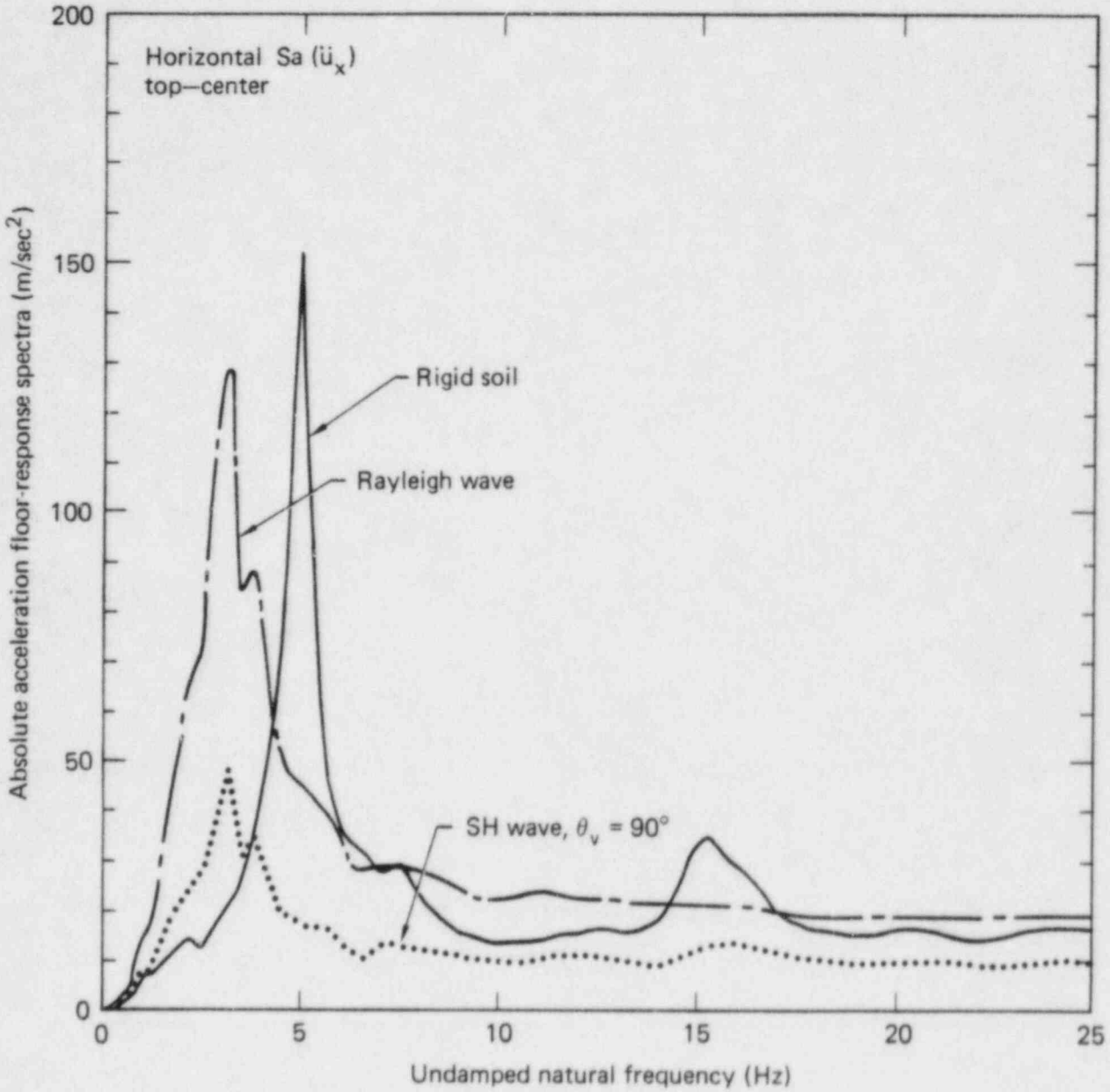

FIG. 7.10. Comparison of floor response spectra at the top of Model 2 for vertically incident SH waves, Rayleigh waves and rigid soil model (2% damping) (Luco and Wong, 1979).

shown in Figure 7.2a. The rocking transfer function at the base, shown in Figure 7.6b, generally follows the rocking input motion except for oscillations in the vicinity of the fixed-base natural frequencies (2, 6, 10, 14 and 18 cps). As expected, the rocking response for Rayleigh (Figures 7.6b and 7.7b) is significantly higher than the corresponding response for vertically incident SH waves (Figures 7.2c and 7.3c).

The vertical response at the center and edge of the base (locations 1 and 5 in Figure 7.1a) shown in Figures 7.6c and 7.7c are twice as large as the horizontal response. In general, the vertical response at the edge is larger than at the center due to the contributions of rocking. The horizontal response at the top (Figures 7.6d and 7.7d) is almost twice as large as the corresponding response for vertically incident SH waves (Figures 7.2e and 7.3e). This amplification results from the large rocking input motion associated with Rayleigh waves. The vertical response at the center and edge of the top of the structures (Figures 7.6e and 7.7e) is not as large as the horizontal response due to the higher stiffness of the structure in the vertical direction and to the large radiation damping associated with vertical vibrations.

The results obtained for the response of Model 1 to Rayleigh waves propagating along the x axis (not shown), as well as those for Model 2 (shown in Figures 7.8 and 7.9), are not significantly different from those already described for Model 1.

The values of the absolute acceleration floor response spectra for a frequency of 25 Hz and Rayleigh wave excitation are also listed in Table 7-2. The results presented in Table 7.2 summarize the effect of obliquely incident seismic waves on the high frequency response components at the different locations shown in Figure 7.1. A comparison of the floor response spectra at the top of Model 2 for vertically incident (Θ_v = 90°) SH waves and for Rayleigh waves is shown in Figure 7.10. The corresponding response for the same structure supported on a rigid soil is also shown in Figure 7.10. The results presented in Figure 7.10 indicate that the response for Rayleigh wave excitation is significantly higher than that for vertically incident SH waves. Comparison with the response for a rigid soil model clearly shows the importance of the effect of soil-structure interaction for this case.

For Rayleigh wave excitation, the horizontal response at the base of the structure is significantly lower than the corresponding response for vertically incident SH waves. The rocking response, on the other hand, is much higher for Rayleigh wave excitation leading to a much higher response at the top. For Model 2, the response at the top for Rayleigh waves is twice that for vertically incident SH waves. For Model 1, increases of 31% and 56% at high frequencies are obtained, depending on the direction of incidence of the wave.

The results obtained by Luco and Wong (1979), described above, are based on a model of the soil corresponding to a uniform half-space. In this case, the phase velocity of the Rayleigh waves is lower than the shear wave velocity in the soil and the vertical component of motion has an amplitude of 1.5 times the amplitude of the horizontal component in the free-field. In a more realistic situation involving soil layers, the phase velocity will be higher than the shear wave velocity in the top layers and the ratio of the vertical to the horizontal component of motion will be lower. As a result the reduction in translational response at base level will not be as marked and the translational response at the top will not differ by a factor of two from the response calculated for vertically incident SH waves. Preliminary results obtained by Luco and Sotiropoulos (1980) for phase velocities of the order of 5 km/sec indicate that the reduction in translational response at foundation level is negligible, while the rocking response may induce an increase in the translational response at the top of a containment-type structure of the order of 30 percent.

The foregoing discussion emphasizes the need for a more complete characterization of the free-field motion.

REFERENCES (7)

Abdel-Ghaffar, A.M. and M.D. Trifunac (1977). Antiplane Dynamic Soil/Bridge Interaction for Incident Plane SH-Waves. *Earthquake Engineering and Structural Dynamics, 5,* 107-128.

Iguchi, M. (1973). Seismic Response with Consideration of Both Phase Differences of Ground Motion and Soil-Structure Interaction. *Proc. Japan Earthquake Engrg. Symp.,* Tokyo, Japan.

Kobori, T. and Y. Shinozaki (1975). Torsional Vibration of Structure Due to Obliquely Incident SH Wave. *Proc. V European Conf. Earthquake Engrg.,* No. 22, Istanbul, Turkey.

Lee, T. H. and D. A. Wesley (1975). Three-Dimensional Soil-Structure Interaction of Nuclear Structures During Earthquakes Considering Ground Rotational Input. *Proc. 2nd ASCE Specialty Conf. on Struct. Design of Nuclear Plant Facilities,* New Orleans, Louisiana.

Lee, T.H. (1977). Three-Dimensional Seismic Response of Multiple Vessels on Common Base Subjected to Translation-Torsion Ground Excitation Input. *Proc. Third International Conference on Pressure Vessel Technology.*

Lee, V. W-S. (1979). *Investigation of Three-Dimensional Soil-Structure Interaction.* Report CE-79-11, Dept. of Civil Engineering, Univ. of Southern California, Los Angeles, California.

Luco, J. E. (1976a). Torsional Response of Structures for Obliquely Incident Seismic Waves. *Earthq. Engrg. and Struct. Dynamics, 4,* 207-219.

Luco, J. E. (1976b). Torsional Response of Structures for SH Waves: The Case of Hemispherical Foundations, *Bull. Seism. Soc. Am., 66,* 1, 109-123.

Luco, J. E. and H. L. Wong (1979). *Response of Structures to Nonvertically Incident Seismic Waves. Dept. of Appl. Mechs. and Engrg. Sci.,* Univ. of California, San Diego, La Jolla, California (October).

Luco, J. E. and D. A. Sotiropoulos (1980). Local Characterization of Free-Field Ground Motion and Effects of Wave Passage. *Bull. Seism. Soc. Am.* (in press).

Matsushima, Y. (1977). Stochastic Response of Structures due to Spatially Variant Earthquake Excitation. *Proc. 6th World Conf. on Earthq. Engrg.,* New Delhi, India, pp. 3-103 to 3-108.

Newmark (1969). Torsion of Symmetrical Buildings, *Proc. 4th World Conf. Earthq. Engrg.,* Santiago, Chile.

Simpson, I. C. (1978). On the Interaction of Rayleigh Surface Waves with Structures. *Earthq. Engrg. and Struct. Dynamics, 6,* 247-263.

Veletsos, A.S., M.D. Erdik and P.T. Kuo (1975). *Response of Structures to Propagating Ground Motions,* Rice University, Houston, Texas (April).

Werner, S. D., L. C. Lee, H. L. Wong and M. D. Trifunac (1977). *An Evaluation of the Effects of Traveling Seismic Waves on the Three-Dimensional Response of Structures.* Report R-7720-4514, Agbabian Associates, El Segundo, California.

Wolf, J. E. (1977). Seismic Response Due to Traveling Shear Wave Including Soil/Structure Interaction with Base-Mat Uplift. *Earthq. Engrg. and Struct. Dyn. 5*, 4, 337-364.

8. INTERACTION THROUGH THE SOIL BETWEEN ADJACENT STRUCTURES

In the case of closely spaced structures it may be necessary to consider not only the interaction between each structure and the soil but also the interaction through the soil between adjacent structures. The formulation of the interaction problem presented in Chapter 2, although derived for the case of an isolated structure, also applies, in a generalized sense, to the case of several (N) structures interacting through the soil. The interaction equation, in this case, is also given by

$$\{U_o\} = \left([I] - \omega^2[C(\omega)]\,([M_o] + [M_b(\omega)])\right)^{-1}\{U_o^*\} \tag{8.1}$$

in which the foundation response vector $\{U_o\}$ and the foundation input motion vector $\{U_o^*\}$ include six degrees of freedom for each of the N foundations (assumed rigid). The matrix [I] corresponds to the $6N \times 6N$ identity matrix and the matrices $[M_o]$ and $[M_b(\omega)]$ are block diagonal of dimensions $6N \times 6N$. The $6N \times 6N$ compliance matrix $[C(\omega)]$ and the foundation input motion $\{U_o^*\}$ incorporate the coupling between foundations. Eq. (8.1) reveals that the problem of determining the through-the-soil coupling effects hinges upon the evaluation of the compliance matrix and foundation input motion for N rigid foundations interacting through the soil. The other elements, i.e. the diagonal blocks of the matrices $[M_o]$ and $[M_b(\omega)]$, correspond to those for an isolated structure.

To discuss the characteristics of the compliance matrix and of the foundation input motion it is convenient to refer, without loss of generality, to the case of two rigid foundations. In this case the force-displacement relationship for the foundations can be written in the form

$$\left\{\begin{array}{c} U_{o1} \\ \hline U_{o2} \end{array}\right\} = \left[\begin{array}{c|c} C_{11} & C_{12} \\ \hline C_{21} & C_{22} \end{array}\right] \left\{\begin{array}{c} F_{S1} \\ \hline F_{S2} \end{array}\right\} + \left\{\begin{array}{c} U_{o1}^* \\ \hline U_{o2}^* \end{array}\right\} \tag{8.2}$$

in which $\{U_{o1}\}$ and $\{U_{o2}\}$ are the 6×1 generalized total displacement vectors for the two foundations, while $\{F_{S1}\}$ and $\{F_{S2}\}$ are the corresponding 6×1 vectors of generalized forces that the foundations exert on the soil. In Eq. (6.2), the 6×1 foundation input motion vectors for both foundations are denoted by $\{U_{o1}^*\}$ and $\{U_{o2}^*\}$. The 6×6 matrices $[C_{11}]$ and $[C_{22}]$ correspond to the diagonal blocks of the partitioned compliance matrix; while the 6×6 coupling matrices $[C_{12}]_T = [C_{21}]^T$ correspond to the off-diagonal blocks. In general, the matrices $[C_{11}]$, $[C_{22}]$, $[C_{12}] = [C_{21}]^T$ and the vectors $\{U_{o1}^*\}$ and $\{U_{o2}^*\}$ depend on the relative position of the two foundations. If the distance between the two foundations is very large then $[C_{12}] = [C_{21}]^T \to 0$ and $[C_{11}]$, $[C_{22}]$, $\{U_{o1}^*\}$ and $\{U_{o2}^*\}$ tend to the corresponding quantities for isolated foundations.

The force-displacement relationship given by Eq. (8.2) can also be written in the form

$$\left\{\begin{array}{c} F_{S1} \\ \hline F_{S2} \end{array}\right\} = \left[\begin{array}{c|c} K_{11} & K_{12} \\ \hline K_{21} & K_{22} \end{array}\right] \left\{\begin{array}{c} U_{o1} \\ \hline U_{o2} \end{array}\right\} - \left\{\begin{array}{c} F_{S1}^* \\ \hline F_{S2}^* \end{array}\right\} \tag{8.3}$$

where the partitioned impedance matrix [K] is defined by

$$\left[\begin{array}{c|c} K_{11} & K_{12} \\ \hline K_{21} & K_{22} \end{array}\right] = \left[\begin{array}{c|c} C_{11} & C_{12} \\ \hline C_{21} & C_{22} \end{array}\right]^{-1} \tag{8.4}$$

and the driving force vector by

$$\left\{\begin{array}{c} F_{S1}^{*} \\ \hline F_{S2}^{*} \end{array}\right\} = \left[\begin{array}{c|c} K_{11} & K_{12} \\ \hline K_{21} & K_{22} \end{array}\right] \left\{\begin{array}{c} U_{o1}^{*} \\ \hline U_{o2}^{*} \end{array}\right\} \tag{8.5}$$

The driving force vector corresponds to the forces that the soil exerts on the foundations when the foundations are kept fixed under the effects of the seismic excitation.

As a first example of the effects of coupling through the soil between two adjacent rigid foundations, consider two infinitely long rigid semicylindrical foundations of radius $r_1 = r_2$ separated by a distance a as shown in Fig. 8.1. The normalized impedance coefficients for vibrations in the direction of the long dimension of the foundations are shown in Fig. 8.1 versus the dimensionless frequency $kr_1 = \omega r_1/\beta$ for three values of the separation ratio $a/r_1 = 4, 10, \infty$ (Luco and Contesse, 1973). It is apparent from Fig. 8.1 that the smaller the distance between foundations the stronger the coupling effects. In particular for $a/r_1 = 4$ the real part of the coupling impedance $K_{12} = K_{21}$ becomes of the same order as the real part of the diagonal terms $K_{11} = K_{22}$. (For $a/r_1 = \infty$, $K_{12} = K_{21} = 0$).

The effects of through-the-soil coupling on the driving forces for vertically incident SH waves with particle motion in the direction of the long dimension of the foundations are shown in Fig. 8.2. In this figure, $S_1 = S_2 = -F_{S1}^{*}/(\pi\mu W_o)$ where μ is the shear modulus of the soil and W_o is the amplitude of the free-field motion on the ground surface. As shown in Fig. 8.2, interaction through the soil introduces significant fluctuations in the driving forces.

As a second example consider two equal rectangular foundations supported on an elastic half-space and separated by a distance S as shown in Fig. 8.3. Some of the static stiffness coefficients for this configuration are presented in Fig. 8.3 versus S/W where W is the half-width of the foundations (Hadjian, Luco and Wong, 1980). As shown in Fig. 8.3, the effects of coupling through the soil become significant for separations of the order of the half-width of the foundations. The effect of through-the-soil coupling on K_{11} increases as the length-to-width ratio (L/W) of the foundations increases. In addition, as the aspect ratio of the foundations increases the coupling stiffness K_{14} becomes progressively more important when compared with K_{11}. These results indicate then that the through-the-soil coupling effects depend not only on the separation between the foundations but also on the aspect ratio of the foundations. For this reason, two-dimensional models (which imply an infinite length to width ratio) will severely distort the interaction effects between adjacent foundations and structures. It is also important to notice that the effects of coupling through the soil are more pronounced on the coupling terms of the impedance matrix (e.g. K_{14}) than on the diagonal terms (Wong, 1977).

In addition to the effects mentioned above, interaction through the soil causes coupling between the different components of motion. For example, a vertical force applied to one foundation may cause not only a translation of the second foundation but also a rocking component may be excited. Similarly, a horizontal force applied to one foundation may cause a torsional response of the second foundation.

The interaction between two rigid circular foundations has been studied experimentally by MacCalden (1969) and analytically by Warburton, Richardson and Webster (1971). Lee and Wesley (1973a,b) used the approximate method proposed by Warburton, et al. to study the coupling through the soil between adjacent structures supported on rigid circular foundations. Wong (1977) has proposed a method to evaluate the through-the-soil coupling effects for several adjacent flat rigid foundations of arbitrary shape.

The two-dimensional anti-plane shear problem of interaction between several infinitely long shear walls supported on semi-cylindrical foundations has been studied by Luco and Contesse (1974), Wong (1975), Wong and Trifunac (1975) and Murakami and Luco (1977). Two-dimensional plane-strain finite element models have been studied by Lysmer, Udaka, Seed and Hwang (1974) and by Liang (1974).

A general formulation of the through-the-soil coupling problem is available for the case of several flat rigid foundations of arbitrary shape (Wong, 1977). This formulation is based on the representation

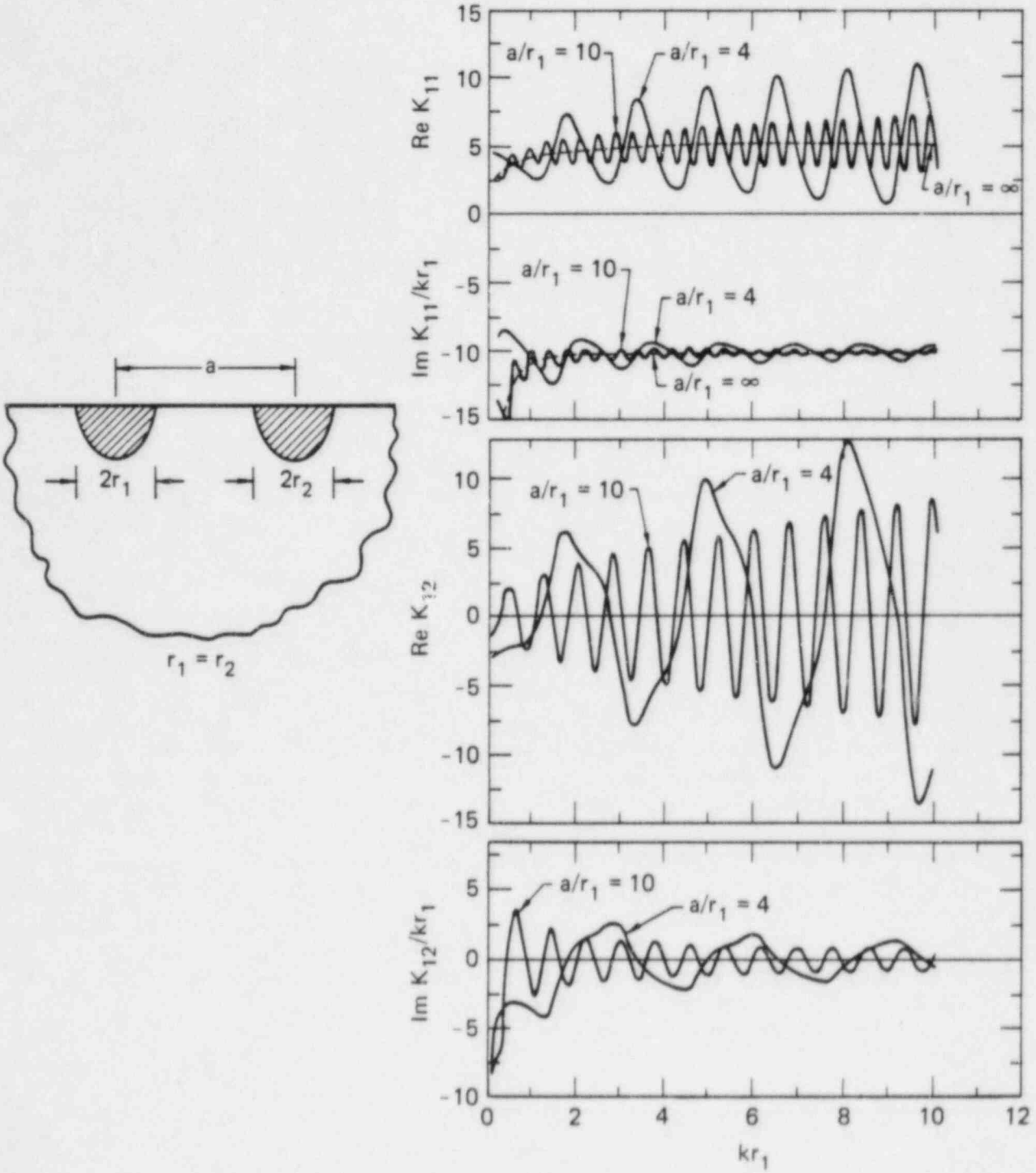

FIG. 8.1. Effect of through-the-soil coupling on the impedance functions (Luco and Contesse, 1973).

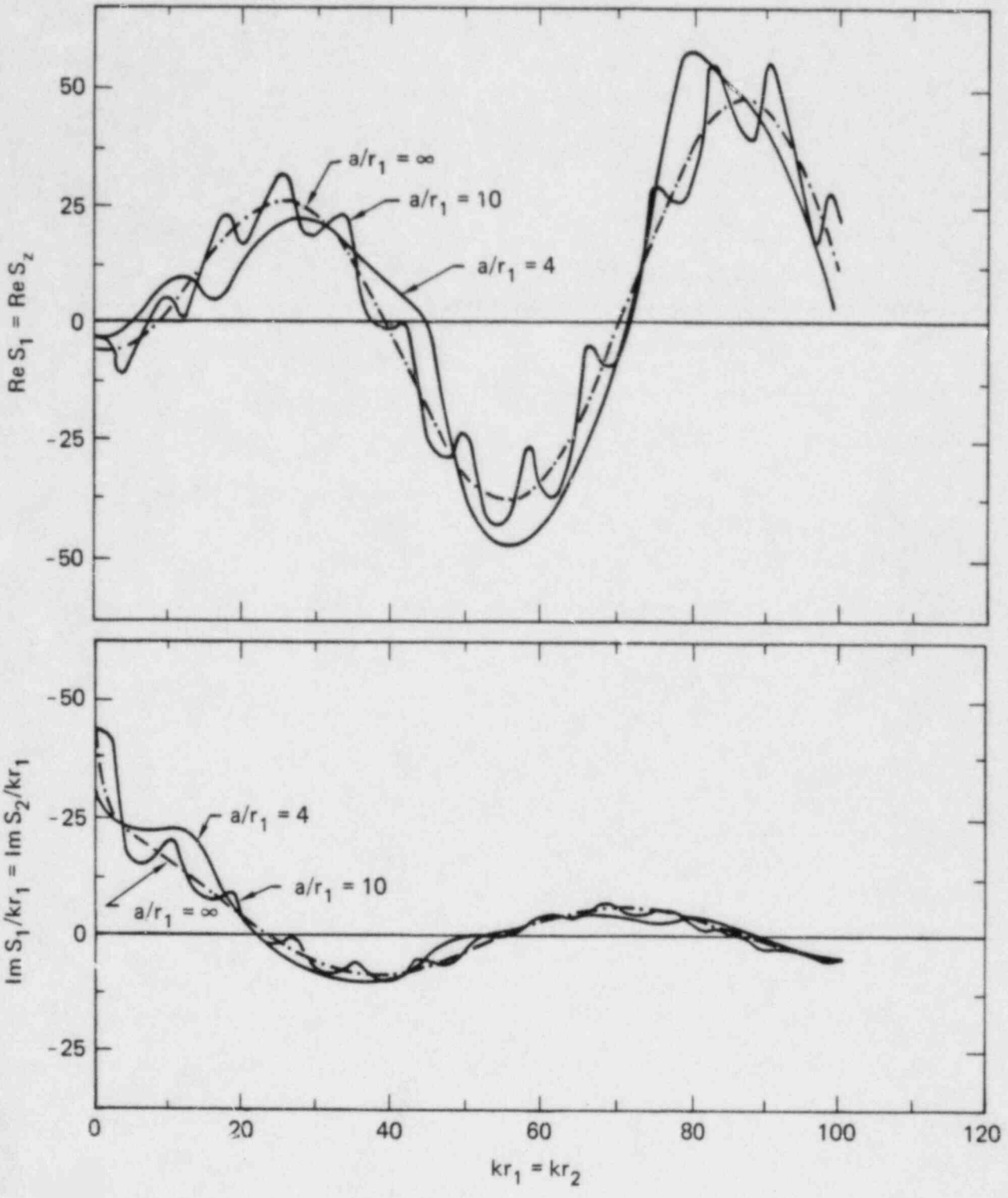

FIG. 8.2. Effect of through-the-soil coupling on the longitudinal driving force (Luco and Contesse, 1973).

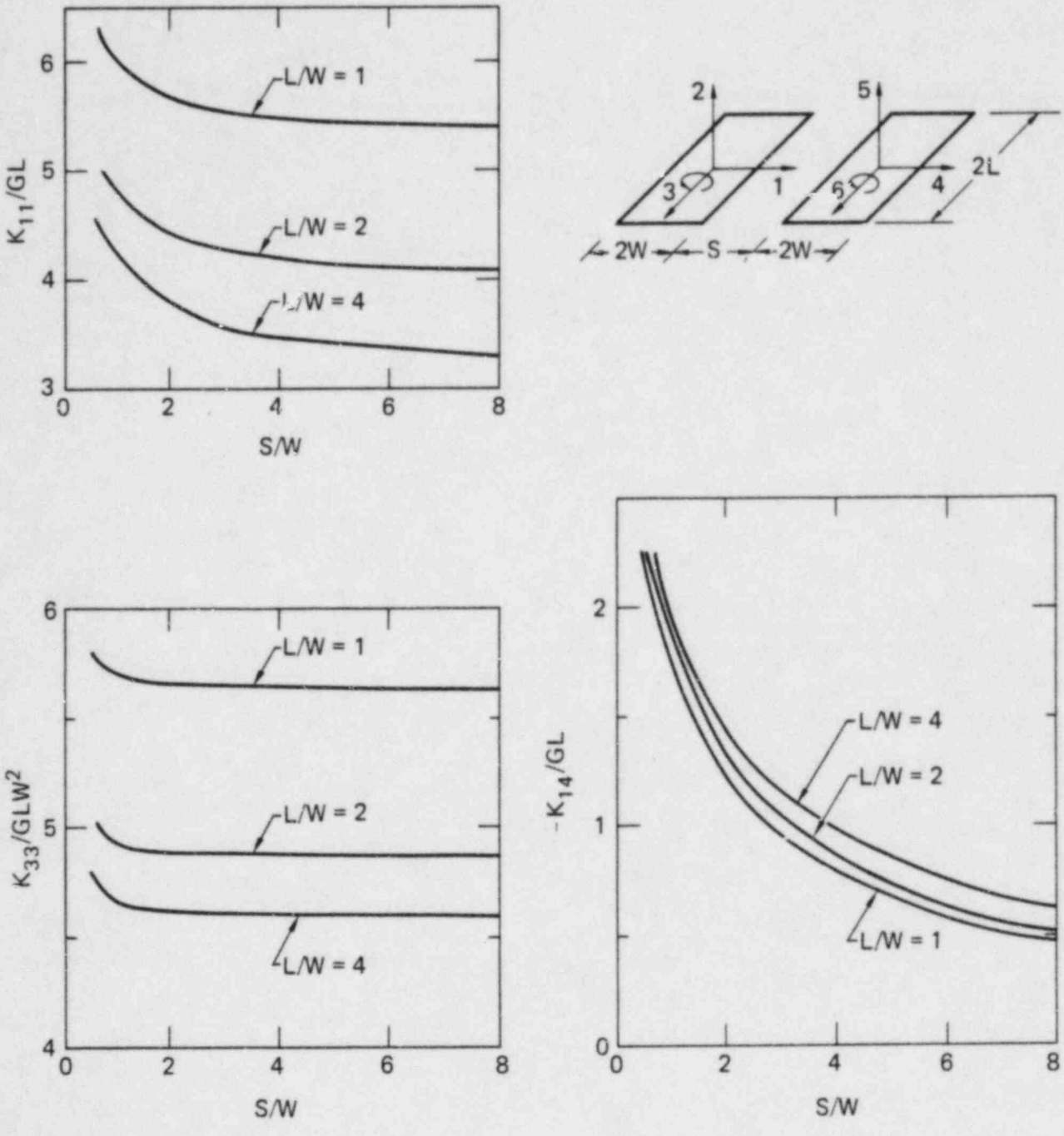

FIG. 8.3. Static stiffnesses for two parallel rectangular foundations (Hadjian, Luco and Wong, 1980).

$$\{U(\vec{x})\} = \sum_{j=1}^{N} \int_{S_j} [G(\vec{x}-\vec{\xi})]\{T_j(\vec{\xi})\}dS_j(\vec{\xi}) + \{U_g(\vec{x})\} \tag{8.6}$$

in which $\{U(\vec{x})\} = (U_x, U_y, U_z)^T$ represents the displacement vector at a point $\vec{x}$ on the soil surface, $\{T_j(\vec{\xi})\}$ the traction vector at a point $\vec{\xi}$ corresponding to the tractions that the jth foundation exerts on the soil, $[G(\vec{x}-\vec{\xi})]$ corresponds to the 3 × 3 matrix of Green's functions, S_j to the area of the jth foundation and $\{U_g(\vec{x})\}$ to the free-field motion on the ground surface.

Dividing each of the N foundations into smaller subregions and assuming that the tractions can be considered constant over each subregion leads to

$$\{\bar{U}_{ik}\} = \sum_{j=1}^{N} [G_{ij}^{kl}]\{R_{jl}\} + \{\bar{U}_{gik}\} \tag{8.7}$$

in which $\{\bar{U}_{ik}\}$ represents the average of the displacement vector over the kth subregion of the ith foundation and $\{\bar{U}_{gik}\}$ the corresponding average of the free-field motion. The vector $\{R_{jl}\}$ corresponds to the resultant of the traction vector over the lth subregion of the jth foundation. The matrix $[G_{ij}^{kl}]$ is defined by

$$[G_{ij}^{kl}] = \frac{1}{S_{ik}S_{jl}} \int_{S_{ik}} \int_{S_{jl}} [G(\vec{x}-\vec{\xi})]dS_{ik}(\vec{x})dS_{jl}(\vec{\xi}) \tag{8.8}$$

in which S_{ik} corresponds to the area of the kth subregion of the ith foundation.

In matrix notation, Eq. (8.7) can be written in the form

$$\begin{Bmatrix} \bar{U}_1 \\ \bar{U}_2 \\ \vdots \\ \bar{U}_N \end{Bmatrix} = \begin{bmatrix} G_{11} & G_{12} & \cdots \\ G_{21} & G_{22} & \cdots \\ \vdots & \vdots & G_{NN} \end{bmatrix} \begin{Bmatrix} R_1 \\ R_2 \\ \vdots \\ R_N \end{Bmatrix} + \begin{Bmatrix} \bar{U}_{g1} \\ \bar{U}_{g2} \\ \vdots \\ \bar{U}_{gN} \end{Bmatrix} \tag{8.9}$$

in which the vector $\{\bar{U}_i\}$ includes the average displacements over each of the subregions of the ith foundations and the vector $\{R_i\}$ includes the resultant forces over each of the subregions of the ith foundation. The vectors $\{\bar{U}_{gi}\}$ and the matrices $[G_{ij}]$ have similar definitions.

If each of the N foundations is assumed rigid, then,

$$\{\bar{U}_i\} = [\alpha_{ii}]\{U_{oi}\} \tag{8.10}$$

where $\{U_{oi}\}$ is the 6 × 1 vector of generalized displacements for the ith foundation and $[\alpha_{ii}]$ the matrix connecting the average motion of each subregion with each of the rigid-body degrees of freedom of the foundation. The vector of generalized forces $\{F_{Si}\}$ that the ith foundation exerts on the soil is given by

$$\{F_{Si}\} = [\alpha_{ii}]^T\{R_i\} \tag{8.11}$$

The force-displacement relationship for the N foundations can be obtained from Eqs. (8.9), (8.10) and (8.11). The resulting expression is

$$\{F_S\} = [K]\{U_o\} - \{F_S^*\} \tag{8.12}$$

where

$$\{F_S\} = (\{F_{S1}\}^T, \{F_{S2}\}^T, \ldots, \{F_{SN}\}^T)^T \tag{8.13}$$

$$\{U_o\} = (\{U_{o1}\}^T, \{U_{o2}\}^T, \ldots, \{U_{oN}\}^T)^T \tag{8.14}$$

$$[K] = [\alpha]^T[G]^{-1}[\alpha] \tag{8.15}$$

and

$$\{F_S^*\} = [\alpha]^T[G]^{-1}\{\bar{U}_g\} \tag{8.16}$$

The matrix $[\alpha]$ appearing in Eqs. (8.15) and (8.16) is block diagonal with blocks defined by $[\alpha_{ij}]$. The matrix [G] corresponds to the matrix of Green's functions appearing in Eq. (8.9) and the vector $\{\bar{U}_g\}$ is defined by

$$\{\bar{U}_g\} = (\{\bar{U}_{g1}\}^T, \{\bar{U}_{g2}\}^T, \ldots, \{\bar{U}_{gN}\}^T)^T \tag{8.17}$$

Once the impedance matrix [K] and the driving force vector $\{F_S^*\}$ have been calculated, the compliance matrix [C] and the foundation input motion vector $\{U_o^*\}$ are obtained from

$$[C] = [K]^{-1} \tag{8.18}$$

and

$$\{U_o^*\} = [C]\{F_S^*\} \tag{8.19}$$

The solution of the interaction problem for several structures including the effects of coupling through the soil is then obtained by use of Eq. (8.1). An alternative, which avoids the calculation of [C] and $\{U_o^*\}$, is to write Eq. (8.1) in the form

$$\{U_o\} = ([K] - \omega^2([M_o] + [M_b]))^{-1}\{F_S^*\} \tag{8.20}$$

which involves the impedance matrix [K] and the driving force vector $\{F_S^*\}$.

When the number of foundations is large, the order of the matrix [G] appearing in Eqs. (8.15) and (8.16) can be large and the required inversion of this matrix for each frequency can become costly. This is particularly true at high frequencies when each foundation has to be divided into a large number of subregions. To avoid this problem Wong (refer to Werner et al., 1977) has proposed an approximate procedure based on the observation that the diagonal blocks of the compliance matrix are only slightly affected by the presence of adjacent foundations. To derive this approximation it is convenient to write the matrix [G] in the form

$$[G] = [G_o]([I] + [A][G_o]) \tag{8.21}$$

in which $[G_o]$ is the block diagonal matrix defined by

$$[G_o] = \begin{bmatrix} G_{11} & 0 & 0 & 0 \\ 0 & G_{22} & 0 & 0 \\ & & & \\ 0 & 0 & 0 & G_{NN} \end{bmatrix} \tag{8.22}$$

and

$$[A] = \begin{bmatrix} 0 & G_{11}^{-1}G_{12}G_{22}^{-1} & G_{11}^{-1}G_{13}C_{33}^{-1} & \\ G_{22}^{-1}G_{21}G_{11}^{-1} & 0 & G_{22}^{-1}G_{23}G_{33}^{-1} & \\ G_{33}^{-1}G_{31}G_{11}^{-1} & G_{33}^{-1}G_{32}G_{22}^{-1} & 0 & \\ & & & \end{bmatrix} \tag{8.23}$$

From Eq. (8.21),

$$[G]^{-1} = ([I] + [A][G_o])^{-1}[G_o]^{-1}. \tag{8.24}$$

Expanding the inverse of the first matrix appearing on the right hand side of Eq. (8.24) and keeping the first two terms leads to

$$[G]^{-1} \cong [G_o]^{-1} - [A] \tag{8.25}$$

By use of Eqs. (8.15), (8.16) and (8.25) the following approximations for [K] and $\{F_S^*\}$ are obtained:

$$[K] \cong [K_o] - [\alpha]^T[A][\alpha] \tag{8.26}$$

$$\{F_S^*\} \cong \{F_{So}^*\} - [\alpha]^T[A]\{\bar{U}_g\} \tag{8.27}$$

in which

$$[K_o] = [\alpha]^T[G_o]^{-1}[\alpha] \tag{8.28}$$

is a block diagonal matrix having for blocks the impedance matrices for each foundation when isolated. The vector $\{F_{So}^*\}$ is given by

$$\{F_{So}^*\} = [\alpha]^T[G_o]^{-1}\{\bar{U}_g\} \tag{8.29}$$

and corresponds to the driving forces when each foundation is isolated from the others. It is interesting to observe that in the approximation to [K] given by Eq. (8.26) the diagonal blocks correspond to the impedance matrices for isolated foundations.

To obtain an approximation to the compliance matrix Eq. (8.26) is written in the form

$$[K] = [K_o]([I]) - [C_o][\alpha]^T[A][\alpha]) \tag{8.30}$$

where $[C_o]$ is the block diagonal matrix

$$[C_o] = [K_o]^{-1} \tag{8.31}$$

having for diagonal blocks the compliance matrices for the foundations when isolated. Following the same procedure used to obtain Eq. (8.31) from Eq. (8.30), the following approximation for [C] is obtained:

$$[C] \cong [C_o] + [C_o][a]^T[A][a][C_o] . \tag{8.32}$$

According to this approximation the submatrices of [C] are given by

$$[C_{ii}] \cong ([a_{ii}]^T[G_{ii}]^{-1}[a_{ii}])^{-1} \tag{8.33}$$

$$[C_{ij}] \cong ([C_{ii}]^T[a_{ii}]^T[G_{ii}]^{-1})[G_{ij}]([G_{jj}]^{-1}[a_{jj}][C_{jj}]) \quad (i \neq j). \tag{8.34}$$

indicating that the diagonal submatrices correspond to the compliance matrices for each foundation when isolated from the others.

An approximation to the foundation input motion vector $\{U_o^*\}$ can be obtained by use of Eqs. (8.19), (8.28) and (8.32). Neglecting higher order terms the approximation is

$$\{U_o^*\} = \{U_{oo}^*\} - [C_o][a]^T[A]\{\bar{U}_g\} \tag{8.35}$$

in which

$$\{U_{oo}^*\} = ([a]^T[G_o]^{-1}[a])^{-1}[a]^T[G_o]^{-1}\{\bar{U}_g\} \tag{8.36}$$

corresponds to the foundation input motion for the foundations when isolated. The subvectors of $\{U_o^*\}$ are given by

$$\{U_{oi}^*\} = \{U_{ooi}^*\} - \sum_{\substack{j=1 \\ j \neq i}}^{N} [C_{ii}][a_{ii}]^T[G_{ii}]^{-1}[G_{ij}][G_{jj}]^{-1}\{\bar{U}_{gj}\} \tag{8.37}$$

in which

$$\{U_{ooi}^*\} = [C_{ii}][a_{ii}]^T[G_{ii}]^{-1}\{\bar{U}_{gi}\} \tag{8.38}$$

corresponds to the foundation input motion for the ith foundation when isolated.

The approximation described above has been utilized to develop a computer program (CLASSI) for the analysis of the response of foundations and structures including the through-the-soil coupling effects.

The problem of evaluating the interaction through the soil between three-dimensional embedded foundations can be solved by extending the general techniques, described in Chapter 6, to calculate the response of isolated embedded foundations. Although the extension of these techniques to the case of several foundations is simple, the resulting computer programs would be complex and costly.

In the case of several embedded foundations an approximation to the compliance matrix and the foundation input motion can be obtained by using Eqs. (8.32) and (8.35) after replacing $[C_o]$ and $\{U_{oo}^*\}$ by the compliance matrices and foundation input motions for the embedded foundations when isolated. In this approximation, the matrix [A] would be the same as in the case in which the foundations are flat. This procedure would preserve the interaction between each embedded foundation and the soil (which is the main effect) and would approximate the coupling through the soil.

REFERENCES (8)

Hadjian, A. H. , J. E. Luco and H. L. Wong (1980). On the Reduction of Three-Dimensional Soil-Structure Interaction Problems to Two-Dimensional Models. (in preparation).

Lee, T. H. and D. A. Wesley (1973a). Soil-Structure Interaction of Nuclear Reactor Structures Considering Through-Soil Coupling between Adjacent Structures, *Nuclear Engineering and Design, 24,* 3, 374-387.

Lee, T. H. and D. A. Wesley (1973b). Influence of Through-Soil Coupling Between Adjacent Structures on Seismic Response of Nuclear Reactors, *Proc. 2nd International Conf. on Structural Mechanics in Reactor Technology,* Berlin, Paper K 2/9.

Liang, V. C. (1974). *Dynamic Response of Structures in Layered Soils,* Report 1274-10, Dept. of Civil Engineering, Massachusetts Institute of Technology, Cambridge, Mass.

Luco, J. E. and L. Contesse (1973). Dynamic Structure-Soil-Structure Interaction, *Bull. Seism. Soc. Am., 63,* 4, 1289-1303.

Lysmer, J. T., T. Udaka, H. B. Seed and R. Hwang (1974). *A Computer Program for Complex Response Analysis of Soil-Structure Interaction,* Report EERC 74-4, Earthquake Engineering Research Center, University of California, Berkeley.

MacCalden, P. B. (1969). *Transmission of Steady-State Vibrations between Circular Footings,* Ph.D. Dissertation, School of Engineering and Applied Science, University of California, Los Angeles.

Murakami, H. and J. E. Luco (1977). Seismic Response of a Periodic Array of Structures, *J. of the Engrg. Mech. Div., ASCE, 103,* EM5, 965-977.

Warburton, G. B., J. D. Richardson and J. J. Webster (1971). Forced Vibrations of Two Masses on an Elastic Half-Space, *J. Appl. Mech., ASME, 38,* 148-156.

Werner, S. D., L. C. Lee, H. L. Wong, and M. D. Trifunac (1977). *An Evaluation of the Effects of Traveling Seismic Waves on the Three-Dimensional Response of Structures,* Report R-7720-4514, Agbabian Associates, El Segundo, California, October.

Wong, H. L. (1975), *Dynamic Soil-Structure Interaction,* Report EERL-75-01, Earthquake Engineering Research Lab., California Institute of Technology, Pasadena, California, May.

Wong, H. L. (1977), The Coupled Translations ad Rotations caused by the Weight Distribution of Nearby Buildings, *Proc. Symp. on Applications of Computer Methods in Engineering,* University of Southern California, Los Angeles, August.

Wong H. L. and M. D. Trifunac (1975). Two Dimensional, Antiplane, Building-Soil-Building Interaction for Two or More Buildings and for Incident Plane SH-Waves, *Bull. Seism. Soc. Am., 65,* 6, 1863-1885.

9. FLEXIBLE FOUNDATIONS

The formulation of the soil-structure interaction problem presented in Chapter 2 is based on the assumption of a rigid foundation. The modifications of the formulation for the case of flexible foundations are discussed here. Although, in general, the foundation by itself cannot be considered to be rigid, it is true in many cases that the stiffening effect of the superstructure prevents any significant deformation of the foundation. In these cases, the assumption of a rigid foundation leads to sufficiently accurate results for all practical purposes. For more flexible superstructures the stiffening effect on the foundation is not as important and the flexibility of the foundations needs to be considered. In general, out-of-plane deformations of the foundation may be more important than in-plane deformations.

An illustration of the flexibility of the foundation is provided by the experimental results obtained by Foutch et al. (1975) for the Millikan Library building. The Millikan Library is a nine-story reinforced concrete building in which lateral loads in the NS direction are resisted by 12-in. reinforced concrete shear walls located on the east and west ends of the building while most of the lateral loads in the EW direction are resisted by a central core. The foundation system of the library consists of a central pad 32 ft. long and 4 ft. wide which runs in the EW direction (Fig. 9.1). Also provided are foundation beams 10 ft. wide by 2 ft. deep which run EW beneath the row of columns at the north and south ends of the building. These beams are connected to the central pad by stepped beams. The contact between the central pad and the underlying soil is approximately 23 ft. below the first-floor level and 18 ft. below grade. The plan dimensions of the foundation are 76.5 × 82.5 ft. with additional areas at the east and west extremes. The foundation rests on alluvium composed of medium to dense sands mixed with gravel. The shear wave velocity at foundation depth is 1250 ft/sec. In an experiment performed in 1974 the Millikan Library building was forced into resonance by a vibration generator located on the roof and the three-dimensional motion at 51 locations on each of four floors, the basement slab and the roof were recorded for shaking in both the NS and EW directions (Foutch et al., 1975). Amplified views of the patterns of deformation of the basement slab for excitation in the NS and EW directions are shown in Fig. (9.2). For vibrations in the NS direction, the stiff shear walls on the east and west ends of the building cause an almost rigid translation of the basement slab together with an almost uniform rotation about the EW axis of symmetry. Some deviations from this average rigid-body motion may be observed at the location of the central core and at the north and south ends of the slab. In this case, the deformation of the basement slab resembles that of a flexible rectangular plate with two rigid edges vibrating on top of an elastic medium. For vibrations in the EW direction, the central core induces large localized deformation of the basement slab. It is apparent that the flexibility of the foundation needs to be considered to properly model the response of the structure in the EW direction.

For the purpose of the discussion it is convenient to consider three types of flexible foundations. The first type corresponds to what may be called flexible-rigid foundations in which the contact region between the foundation and the load-carrying elements of the superstructure can be considered to be rigid. The second type corresponds to foundation systems consisting of several footings interconnected by foundation beams. The last type corresponds to fully flexible continuous foundations. The methods of analysis for these types of foundations are discussed below.

An example of flexible-rigid foundations is provided by the foundation of the Millikan Library building. In this case and for vibrations in the NS direction, the contact between the east and west shear walls and the foundation can be assumed to be rigid as shown in Fig. 9.2a. For vibrations in the EW direction the contact region between the central core (which carries most of the lateral loads in the EW direction) and the foundation can be considered rigid as shown in Fig. 9.2b. In these two cases the rest of the foundation is clearly flexible.

If the rigid portion of the foundation is connected then only six degrees of freedom are needed to describe its motion. If, in addition, the motion of the superstructure is controlled by the motion of the rigid portion of the foundation, then the formulation of the soil-structure interaction problem presented in

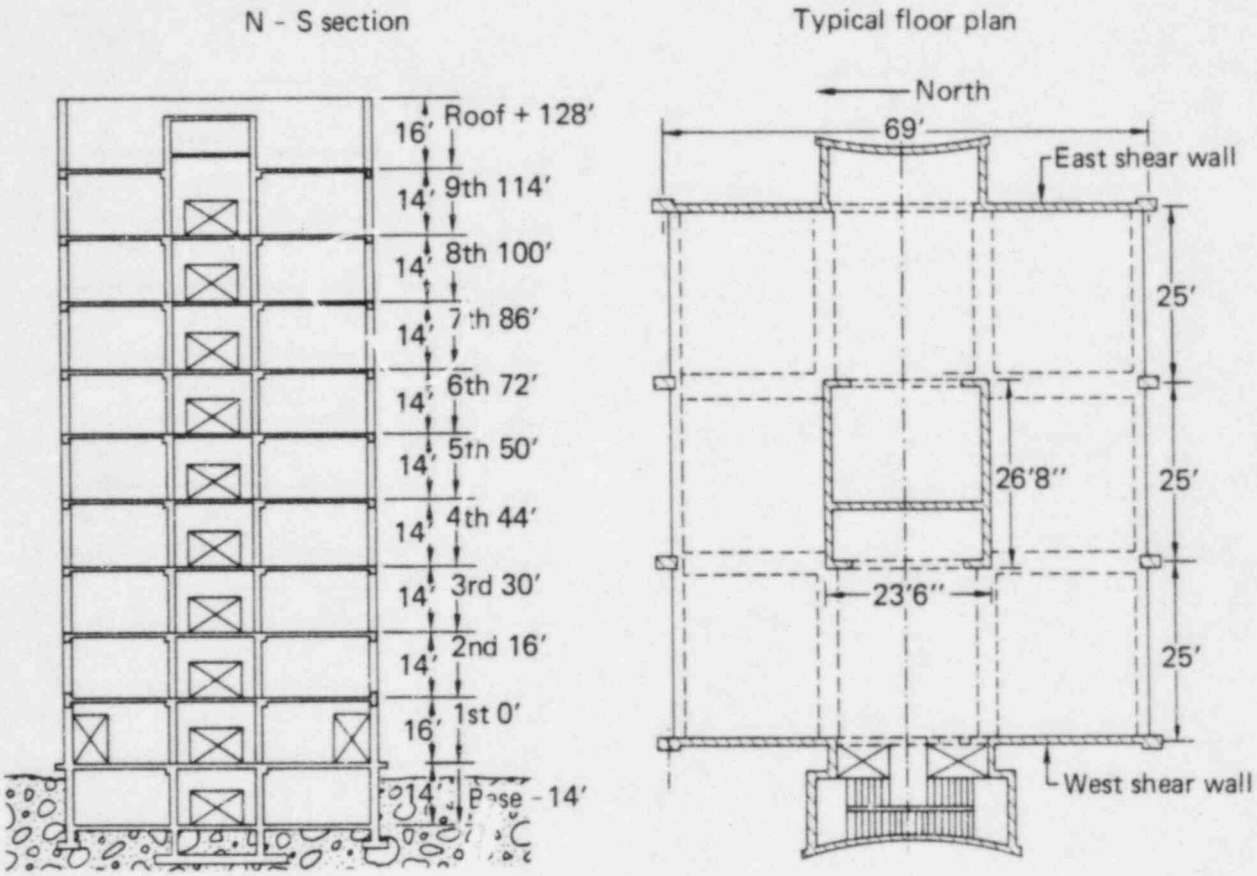

FIG. 9.1. Description of the Millikan Library building.

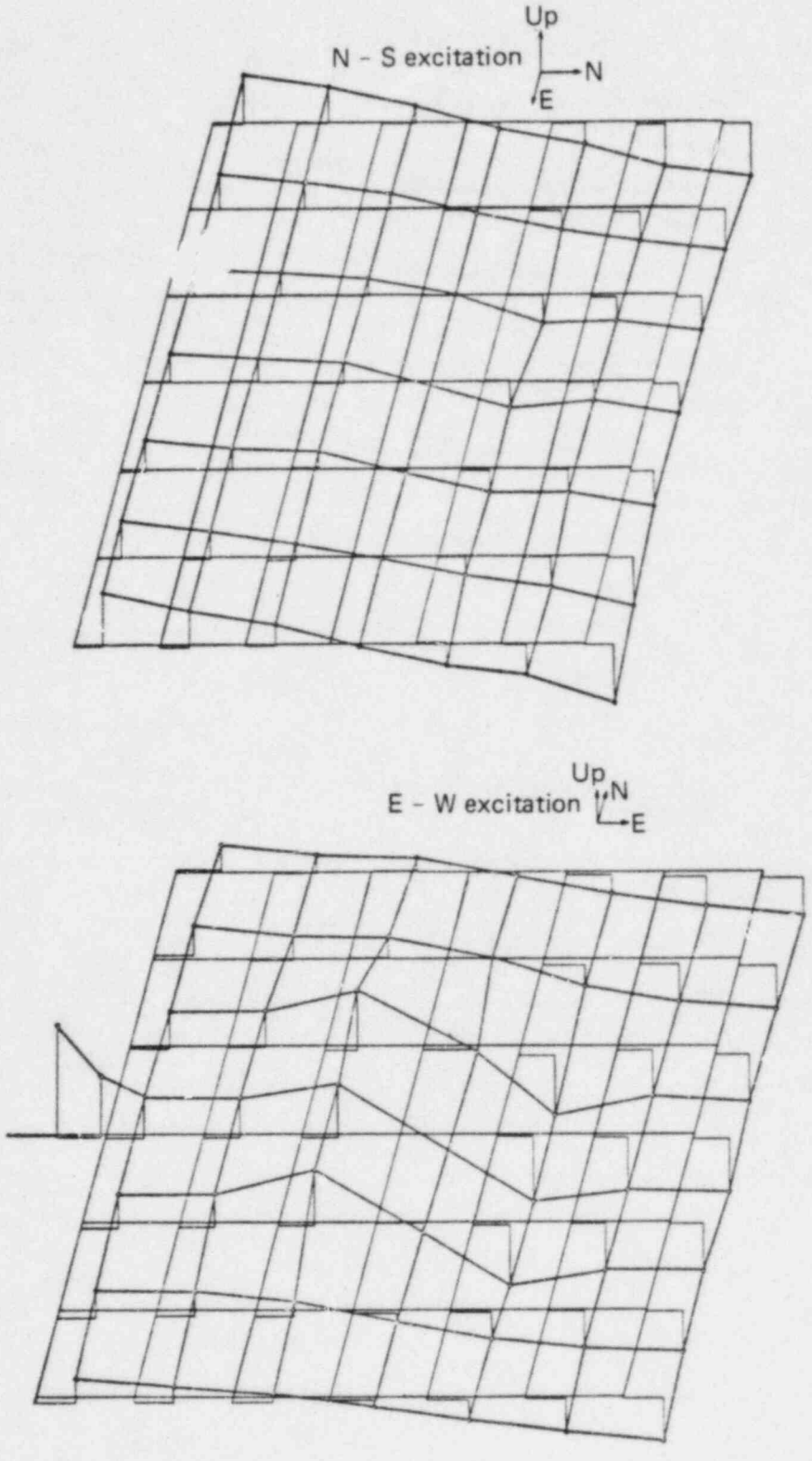

FIG. 9.2. Deformation patterns of the basement slab of the Millikan Library building (Foutch et al., 1975).

Chapter 2 and, in particular, Eq. (2.7) remain valid. In this case the compliance matrix relates the generalized forces and displacements of the rigid portion of the foundation while the foundation input motion vector represents the motion of the rigid portion of the foundation when subjected to seismic excitation in absence of external forces. The equivalent mass matrix for the superstructure $[M_b(\omega)]$ relates in this case the generalized forces that the superstructure exerts on the rigid portion of the foundation with the generalized motion of this portion of the foundation.

For flexible-rigid foundations the compliance and impedance matrices as well as the foundation input motion depend on the flexibility of the deformable portion of the foundation. An example of this effect is provided by the results obtained by Iguchi and Luco (1980) for the two models of flexible-rigid foundations shown in Fig. 9.3. Both models correspond to a square flexible plate of thickness t_f, Young's modulus E and plan dimension $2a \times 2a$. In model (a) the perimeter of the foundation is assumed rigid, while in model (b) the plate has a rigid central zone of dimensions $a \times a$. The effects of the flexibility of the foundation plate on the vertical and rocking impedance functions are illustrated in Figs. 9.4 and 9.5, respectively. In these figures, the normalized stiffness coefficients are shown on the left while the normalized damping coefficients are shown on the right. Results are presented for different values of the relative stiffness δ defined by

$$\delta = Et_f^3/[\mu a^3(1 - \nu_f^2)] \tag{9.1}$$

where μ is the shear modulus for the soil and ν_f corresponds to the Poisson's ratio for the plate. The results presented indicate that, at low frequencies, the dynamic stiffness coefficients ($_eK_V$, $_eK_M$) for a flexible-rigid foundation plate can be significantly lower than those for a rigid plate. At high frequencies, however, the dynamic stiffness coefficients for flexible-rigid foundations can be higher than those for a rigid plate. For model (a), the effects of flexibility of the foundation plate on the vertical and rocking stiffness coefficients are similar. For model (b), the effects on the rocking stiffness coefficients are more pronounced.

Perhaps the most significant effect shown in Figs. 9.4 and 9.5 corresponds to the reduction of the damping coefficients ($_eC_V$, $_eC_M$). It is apparent that flexible foundation plates are less efficient than rigid foundations in radiating energy into the ground. For model (a) the reduction of the vertical damping coefficient is more pronounced while for model (b) the reduction of the rocking damping coefficient is more significant.

The study of the dynamic response of flexible or flexible-rigid foundations has received less attention than that of rigid foundations. Several authors, however, studied various cases and some information is readily available [Oien (1973), Iguchi (1976, 1978), Lin (1978), Matsui and Seya (1978), Savidis and Richter (1979), Iguchi and Luco (1980)].

One method to determine the response of flat flexible-rigid foundations is based on discretizing the flexible foundation plate and the contact region between the foundation plate and the soil by subdivision into a number of rectangular subregions (Iguchi and Luco, 1980). Neglecting the inertia of the flexible plate it is possible to write

$$\left[\begin{array}{c|c} K_{11}^f & K_{12}^f \\ \hline K_{21}^f & K_{22}^f \end{array}\right] \left\{\begin{array}{c} U_1 \\ \hline U_2 \end{array}\right\} = \left\{\begin{array}{c} P_1 \\ \hline P_2 \end{array}\right\} - \left\{\begin{array}{c} R_1 \\ \hline 0 \end{array}\right\} \tag{9.2}$$

where U_1 and P_1 represent the vectors of vertical components of the nodal displacements and nodal external forces, respectively. The vectors U_2 and P_2 include the remaining components of the nodal displacements and nodal external forces, respectively. The vector R_1 corresponds to the nodal forces (assumed vertical) that the soil exerts on the foundation. The stiffness matrix for the plate $[K^f]$ may be obtained by a finite element representation.

Referring to the soil, the average vertical displacement over each subregion can be written in the form (Wong and Luco, 1978)

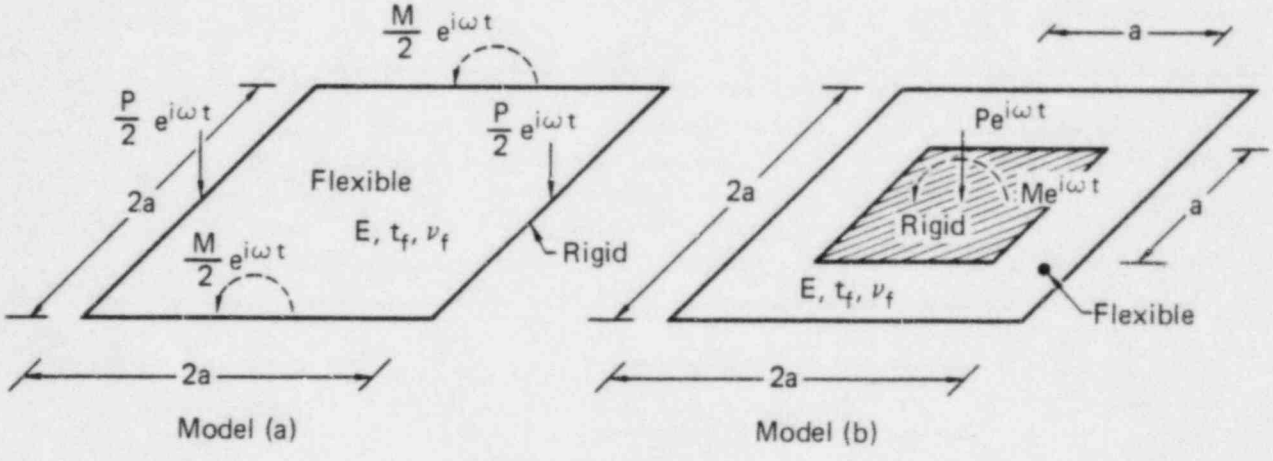

FIG. 9.3. Models of flexible foundations resting on a homogeneous elastic soil. Model (a): Flexible plate with a rigid perimeter. Model (b): Flexible plate with a rigid central region.

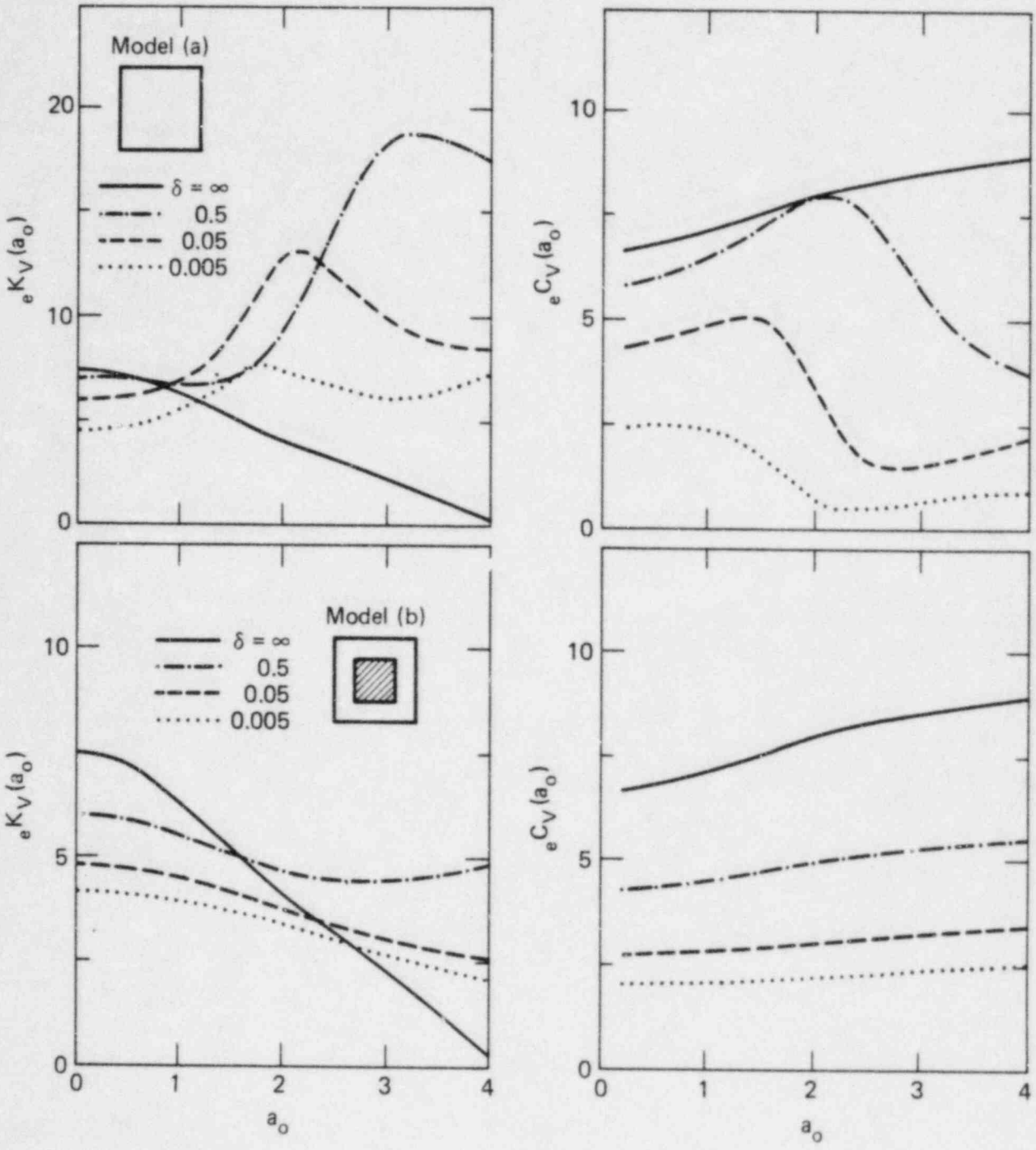

FIG. 9.4. Effects of flexibility of the foundations on the vertical impedance functions ($\nu = 0.4$, $\nu_f = 0.$) (Iguchi and Luco, 1380).

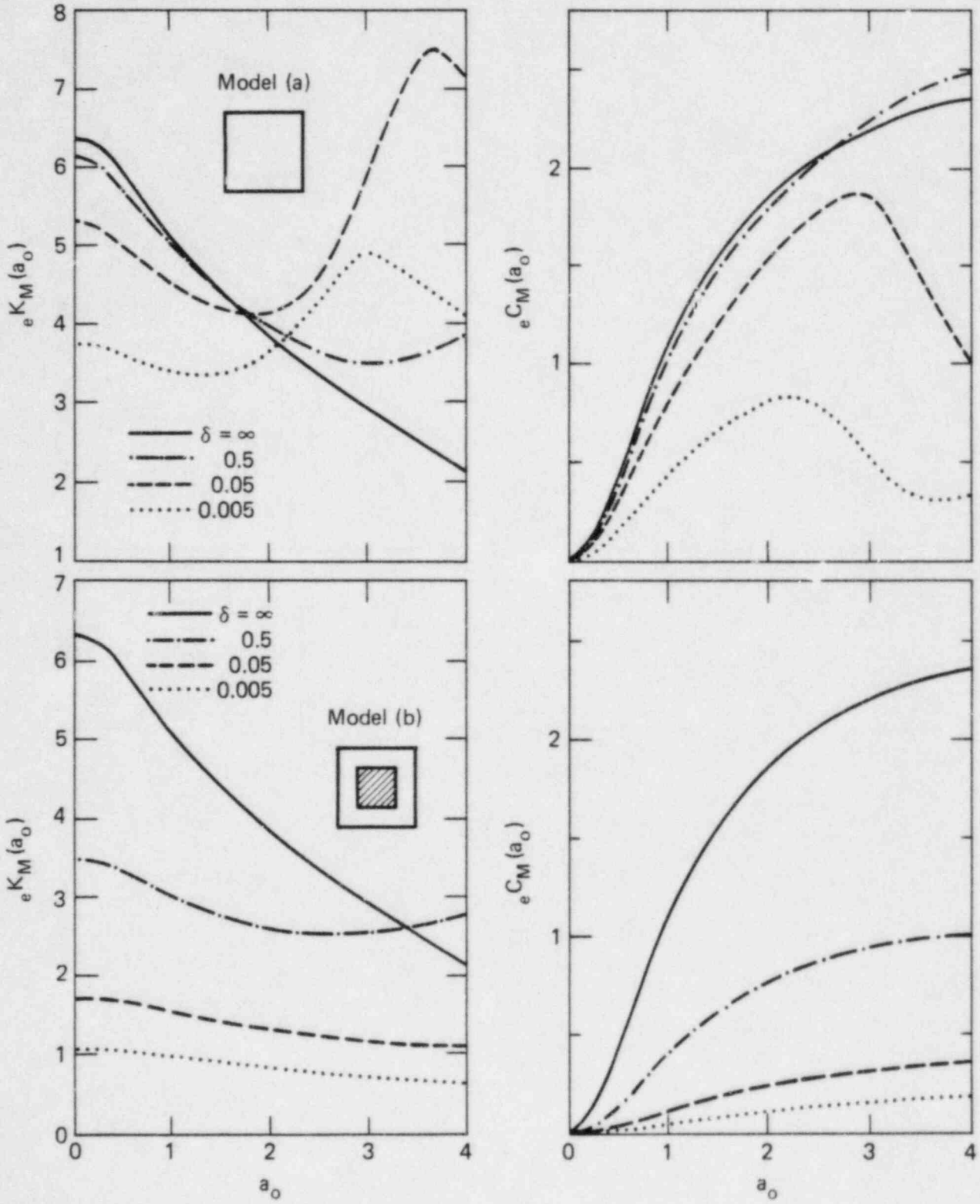

FIG. 9.5. Effects of flexibility of the foundations on the rocking impedance functions ($\nu = 0.4$, $\nu_f = 0.$) (Iguchi and Luco, 1980).

$$\bar{U}_1 = A_g \bar{R}_1 + \bar{U}_g \tag{9.3}$$

where $\bar{U}_1$ represents the vector of average vertical displacements over each subregion, $\bar{R}_1$ the vector of resultant vertical forces (over each subregion) that the foundation exerts on the soil and $\bar{U}_g$ represents the averages of the vertical components of the free-field motion over each subregion. The matrix A_g corresponds to the dynamic flexibility matrix for the soil.

As a first approximation the average displacement over each subregion $\bar{U}_1$ can be represented as a mean of the nodal displacements U_1. Similarly, the resultant force $\bar{R}_1$ over each subregion can be partitioned into four equal nodal forces R_1. In this case, it is possible to write

$$\bar{U}_1 = T U_1 \quad , \quad R_1 = T^T \bar{R}_1 \tag{9.4}$$

in which T represents an averaging matrix. From Eqs. (9.3) and (9.4) it is found that

$$R_1 = K_g U_1 - R_g^* \tag{9.5}$$

where

$$K_g = T^T A_g^{-1} T \quad , \quad R_g^* = T^T A_g^{-1} \bar{U}_g \tag{9.6}$$

The matrix K_g corresponds to the dynamic stiffness matrix for the soil.

Substitution from Eq. (9.6) into Eq. (9.2) leads to

$$\left[\begin{array}{c|c} K_{11}^f + K_g & K_{12}^f \\ \hline K_{21}^f & K_{22}^f \end{array}\right] \left\{\begin{array}{c} U_1 \\ \hline U_2 \end{array}\right\} = \left\{\begin{array}{c} P_1 \\ \hline P_2 \end{array}\right\} + \left\{\begin{array}{c} R_g^* \\ \hline 0 \end{array}\right\} \tag{9.7}$$

from where the response of the foundation to external forces and seismic waves can be easily obtained. For flexible-rigid foundations it is assumed that the external forces are applied on the rigid portion of the foundation. In this case, the six components of motion of the rigid portion define the compliance matrix and the foundation input motion to be used in conjunction with Eq. (2.7).

In the case of foundation systems consisting of several rigid footings the total response of the footings can be described by the (6N × 1) vector $\{U_o\}$. This displacement vector has six components (corresponding to the six degrees of freedom) for each of the N rigid footings. Considering the motion of the soil in contact with the footings it is possible to write

$$\{U_o\} = [C(\omega)]\{F_S\} + \{U_o^*\} \tag{9.8}$$

in which $[C(\omega)]$ is the (6N × 6N) compliance matrix, $\{F_S\}$ is the (6N × 1) vector of generalized forces that the footings exert on the soil and $\{U_o^*\}$ is the (6N × 1) foundation input motion vector. The compliance matrix $[C(\omega)]$ and the foundation input motion vector $\{U_o^*\}$ for N rigid footings are calculated as described in Chapter 8. To solve the interaction problem it is necessary to express $\{F_S\}$ in terms of $\{U_o\}$ and of the properties of the superstructure.

The equations of motion for the superstructure-foundation system can be written in the form

$$\left(-\omega^2 \left[\begin{array}{c|c} M_{bb} & 0 \\ \hline 0 & M_o \end{array}\right] + i\omega \left[\begin{array}{c|c} C_{bb} & C_{bo} \\ \hline C_{ob} & C_{oo} \end{array}\right] + \left[\begin{array}{c|c} K_{bb} & K_{bo} \\ \hline K_{ob} & K_{oo} \end{array}\right]\right) \left\{\begin{array}{c} U_b \\ \hline U_o \end{array}\right\} = \left\{\begin{array}{c} 0 \\ \hline -F_S \end{array}\right\} \tag{9.9}$$

where $\{U_b\}$ represents the generalized displacements for the superstructure while $\{U_o\}$ corresponds to the generalized displacement of the footings.

Eliminating $\{U_b\}$ from Eq. (9.9) leads to

$$\{F_S\} = -[K_b(\omega)]\{U_o\} + \omega^2([M_o] + [M_b(\omega)]\{U_o\} \tag{9.10}$$

in which

$$[K_b(\omega)] = ([K_{oo}] + i\omega[C_{oo}]) - ([K_{ob}] + i\omega[C_{ob}])([K_{bb}] + i\omega[C_{bb}])^{-1}([K_{bo}] + i\omega[C_{bo}]) \tag{9.11}$$

and

$$[M_b(\omega)] = ([K_{ob}] + i\omega[C_{ob}])(-\omega^2[M_{bb}] + i\omega[C_{bb}] + [K_{bb}])^{-1}[M_{bb}]$$
$$([K_{bb}] + i\omega[C_{bb}])^{-1}([K_{bo}] + i\omega[C_{bo}]) \tag{9.12}$$

The frequency-dependent matrix $[M_b(\omega)]$ can be thought of as an equivalent mass matrix. This matrix is zero if the superstructure is massless. The matrix $[K_b(\omega)]$ corresponds to an equivalent stiffness matrix. In the static case, $[K_b(0)]$ corresponds to the stiffness matrix for the foundation degrees of freedom when the superstructure is free to move.

From Eqs. (9.8) and (9.10) it is found that the solution of the interaction problem is given by

$$\{U_o\} = ([I] + [C(\omega)][K_b(\omega)] - \omega^2[C(\omega)]([M_o] + [M_b(\omega)]))^{-1}\{U_o^*\} \tag{9.13}$$

where $[I]$ is the $6N \times 6N$ identity matrix. Once the generalized displacements of the footings have been obtained from Eq. (9.13) the response of the superstructure can be obtained by use of Eq. (9.9).

The calculation of the matrices $[M_b(\omega)]$ and $[K_b(\omega)]$ can be simplified by use of the fixed-base modes of vibration of the superstructure. Let $[\Phi]$ be the modal matrix for the superstructure on a fixed-base. The modal matrix $[\Phi]$ is such that

$$-[M_{bb}][\Phi][\omega_r^2] + [K_{bb}][\Phi] = 0 \tag{9.14}$$

and

$$[\Phi]^T[M_{bb}][\Phi] = [I] \tag{9.15}$$

in which ω_r $(r = 1,2,\ldots)$ are the fixed-base natural frequencies of the superstructure. After some algebra, it can be shown that

$$[K_b(\omega)] = ([K_{oo}] + i\omega[C_{oo}]) - ([\Gamma_1] + i\omega[\Gamma_2])^T[D_1(\omega)]([\Gamma_1] + i\omega[\Gamma_2]) \tag{9.16}$$

and

$$[M_b(\omega)] = ([\Gamma_1] + i\omega[\Gamma_2])^T[D_2(\omega)]([\Gamma_1] + i\omega[\Gamma_2]) \tag{9.17}$$

where $[\Gamma_1]$ and $[\Gamma_2]$ are the matrices defined by

$$[\Gamma_1] = [\Phi]^T[K_{bo}] \tag{9.18}$$

$$[\Gamma_2] = [\Phi]^T[C_{bo}] \tag{9.19}$$

The matrices $[D_1(\omega)]$ and $[D_2(\omega)]$ correspond to the diagonal matrices having for elements

$$D_{1r}(\omega) = (\omega_r^2 + 2i\xi_r\omega\omega_r)^{-1} \tag{9.20}$$

$$D_{2r}(\omega) = (\omega_r^2 - \omega^2 + 2i\xi_r\omega\omega_r)^{-1}(\omega_r^2 + 2i\xi_r\omega\omega_r)^{-1} \tag{9.21}$$

in which ξ_r denotes the rth modal damping ratio.

The generalized displacement for the superstructure can be written in the form

$$\{U_b\} = -[\Phi][D_1(\omega)]([\Gamma_1] + i\omega[\Gamma_2])\{U_o\} - \omega^2[\Phi][D_2(\omega)]([\Gamma_1] + i\omega[\Gamma_2])\{U_o\} \tag{9.22}$$

from which the response of the superstructure can be calculated once $\{U_o\}$ is known.

The procedure described above is similar to the method employed by Werner, Lee, Wong and Trifunac (1977) to analyze the response of a single span bridge supported on two rigid foundations.

As indicated by Eq. (9.13) the key elements entering into the solution of the interaction problem for a structure supported on several footings are the compliance matrix $[C(\omega)]$ and the foundation input motion $\{U_o^*\}$. The other elements can be obtained by conventional structural analysis. As mentioned in Chapter 8, a method and the associated computer programs (CLASSI) has been developed to generate the compliance matrix and the foundation input motion for several surface footings interacting through the soil modeled as a layered viscoelastic half-space.

Finally, it remains to discuss the case of fully flexible foundations. In this case Eq. (9.13) remains valid but for its use it is convenient to rewrite it in the form

$$\{U_c\} = ([K_g(\omega)] + [K_b(\omega)] - \omega^2([M_o] + [M_b(\omega)]))^{-1}\{F_o^*\} \tag{9.23}$$

where

$$[K_g(\omega)] = [C(\omega)]^{-1} \tag{9.24}$$

and

$$\{F_o^*\} = [K_g(\omega)]\{U_o^*\} \quad . \tag{9.25}$$

In Eq. (9.23), $\{U_o\}$ corresponds now to the nodal displacements along the contact region between the foundation and the soil. The matrix $[K_g(\omega)]$ corresponds to the nodal impedance matrix for the soil and $\{F_o^*\}$ to the modal "driving force" vector. The vector $\{F_o^*\}$ corresponds to the forces that must be applied to the nodes of the foundation-soil interface to keep this interface fixed while under the action of the seismic excitation and in absence of the superstructure and foundation. The matrices $[K_b(\omega)]$ and $[M_b(\omega)]$ are given by Eqs. (9.11) and (9.12) or Eqs. (9.16) and (9.17), respectively. Again, the elements most difficult to determine are $[K_g]$ and $\{F_o^*\}$.

For flat foundations resting on a layered viscoelastic half-space it is possible to use the technique described by Wong and Luco (1978) and Iguchi and Luco (1980) to determine $[K_g]$ and $\{F_o^*\}$. The resulting expressions for $[K_g]$ and $\{F_o^*\}$ are given by Eq. (9.6) ($F_o^* = R_g^*$).

For embedded foundations, the matrices $[K_g]$ and $\{F_o^*\}$ can be determined by the same techniques employed to calculate impedance matrices and input motion for rigid embedded foundations (Chapter 6).

The major difficulty of analyzing fully flexible foundations resides on the large number of degrees of freedom along the foundation-soil interface that must be considered. This situation can be ameliorated by employing distributed coordinates as suggested by Gutierrez and Chopra (1978). Let $\{\tilde{U}_o\}$ be a set of distributed coordinates such that $\{U_o\}$ can be approximated by

$$\{U_o\} = [\Phi_o]\{\tilde{U}_o\} \tag{9.26}$$

in which the influence or transformation matrix $[\Phi_o]$ is given. Then, Eq. (9.23) can be written in the form

$$\{\tilde{U}_o\} = ([\tilde{K}_g] + [\tilde{K}_b] - \omega^2([\tilde{M}_o] + [\tilde{M}_b]))^{-1}\{\tilde{F}_o^*\} \tag{9.27}$$

in which

$$([\tilde{K}_g],[\tilde{K}_b],[\tilde{M}_o],[\tilde{M}_b]) = [\Phi_o]^T([K_g],[K_b],[M_o],[M_b])[\Phi_o] \tag{9.28}$$

and

$$\{\tilde{F}_o^*\} = [\Phi_o]^T\{F_o^*\}. \tag{9.29}$$

Finally, defining

$$[\tilde{C}_g] = [\tilde{K}_g]^{-1} \tag{9.30}$$

and

$$\{\tilde{U}_o^*\} = [\tilde{C}_g]\{\tilde{F}_o^*\} \tag{9.31}$$

Eq. (9.27) can be written in the form

$$\{\tilde{U}_o\} = ([I] + [\tilde{C}_g][\tilde{K}_b] - \omega^2[\tilde{C}_g]([\tilde{M}_o] + [\tilde{M}_b]))^{-1}\{\tilde{U}_o^*\} \tag{9.32}$$

In most cases it is possible to obtain adequate accuracy by judicious choice of a small number of distributed coordinates.

REFERENCES (9)

Foutch, D. A., J. E. Luco, M. D. Trifunac and F. E. Udwadia (1975). Full Scale, Three-Dimensional Tests of Structural Deformations during Forced Excitation of a Nine-Story Reinforced Concrete Building, *Proceedings, U. S. National Conference on Earthquake Engineering,* Ann Arbor, Michigan. 206-215.

Gutierrez, J. A. and A. K. Chopra (1978). A Substructure Method for Earthquake Analysis of Structures Including Structure-Soil Interaction, *Earthquake Engineering and Structural Dynamics,* Vol. 6, pp. 51-69.

Hudson, D. E. (1977). Dynamic Tests of Full-Scale Structures, *J. Engng. Mech. Div.,* ASCE, Vol. 103, EM6, 1141-1157.

Iguchi, M., (1976). A Basic Study on the Behavior of Long Dimensional Size Buildings During Earthquakes, *Proc. 6th World Conf. on Earthquake Engng.,* New Delhi, India, Vol. 4, 4-37 to 4-42.

Iguchi, M., (1978). Dynamic Interaction of Soil-Structure with Elastic Rectangular Foundation, *Proc. 5th Japan Earthquake Engng. Symp.*, Tokyo, Japan, 457-464 .

Iguchi, M. and J. E. Luco, (1980) Dynamic Response of Flexible Rectangular Foundations, Department of Applied Mechanics and Engineering Sciences, University of California, San Diego, La Jolla, California.

Lin, Y. J., (1978). Dynamic Response of Circular Plates Resting on Viscoelastic Half Space, *J. Appl. Mech. ASME,* Vol. 45, 379-384.

Matsui, G. and H. Seya, (1978). Seismic Response of Shell Structure Subjected to Spatially Variant Waves, *Trans. Arch. Inst. of Japan,* No. 266, 73-85.

Oien, M. A., (1973). Steady Motion of a Plate on an Elastic Half Space, *J. Appl. Mech.* ASME, Vol. 40, 478-484.

Savidis, S.A. and T. Richter, (1979). Dynamic Response of Elastic Plates on the Surface of the Half-Space, *Int. J. Numer. Anal. Methods Geomech.*, Vol. 3, 245-254 .

Werner, S.D., L. C. Lee, H. L. Wong and M. D. Trifunac, (1977). An Evaluation of the Effects of Traveling Seismic Waves on the Three-Dimensional Response of Structures, Report R-7720-4514, Agbabian and Associates.

Whitman, R.V., J. N. Protonotarios and M. F. Nelson, (1973). Case Study of Dynamic Soil-Structure Interaction, *J. Soil Mech. Div.* ASCE, Vol. 99, SM11, 997-1009.

Wong, H.L. and J. E. Luco, (1976). Dynamic Response of Rigid Foundations of Arbitrary Shape, *Earthquake Engng. Struct. Dyn.*, Vol. 4, 579-587.

Wong, H.L., J. E. Luco and M. D. Trifunac, (1977). Contact Stresses and Ground Motion Generated by Soil-Structure Interaction, *Earthquake Engng. Struct. Dyn.*, Vol. 5, 67-79.

Wong, H.L. and J. E. Luco, (1978). Dynamic Response of Rectangular Foundations to Obliquely Incident Seismic Waves, *Earthquake Engng. Struct. Dyn.*, Vol. 6, 3-16.

10. REVIEW OF VARIOUS FORMULATIONS OF THE LINEAR INTERACTION PROBLEM

A number of formulations of the interaction between structures and the ground have been proposed. These formulations differ in generality, analytical approach, or, in the basic concepts involved. In some cases, alternative formulations lead to the same final equations but differ in derivation. In other cases, differences resulting from the approximations or assumptions introduced in the analysis are apparent.

It is convenient to start by considering the substructure formulation proposed by Gutierrez and Chopra (1978). In this formulation the complete system is separated into two subsystems. The first subsystem corresponds to the superstructure and the foundation and is designated as structure. The second subsystem corresponds to the soil region *after* the cavity for the foundation has been excavated. In the case of "spatially varying" ground motion the discretized equations of motion for the structure are written in the form

$$\left(-\omega^2 \begin{bmatrix} M_{bb} & 0 \\ 0 & M_o \end{bmatrix} + (1 + i\eta) \begin{bmatrix} K_{bb} & K_{bo} \\ K_{ob} & K_{oo} \end{bmatrix} \right) \begin{Bmatrix} U_b \\ U_o \end{Bmatrix} = \begin{Bmatrix} 0 \\ -F_S \end{Bmatrix} \tag{10.1}$$

in which U_b represents the total displacement vector for nodes not on the structure-soil interface, while U_o represents the total displacement vector for nodes on that interface. In Eq. (10.1), F_S represents the vector of nodal forces that the structure exerts on the soil and η the hysteretic damping factor for the structure. The mass and stiffness matrices appearing in Eq. (10.1) would be calculated from a finite element model of the structure.

The next step in this formulation is to write the vector U_o in the form

$$U_o = U_g^* + U_S \tag{10.2}$$

in which U_g^* corresponds to the displacement along the structure-soil interface resulting from the seismic excitation in absence of the structure. The vector U_S corresponds to the displacement along the structure-soil interface caused by the forces that the structure exerts on the soil. The displacement U_g^* is called free-field motion by Gutierrez and Chopra but will be called here modified free-field motion. This motion includes the scattering of the incident seismic motion by the cavity for the foundation, and, consequently, differs from the free-field motion at the same location on a half-space without the cavity for the foundation. The formulation of Gutierrez and Chopra proceeds on the assumption that this modified free-field motion is prescribed. In practice and with exception of the case of flat foundations, the modified free-field motion must be calculated from the actual free-field motion.

Considering the dynamics of the soil region, the vectors F_S and U_S are related by means of the equation

$$F_S = K_S U_S \tag{10.3}$$

in which $K_S(\omega)$ is the complex valued, dynamic stiffness (or impedance) matrix for the soil region. The elements of this matrix are defined as the nodal forces acting on the soil-structure interface required to keep all nodes fixed except for a unit displacement of a given node. In the definition, Gutierrez and Chopra (Fig. 2, 1978) assume a linear variation of displacement in the region between the node subjected to the unit displacement and the surrounding fixed nodes. Although Eq. (10.3) is valid, the definition of the dynamic stiffness matrix involving linear interpolation of soil displacements leads to serious errors as revealed by the calculations performed by Chopra et al. (1976), Dasgupta (1976) and Dasgupta and Chopra (1979).

The formulation continues by writing

$$U_b = LU_g^* + U \tag{10.4}$$

in which

$$L = -K_{bb}^{-1} K_{bo} \ . \tag{10.5}$$

and U represents displacements of the structure relative to the "pseudo-static" displacement LU_g^*. Substitution from Eqs. (10.2), (10.3) and (10.4) into Eq. (10.1) leads to

$$\left[\begin{array}{c|c} -\omega^2 M_{bb} + (1 + i\eta)K_{bb} & (1 + i\eta)K_{bo} \\ \hline (1 + i\eta)K_{oo} & -\omega M_o + (1 + i\eta)K_{oo} + K_S \end{array}\right] \left\{\begin{array}{c} U \\ \hline U_S \end{array}\right\} =$$

$$\left\{\begin{array}{c} \omega^2 M_{bb} L U_g^* \\ \hline \omega^2 M_o U_g^* - K_b U_g^* \end{array}\right\} \tag{10.6}$$

in which

$$K_b = (1 + i\eta)(K_{oo} - K_{ob} K_{bb}^{-1} K_{bo}) \tag{10.7}$$

In the next step, the relative displacement of the superstructure U and the relative displacement U_S of the structure-soil interface are written in the form

$$\left\{\begin{array}{c} U \\ \hline U_S \end{array}\right\} = \left[\begin{array}{c|c} \Phi & L\Phi_o \\ \hline o & \Phi_o \end{array}\right] \left\{\begin{array}{c} Y \\ \hline Z \end{array}\right\} \tag{10.8}$$

in which Φ is the matrix of fixed-base normal modes for the structure and Φ_o is a matrix of deformation patterns for the soil-interface. The vectors Y and Z appearing in Eq. (10.8) represent generalized coordinates. The idea of reducing the number of degrees of freedom along the structure-soil interface by introducing displacement patterns for this interface is good in principle. Unfortunately, Gutierrez and Chopra apply this representation to the relative displacement of the structure-soil interface. For structures with sufficiently rigid foundations it is possible to represent the *total* displacement along the interface by combination of a few displacement patterns. If the modified free-field motion U_g^* is highly variable along the interface, as it occurs for embedded foundations at high frequencies and for flat foundations subjected to nonvertically incident waves, the representation in terms of a few displacement patterns may be valid for the total displacement U_o but it is not valid for the relative displacement U_S. The representation given by Eq. (10.8) is then only adequate for flat foundation and vertically incident waves. It must be noted that Gutierrez and Chopra have tested this procedure only for the case in which U_g^* is spatially invariant.

From Eqs. (10.6) and (10.8) it may be found that

$$\left[\begin{array}{c|c} -\omega^2 I + (1 + i\eta)\Omega & -\omega^2 \Phi^T M_{bb} L \Phi_o \\ \hline -\omega^2 \Phi_o^T L^T M_{bb} \Phi & \Phi_o^T(-\omega^2 M_o - \omega^2 L^T M_{bb} L + K_b + K_S)\Phi_o \end{array}\right] \left\{\begin{array}{c} Y \\ \hline Z \end{array}\right\} =$$

$$\left\{\begin{array}{c} \omega^2\Phi^T M_{bb} L\, U_g^* \\ \hline \Phi_o^T(\omega^2 M_o + \omega^2 L^T M_{bb} L - K_b)U_g^* \end{array}\right\} \tag{10.9}$$

in which it has been assumed that the fixed-base modes of the superstructure are such that

$$\Phi^T M_{bb} \Phi = I \tag{10.10}$$

and

$$\Phi^T K_{bb} \Phi = \Omega \tag{10.11}$$

The matrix Ω is diagonal and it has for elements the squares of the fixed-base natural frequencies of the superstructure.

Finally, eliminating Y from Eq. (10.9) leads to

$$Y = (-\omega^2 I + (1 + i\eta)\Omega)^{-1}\omega^2\Phi^T M_{bb} L(\Phi_o Z + U_g^*) \tag{10.12}$$

and

$$Z = (\tilde{K}_S + \tilde{K}_b - \omega^2(\tilde{M}_o + \tilde{M}_b))^{-1}\, \Phi_o^T[\omega^2(M_o + M_b) - K_b]U_g^* \tag{10.13}$$

in which

$$(\tilde{K}_S, \tilde{K}_b, \tilde{M}_o \tilde{M}_b) = \Phi_o^T(K_S, K_b, M_o, M_b)\Phi_o \tag{10.14}$$

and

$$M_b = L^T M_{bb} L + \omega^2 L^T M_{bb} \Phi(-\omega^2 I + (1 + i\eta)\Omega)^{-1}\Phi^T M_{bb} L \tag{10.15}$$

Once the generalized coordinates are obtained from Eq. (10.13), the total displacement of the superstructure and of the structure can be obtained from

$$U_b = L(U_g^* + \Phi_o Z) + \Phi Y \tag{10.16}$$

$$U_o = U_g^* + \Phi_o Z \tag{10.17}$$

in which Y is given by Eq. (10.12).

In summary, the advantages of the substructure formulation proposed by Gutierrez and Chopra are: (i) The finite-element model is restricted to the structure, (ii) fixed-base normal modes of the structure are used to describe the relative motion of the superstructure, (iii) the idea of utilizing displacement patterns to describe the displacement of the structure-soil interface is introduced and (iv) the formulation is addressed to the case of the flexible foundations. The shortcomings of the formulation are: (i) It assumes that the modified free-field motion is prescribed. In practice the modified free-field motion needs to be determined from the actual free-field motion. In this sense, the formulation is not complete since it does not include a procedure to calculate the modified free-field motion. (ii) The procedure suggested to calculate the dynamic stiffness matrix for the soil is not adequate and leads to large errors. (iii) The formulation assumes that the displacement of the structure-soil interface relative to the

modified free-field motion can be expressed in terms of a few displacement patterns. Although for sufficiently stiff foundations it is possible to represent the *total* displacement of the structure-soil interface by combination of a few displacement patterns it is not possible to do so for the relative displacement. This is particulary true for embedded foundations and flat foundations subjected to nonvertically incident ground motion.

The last disadvantage indicated above can be removed by noting from Eqs.(10.16) and (10.12) that the total response of the superstructure depends on the total displacement of the structure-soil interface nodes. After some algebra it can be found that if U_o is written in the form

$$U_o = \Phi_o \tilde{U}_o \tag{10.18}$$

where $\tilde{U}_o$ represents the generalized coordinates for the soil-structure interface, then

$$U_b = L\Phi_o \tilde{U}_o + \Phi Y \tag{10.19}$$

$$Y = (-\omega^2 I + (1 + i\eta)\Omega)^{-1} \omega^2 \Phi^T M_{bb} L\Phi_o \tilde{U}_o \tag{10.20}$$

and

$$\tilde{U}_o = (I + \tilde{C}_S \tilde{K}_b - \omega^2 \tilde{C}_S (\tilde{M}_o + \tilde{M}_b))^{-1} \tilde{U}_o^* \tag{10.21}$$

in which $\tilde{C}_S = \tilde{K}_S^{-1}$ and

$$U_o^* = \tilde{C}_S \Phi_o^T K_S U_g^* \tag{10.22}$$

With these modifications the formulation of Gutierrez and Chopra coincides with that presented in the previous chapter.

An alternative substructure formulation has been presented by Kausel, Whitman, Morray and Elsabee (1977). The derivation of this formulation is based on a finite element discretization of the structure and of a portion of the soil. The formulation is based on writing the discretized equations of motion for the superstructure and portion of the soil in the form

$$\left[\begin{array}{c|c} K_{bb} & K_{bo} \\ \hline K_{ob} & K_{oo}^{b} \end{array}\right] \left\{\begin{array}{c} U_b \\ \hline U_o \end{array}\right\} = \left\{\begin{array}{c} 0 \\ \hline -F_S \end{array}\right\} \tag{10.23}$$

and

$$\left[\begin{array}{c|c} K_{oo}^{S} & K_{or} \\ \hline K_{ro} & K_{rr}^{S} \end{array}\right] \left\{\begin{array}{c} U_o \\ \hline U_r \end{array}\right\} = \left\{\begin{array}{c} F_S \\ \hline F_r^* \end{array}\right\} \tag{10.24}$$

in which, for brevity, the stiffness matrices represent the sum $(-\omega^2 M + i\omega C + K)$. In Eq. (10.23) the vector U_b represents the total displacement on nodes of the structure not on the structure-soil interface, while the vector U_o represents total displacement on nodes at the structure-soil interface. The vector F_S represents the nodal forces that the structure exerts on the soil. In Eq. (10.24), U_r and F_r^* represent the vectors of total displacement and nodal forces along the portion of the external boundary of the finite element model of the soil designated by r in Fig. 10.1c. As in finite element analyses, the displacement U_r is assumed to be prescribed. In Eq. (10.24) the displacements associated with internal nodes as well as with nodes on the unloaded soil surface have been condensed.

A third equation is obtained by considering the "free-field" problem illustrated in Fig. 10.1d.

Separating the portion of the soil that will be excavated for the foundation as shown in Figs. 10.1e and 10.1f, it is possible to write

$$\left[\begin{array}{c|c} K_{oo}^{S} & K_{or} \\ \hline K_{ro} & K_{rr}^{S} \end{array}\right] \left\{\begin{array}{c} U_g \\ \hline U_r \end{array}\right\} = \left\{\begin{array}{c} T_g \\ \hline F_r \end{array}\right\} \tag{10.25}$$

where U_g represents the free-field displacement at the nodes where the structure-soil interface will be located. It is important to notice that U_g represents the free-field displacement vector before the cavity has been excavated. The vector T_g corresponds to the free-field tractions that the portion of the soil to be excavated exerts on the rest of the soil. The excitation U_r along the external boundary of the soil for the free-field problem is assumed to be the same as that for the soil-structure interaction problem.

Subtracting Eq. (10.25) from Eq. (10.24) leads to

$$\left[\begin{array}{c|c} K_{oo}^{S} & K_{or} \\ \hline K_{ro} & K_{rr}^{S} \end{array}\right] \left\{\begin{array}{c} U_o - U_g \\ \hline 0 \end{array}\right\} = \left\{\begin{array}{c} F_S - T_g \\ \hline F_r^* - F_r \end{array}\right\} \tag{10.26}$$

from where

$$F_S - T_g = K_{oo}^{S} (U_o - U_g) \ . \tag{10.27}$$

In Eq. (10.27), K_{oo}^{S} represents the stiffness matrix for the soil. Eliminating F_S from Eqs. (10.23) and (10.27) leads to

$$\left[\begin{array}{c|c} -\omega^2 M_{bb} + i\omega C_{bb} + K_{bb} & i\omega C_{bo} + K_{bo} \\ \hline i\omega C_{ob} + K_{ob} & -\omega^2 M_{oo} + i\omega C_{oo} + K_{oo} + K_{oo}^{S} \end{array}\right] \left\{\begin{array}{c} U_b \\ \hline U_o \end{array}\right\} = \left\{\begin{array}{c} 0 \\ \hline K_{oo}^{S} U_g - T_g \end{array}\right\} \tag{10.28}$$

where the matrices K_{bb}, ..., have been replaced by the full expressions $-\omega^2 M_{bb} + i\omega C_{bb} + K_{bb}$, ... etc.

The formulation proposed by Kausel et al. is similar to that presented by Gutierrez and Chopra. The differences are in the method of derivation and in the fact that the formulation of Kausel et al. involves the free-field motion U_g and the free-field tractions T_g on the surface which will correspond to the structure-soil interface. The formulation of Gutierrez and Chopra involves the modified free-field motion U_g^* after the cavity for the foundation has been excavated. It is interesting to notice that U_g^*, U_g, and T_g are related by

$$U_g^* = U_g + K_{oo}^{S} T_g \ . \tag{10.29}$$

If the terms K_{oo}^{S}, U_g and T_g appearing in Eq. (10.28) are interpreted as the stiffness matrix, free-field motion and free-field tractions for an unbounded soil, then Eq. (10.28) is exact and coincides with a derivation based on a continuum approach. On the other hand, if these terms are calculated via the finite element method, then Eq. (10.28) provides only an approximation to the real situation.

The approximations introduced in the derivation of the formulation presented by Kausel et al. are the same as in direct (one-pass) finite element analyses and should be reviewed carefully. In the first place, in writing Eqs. (10.24) and (10.25) it has been assumed that the excitation along the external soil boundary is common for both the soil-structure interaction problem and for the free-field problem. It is obvious that this cannot be the case since the presence of the structure in the soil-structure in-

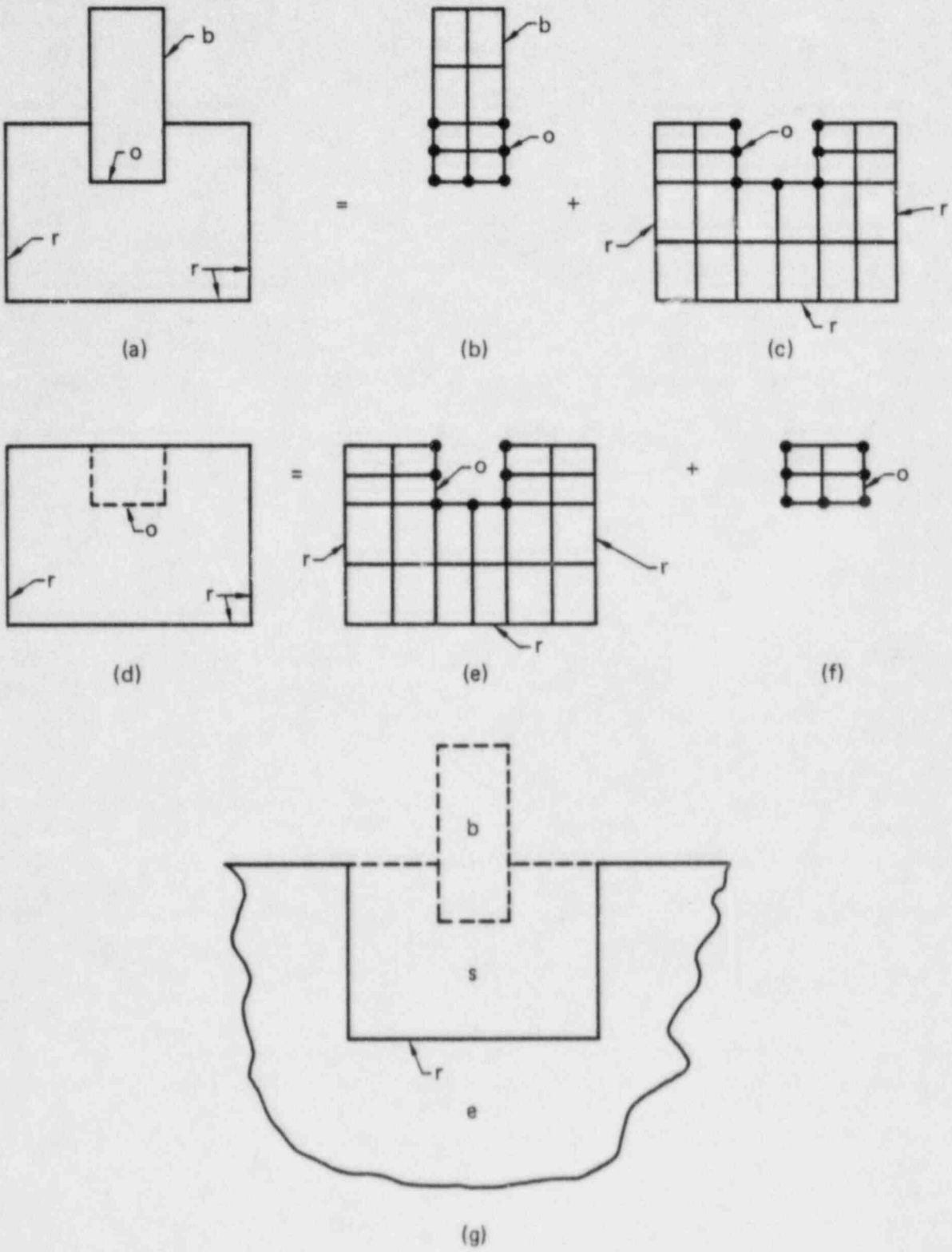

FIG. 10.1. Description of the substructure approach of Kausel et al. (1977).

teraction problem will lead to scattering of waves which in turn will modify the motion throughout the soil. If the total motion along the external boundary of the soil model for the soil-structure interaction problem is denoted by U_r^* ($U_r^* \neq U_r$), then U_r in Eq. (10.24) should be replaced by U_r^*. Subtracting Eq. (10.25) from the modified version of Eq. (10.24) leads to

$$\left[\begin{array}{c|c} K_{oo}^S & K_{or} \\ \hline K_{ro} & K_{rr}^S \end{array}\right] \left\{\begin{array}{c} U_o - U_g \\ \hline U_r^* - U_r \end{array}\right\} = \left\{\begin{array}{c} F_S - T_g \\ \hline F_r^* - F_r \end{array}\right\} \tag{10.30}$$

which should be compared with Eq. (10.26)

Considering the soil outside the region covered by the finite element model it is possible to write

$$F_r^* - F_r = -K_{rr}^e(U_r^* - U_r) \tag{10.31}$$

where K_{rr}^e represents the dynamic stiffness matrix for the soil not considered in the finite element model (Fig. 10.1g).

From Eqs. (10.30) and (10.31) it is found that

$$F_S - T_g = K_S(U_o - U_g) \tag{10.32}$$

where

$$K_S = K_{oo}^S - K_{or}(K_{rr}^S + K_{rr}^e)^{-1}K_{ro} \tag{10.33}$$

represents the correct stiffness matrix of the soil for nodes along the structure-soil interface. The finite element stiffness matrix K_{oo}^S will be equal to the real stiffness matrix K_S only when the soil outside the region considered in the finite element model is rigid, i.e. when $(K_{rr}^e)^{-1} = 0$. A number of studies have shown that the stiffness matrix K_{oo}^S calculated by use of a finite element model exhibits artificial characteristics not present in the matrix K_S.

Finally, substitution from Eq. (10.32) into Eq. (10.23) leads to an equation of the same form as Eq. (10.28) except that K_{oo}^S should be replaced by K_S given by Eq. (10.33). If the vectors U_g and T_g appearing in the modified version of Eq. (10.28) are calculated considering an unbounded soil, then this modified version of Eq. (10.28) would be correct. Although the quantities U_g and T_g are not calculated expiicitly in the direct finite element method the results of such analyses should coincide with those obtained by use of Eq. (10.28)(unmodified). In this case, additional errors which affect U_g and T_g result from the evaluation (deconvolution) of the input motion U_r to be used along the external boundary of the soil model. Typically, the input motion U_r must be determined from a prescribed free-field motion on the ground surface. For vertically incident waves it is possible to determine U_r with some confidence. For more general seismic excitation the problem has not been adequately solved.

In recent years a curious situation has developed in the field of soil-structure interaction in which the finite element method, in spite of the shortcomings mentioned above and of other limitations (filtering of high frequencies due to size of elements, two-dimensional character of most finite-element models), continues to be employed as a yardstick by which other formulations are judged. As example, the derivation presented by Kausel et al. (1977) and discussed above is based on a finite element model and was employed to justify the use of a continuum approach. It is fortunate in this case that, although the derivation is not exactly correct, the final equation, when properly interpreted, does coincide with the result obtained by use of the continuum approach.

A number of approximate formulations of the soil-structure interaction problem for the case of rigid foundations have been presented. One of the most common approximations introduced is to neglect the frequency dependence of the impedance functions and to represent the force-displacement rela-

tionship for the foundation by means of frequency independent springs and dashpots. The basic equations, in the time domain, are, in this case:

$$[M_{bb}]\{\ddot{U}_t\} + [C_{bb}]\{\dot{U}\} + [K_{bb}]\{U\} = \{0\} \tag{10.34}$$

$$\{U_t\} = [a]\{U_o\} + \{U\} \tag{10.35}$$

$$[M_o]\{\ddot{U}_o\} + [C_S]\{\dot{U}_S\} + [K_S]\{U_S\} = -[a]^T[M_{bb}]\{\ddot{U}_t\} \tag{10.36}$$

$$\{U_o\} = \{U_o^*\} + \{U_S\} \tag{10.37}$$

in which $[M_{bb}]$, $[C_{bb}]$ and $[K_{bb}]$ represent, respectively, the mass, damping and stiffness matrices for the superstructure on a fixed base. The relative displacement vector for the superstructure $\{U\}$ is defined by Eq. (6.1) and represents the relative motion of the superstructure with respect to a frame of reference fixed to the moving rigid foundation. The total displacement vector for the superstructure $\{U_t\}$ is given by Eq. (10.35) in which $\{U_o\}$ represents the total displacement vector for the foundation and $[a]$ is the matrix defined by Eq. (6.3).

The equation of motion for the foundation is given by Eq. (10.36) in which $[M_o]$ denotes the mass matrix for the rigid foundation. The matrices $[K_S]$ and $[C_S]$ correspond to the approximate stiffness and damping matrices for the soil, respectively. The vector $\{U_S\}$ appearing in Eq. (10.36) corresponds, as indicated by Eq. (10.37), to the relative displacement of the foundation with respect to the foundation input motion vector $\{U_o^*\}$. The foundation input motion vector $\{U_o^*\}$ which in general includes three translational and three rotational components is assumed to be known. In most of the approximate formulations it is assumed that the foundation is flat and that the excitation can be represented by vertically incident seismic waves. In this case, $\{U_o^*\} = (U_{gx}, 0, U_{gy}, 0\ U_{gz}, 0)^T$ in which (U_{gx}, U_{gy}, U_{gz}) represents the free-field motion on the ground surface.

The basic equations given by Eqs. (10.34) - (10.37) can be rearranged in various forms. One form involving the relative displacement vectors $\{U\}$ and $\{U_S\}$ is:

$$\left[\begin{array}{c|c} M_{bb} & M_{bb}a \\ \hline a^T M_{bb} & M_o + a^T M_{bb} a \end{array}\right] \left\{\begin{array}{c} \ddot{U} \\ \hline \ddot{U}_S \end{array}\right\} + \left[\begin{array}{c|c} C_{bb} & 0 \\ \hline 0 & C_S \end{array}\right] \left\{\begin{array}{c} \dot{U} \\ \hline \dot{U}_S \end{array}\right\} + \left[\begin{array}{c|c} K_{bb} & 0 \\ \hline 0 & K_S \end{array}\right] \left\{\begin{array}{c} U \\ \hline U_S \end{array}\right\} =$$

$$- \left\{\begin{array}{c} M_{bb} a \ddot{U}_o^* \\ \hline (M_o + a^T M_{bb} a)\ddot{U}_o^* \end{array}\right\} \tag{10.38}$$

which corresponds to a generalization of the equation formulated by Parmelee et al. (1969) This equation can be solved by direct integration, Foss's method, or by modal analysis in the time domain.

In general, Eq. (10.38) does not admit classical normal modes and consequently a solution in terms of normal modes can only be considered as an approximation. The approximate classical normal mode solution obtained by generalizing the formulation presented by Bielak (1975) to the three-dimensional case would be:

$$\left\{\begin{array}{c} U \\ U_S \end{array}\right\} = \sum_r \{\psi_r\} q_r(t) \tag{10.39}$$

in which the rth mode for the complete system $\{\psi_r\}$ is defined by

$$\tilde{\omega}_r^2 \left[\begin{array}{c|c} M_{bb} & M_{bb}\alpha \\ \hline \alpha^T M_{bb} & M_o + \alpha^T M_{bb}\alpha \end{array}\right] \{\psi_r\} = \left[\begin{array}{c|c} K_{bb} & 0 \\ \hline 0 & K_S \end{array}\right] \{\psi_r\} \tag{10.40}$$

and

$$\{\psi_r\}^T \left[\begin{array}{c|c} M_{bb} & M_{bb}\alpha \\ \hline \alpha^T M_{bb} & M_o + \alpha^T M_{bb}\alpha \end{array}\right] \{\psi_r\} = 1 \tag{10.41}$$

The modal coordinates $q_r(t)$ would be given by

$$\ddot{q}_r + 2\tilde{\xi}_r\tilde{\omega}_r\dot{q}_r + \tilde{\omega}_r^2 q_r = -\{\psi_r\}^T \left\{\begin{array}{c} M_{bb}\alpha\ddot{U}_o^* \\ \hline (M_o + \alpha^T M_{bb}\alpha)\ddot{U}_o^* \end{array}\right\} \tag{10.42}$$

in which $\tilde{\omega}_r$ and $\tilde{\xi}_r$, the rth system frequency and equivalent modal damping ratio, respectively, are given by

$$\tilde{\omega}_r^2 = \{\psi_r\}^T \left[\begin{array}{c|c} K_{bb} & 0 \\ \hline 0 & K_S \end{array}\right] \{\psi_r\} \tag{10.43}$$

$$\tilde{\xi}_r = \frac{1}{2\tilde{\omega}_r} \{\psi_r\}^T \left[\begin{array}{c|c} C_{bb} & 0 \\ \hline 0 & C_S \end{array}\right] \{\psi_r\} \tag{10.44}$$

It is important that the values selected for $[K_S]$ and $[C_S]$ be consistent with the system frequencies obtained. For this reason an iterative process may be required to determine $\tilde{\omega}_r$.

In many cases, damping in the superstructure is given in terms of fixed-base modal damping ratios. In these cases it is convenient to write the vector $\{U\}$ in the form

$$\{U\} = [\Phi]\{\eta\} \tag{10.45}$$

in which $[\Phi]$ is the fixed-base modal matrix for the superstructure normalized in such a way that

$$[\Phi]^T [M_{bb}] [\Phi] = [I] \tag{10.46}$$

Substitution from Eq. (10.45) into Eq. (10.38) leads to

$$\left[\begin{array}{c|c} I & \beta^T \\ \hline \beta & M_o + \alpha^T M_{bb}\alpha \end{array}\right] \left\{\begin{array}{c} \ddot{\eta} \\ \hline \ddot{U}_S \end{array}\right\} + \left[\begin{array}{c|c} 2D\Omega & 0 \\ \hline 0 & C_S \end{array}\right] \left\{\begin{array}{c} \dot{\eta} \\ \hline \dot{U}_S \end{array}\right\} + \left[\begin{array}{c|c} \Omega^2 & 0 \\ \hline 0 & K_S \end{array}\right] \left\{\begin{array}{c} \eta \\ \hline U_S \end{array}\right\} =$$

$$- \left\{\begin{array}{c} \beta^T\ddot{U}_o^* \\ \hline (M_o + \alpha^T M_{bb}\alpha)\ddot{U}_o^* \end{array}\right\} \tag{10.47}$$

in which $[I]$ is the identity matrix, $[D] = [\xi_r]$ is a diagonal matrix having for elements the fixed-base modal damping ratios for the superstructure, $[\Omega] = [\omega_r]$ is a diagonal matrix having for elements the

fixed-base natural frequencies of the superstructure, and $[\beta] = [\alpha]^T[M_{bb}][\Phi]$ is the matrix of participation factors for the superstructure on a fixed base.

Expanding $\{\eta\}$ and $\{U_S\}$ in the form

$$\{\eta\} = \sum_r \{\Phi_r^b\}q_r \quad , \quad \{U_S\} = \sum_r \{\Phi_r^S\}q_r \tag{10.48}$$

in which the eigen-vectors $\{\Phi_r^b\}$ and $\{\Phi_r^S\}$ are defined by

$$\left(-\tilde{\omega}_r^2 \left[\begin{array}{c|c} I & \beta^T \\ \hline \beta & M_o + \alpha^T M_{bb}\alpha \end{array}\right] + \left[\begin{array}{c|c} \Omega^2 & 0 \\ \hline 0 & K_S \end{array}\right] \right) \left\{\begin{array}{c} \Phi_r^b \\ \hline \Phi_r^S \end{array}\right\} = 0 \tag{10.49}$$

and

$$\left\{\begin{array}{c} \Phi_r^b \\ \hline \Phi_r^S \end{array}\right\}^T \left[\begin{array}{c|c} I & \beta^T \\ \hline \beta & M_o + \alpha^T M_{bb}\alpha \end{array}\right] \left\{\begin{array}{c} \Phi_r^b \\ \hline \Phi_r^S \end{array}\right\} = 1 \tag{10.50}$$

leads to

$$\ddot{q}_r + 2\tilde{\xi}_r\tilde{\omega}_r\dot{q}_r + \tilde{\omega}_r^2 q_r = -\{\tilde{\beta}_r\}^T\{\ddot{U}_o^*\} \tag{10.51}$$

in which

$$\tilde{\omega}_r^2 = \{\Phi_r^b\}^T[\Omega^2]\{\Phi_r^b\} + \{\Phi_r^S\}^T[K_S]\{\Phi_r^S\} \tag{10.52}$$

$$\tilde{\xi}_r = \frac{1}{\tilde{\omega}_r}\{\Phi_r^b\}^T[D][\Omega]\{\Phi_r^b\} + \frac{1}{2\tilde{\omega}_r}\{\Phi_r^S\}^T[C_S]\{\Phi_r^S\} \tag{10.53}$$

and

$$\{\tilde{\beta}_r\} = [\beta]\{\Phi_r^b\} + ([M_o] + [\alpha]^T[M_{bb}][\alpha])\{\Phi_r^S\} \quad . \tag{10.54}$$

Once $q_r(t)$ has been obtained from Eq. (10.51), the total response of the foundation and of the superstructure can be obtained from

$$\{U_o(t)\} = \{U_o^*(t)\} + \sum_r \{\Phi_r^S\}q_r(t) \tag{10.55}$$

$$\{U_t(t)\} = [\alpha]\{U_o^*(t)\} + \sum_r [\alpha]\{\Phi_r^S\}q_r(t) + \sum_r [\Phi]\{\Phi_r^b\}\, q_r(t) \tag{10.56}$$

In addition to the estimates of the equivalent modal damping proposed by Bielak (Eqs. (10.44) and (10.53)) various other forms have been suggested. (Roesset, Whitman and Dobry (1973), Novak (1974), and Rainer (1975)). A somewhat different approach to determine the equivalent modal damping has been proposed by Tsai (1974). In this approach the equivalent modal damping ratios are determined by matching the amplitudes of the transfer functions obtained by modal analysis and by direct use of Eq. (10.38).

Although modal superposition cannot be considered exact it is convenient in the sense that it gives

physical insight into the interaction problem. The main disadvantage of this procedure is that the frequency dependence of the impedance function is not considered, or, at best, is approximated by considering the values of the impedance functions in the vicinity of the system frequencies. In the case of layered soil deposits with marked changes in stiffness, the frequency dependence of the impedance functions is strong and the approximation by means of frequency independent spring and dashpots may be inadequate. Previous studies based on the use of modal analysis have been limited to the case in which the foundation input motion is equal to the free-field motion on the ground surface, and, consequently, refer only to the case of flat foundations and vertically incident seismic excitation. Solutions of Eq. (10.38) by direct step-by-step numerical integration (Parmelee, Perelman and Lee, 1969) and by Foss's method (Jennings and Bielak (1973), Tsai, Niehoff, Swatta and Hadjian (1974)), although not involving equivalent modal damping ratios, present the same disadvantages and limitations described above.

An alternative arrangement of the approximate interaction equations for the case of frequency independent impedance functions has been presented by Ibrahim and Hadjian (1975). A generalized version of this formulation, for the case of a general seismic excitation, can be obtained by defining

$$\{U_r\} = [\alpha]\{U_S\} + \{U\} \tag{10.57}$$

in which $\{U_r\}$ represents a displacement of the superstructure relative to a rigid body motion consistent with the foundation input motion $\{U_o^*\}$. Substitution from Eq. (10.57) into Eqs. (10.34)-(10.37) leads to

$$\begin{bmatrix} M_{bb} & 0 \\ 0 & M_o \end{bmatrix} \begin{Bmatrix} \ddot{U}_r \\ \ddot{U}_S \end{Bmatrix} + \begin{bmatrix} C_{bb} & -C_{bb}\alpha \\ -\alpha^T C_{bb} & C_S + \alpha^T C_{bb}\alpha \end{bmatrix} \begin{Bmatrix} \dot{U}_r \\ \dot{U}_S \end{Bmatrix} +$$

$$+ \begin{bmatrix} K_{bb} & -K_{bb}\alpha \\ -\alpha^T K_{bb} & K_S + \alpha^T K_{bb}\alpha \end{bmatrix} \begin{Bmatrix} U_r \\ U_S \end{Bmatrix} = - \begin{Bmatrix} M_{bb}\alpha\ddot{U}_o^* \\ M_o\ddot{U}_o^* \end{Bmatrix} \tag{10.58}$$

This particular arrangement of the interaction equations involves the displacement vector $\{U_r\}$, which, as indicated by Eq. (10.57), corresponds to a combination of rigid-body motion and deformation of the superstructure. For this reason, this formulation is less convenient than that given by Eq. (10.38).

REFERENCES (10)

Bielak, J. (1975). Modal Analysis for Building-Soil Interaction. Report E17, Instituto de Ingenieria, Universidad Nacional Autonoma de Mexico.

Chopra, A. K., P. Chakrabarti, and G. Dasgupta (1976). Dynamic Stiffness Matrices for Viscoelastic Half-Plane Foundations. *J. Engrg. Mech. Div., ASCE, 102,* 497-514.

Dasgupta, G. (1976). A Numerical Solution for Viscoelastic Half Planes. *J. Engrg. Mech. Div., ASCE. 102,* 601-612.

Gutierrez, J. A. and A. K. Chopra (1978). A Substructure Method for Earthquake Analysis of Structures Including Structure-Soil Interaction. *Earthq. Engrg. and Struct. Dyn., 6,* 51-69.

Ibrahim, A. M. and A. H. Hadjian (1975). The Composite Damping Matrix for Three-Dimensional Soil-Structure Systems. *Proc. Second ASCE Specialty Conference on Structural Design of Nuclear Plant Facilities,* New Orleans, Louisiana, Volume 1-B, 932-960.

Jennings, P. C. and J. Bielak (1973). Dynamics of Building-Soil Interaction. *Bull. Seism. Soc. Am., 63,* 9-48.

Kausel, E., R. V. Whitman, J. P. Morray and F. Elsabee (1977). The Spring Method for Embedded Foundations. *Transactions 4th International Conference on Struct. Mech. in Reactor Technology,* San Francisco, California, Paper K2/6.

Novak, M. (1974). Effect of Soil on Structural Response to Wind and Earthquake, *Earthq. Engrg. and Struct. Dyn.,* 3, 79-96.

Rainer, S. H. (1975). Damping in Dynamic Structure-Foundation Interaction. *Canadian Geotechnical Journal, 12,* 13-22.

Roesset, J. M. R. V. Whitman and R. Dobry (1973). Modal Analysis for Structures with Foundation Interaction. *J. Structural Div., ASCE, 99,* 399-416.

Tsai, N. C. (1974). Modal Damping for Soil-Structure Interaction. *J. Engineering Mechanics Div., ASCE, 100,* 323-341.

Tsai, N. C., D. Niehoff, M. Swatta and A. H. Hadjian (1974). The Use of Frequency-Independent Soil-Structure Interaction Parameters. *Nuclear Engineering and Design, 31,* 168-183.

11. APPROXIMATE SOLUTION AND INTERACTION EFFECTS ON STRUCTURAL IDENTIFICATION

The first objective of this chapter is to present and discuss the approximate solution of the interaction problem presented by Bielak (1971) and Jennings and Bielak (1973). This approximate solution provides a clear description of some of the interaction effects. The second objective of this chapter is to discuss the effects of soil-structure interaction on the interpretation of results obtained by structural identification techniques. These techniques typically do not consider the effects of soil-structure and lead to apparent modal frequencies and damping ratios that may not reflect the characteristics of the superstructure (Luco, 1980).

Jennings and Bielak (1973) obtained an exact solution for the case of a one-story structure supported on a flat rigid foundation when subjected to vertically incident SH waves. An approximate solution was then obtained by neglecting certain second order terms. An approximate solution for the fundamental mode of a multistory structure was also obtained by modification of the results for a single-story building. An alternative derivation is described here (Luco, 1980).

Consider in-plane vibrations of an elastic structure supported on a flat rigid foundation resting on a viscoelastic half-space. The equation of motion for the superstructure, in the frequency domain, can be written in the form

$$-\omega^2[M]\{U_T\} + i\omega[C]\{U\} + [K]\{U\} = \{0\} \tag{11.1}$$

in which [M], [C] and [K] are the fixed-base mass, damping and stiffness matrices for the superstructure. The displacement vector $\{U_T\}$ corresponds to the total displacement of the mass points, while $\{U\}$ represents the displacement of the mass points relative to a moving frame of reference attached to the rigid foundation. The displacements $\{U_T\}$ and $\{U\}$ are related by

$$\{U_T\} = \{1\}(U_g + U_s) + \{h\}\phi_s + \{U\} \tag{11.2}$$

in which U_g corresponds to the free-field motion on the ground surface, U_s to the additional translational motion of the foundation associated with interaction, and ϕ_s to the angle of rocking of the foundation. The vectors $\{1\}$ and $\{h\}$ appearing in Eq. (11.2) are defined by $\{1\}^T = (1,1,\ldots,1)$ and $\{h\}^T = (h_1, h_2,\ldots,h_n)$, where h_i denotes the height of the ith mass. In writing Eq. (11.2) it has been assumed that the seismic excitation corresponds to vertically incident SH waves.

Neglecting the mass of the foundation and the rotary inertia of the superstructure it is possible to write the equations of motion for the foundation in the form

$$-\omega^2\{1\}[M]\{U_T\} + Gr\,[(1 + 2i\xi_s)k_H + i\omega c_H]\,U_s = 0 \tag{11.3}$$

$$-\omega^2\{h\}[M]\{U_T\} + Gr^3\,[(1 + 2i\xi_s)k_R + i\omega c_R]\,\phi_s = 0 \tag{11.4}$$

in which G is a shear modulus of reference for the soil, r the equivalent radius of the foundation, ξ_s the hysteretic damping constant for the soil, k_H and k_R the frequency-dependent horizontal and rocking stiffness coefficients for the foundation, and c_H and c_R the frequency-dependent horizontal and rocking radiation damping coefficients for the foundation. In Eqs. (11.3) and (11.4), the coupling impedance functions for the foundation have been assumed negligible and the normalized horizontal and rocking impedance functions have been written in the form $[k + i(2\xi_s + \omega c)]$ which separates the material and radiation damping in the soil.

For vibrations in the neighborhood of the fundamental fixed-base natural frequency of the superstructure it is possible to neglect the contributions of the higher modes. In this case, the relative

displacement {U} can be approximated by

$$\{U\} = \{\psi_1\}U_b \tag{11.5}$$

where U_b represents the relative displacement at the top of the structure and $\{\psi_1\}$ denotes the fundamental fixed-base mode normalized to unity at the top of the structure.

Substitution from Eqs. (11.2) and (11.5) into Eqs. (11.1), (11.3) and (11.4) leads to the following system of equations for U_b, U_s and ϕ_s:

$$[D(\omega)] \begin{Bmatrix} U_b/\beta_1 \\ (\omega_H/\omega_1)U_s \\ (\omega_R/\omega_1)H_1\phi_s \end{Bmatrix} = \begin{Bmatrix} 1 \\ (\omega_1/\omega_H) \\ (\omega_1/\omega_R) \end{Bmatrix} U_g \tag{11.6}$$

in which the matrix $[D(\omega)]$ is given by

$$[D(\omega)] = \begin{bmatrix} 1 - (\omega/\omega_1)^2 + 2i(\omega/\omega_1)\xi_1 & -(\omega/\omega_1)(\omega/\omega_H) & -(\omega/\omega_1)(\omega/\omega_R) \\ -(\omega/\omega_1)(\omega/\omega_H) & 1-(\omega/\omega_H)^2 + 2i[\xi_s + (\omega/\omega_H)\xi_H] & -(\omega/\omega_H)(\omega/\omega_R) \\ -(\omega/\omega_1)(\omega/\omega_R) & -(\omega/\omega_R)(\omega/\omega_H) & 1 - (\omega/\omega_R)^2 + 2i[\xi_S + (\omega/\omega_R)\xi_R] \end{bmatrix} \tag{11.7}$$

In Eqs. (11.6) and (11.7), ω_1 and ξ_1 represent, respectively, the fixed-base natural frequency and modal damping ratio of the superstructure, while β_1 and H_1 defined by

$$\beta_1 = \{\psi_1\}^T[M]\{1\}/\{\psi_1\}^T[M]\{\psi_1\} \tag{11.8}$$

and

$$H_1 = \{\psi_1\}^T[M]\{h\}/\{\psi_1\}^T[M]\{1\} \tag{11.9}$$

represent the modal participation factor and modal height, respectively. The frequency-dependent quantities $\omega_H(\omega)$ and $\omega_R(\omega)$ are defined by

$$\omega_H^2 = Gr\, k_H(\omega)/M_1 \tag{11.10}$$

$$\omega_R^2 = Gr^3\, k_R(\omega)/M_1H_1^2 \tag{11.11}$$

in which M_1 corresponds to the modal mass

$$M_1 = \beta_1^2\{\psi_1\}^T[M]\{\psi_1\}. \tag{11.12}$$

Finally, the frequency-dependent quantities $\xi_H(\omega)$ and $\xi_R(\omega)$ are defined by

$$\xi_H = \omega_H c_H(\omega)/2k_H(\omega) \tag{11.13}$$

$$\xi_R = \omega_R c_R(\omega)/2k_R(\omega)\ . \tag{11.14}$$

It should be noted that the approximations

$$\{1\}^T[M]\{1\}\sim M_1,\ \{h\}^T[M]\{1\}\sim M_1H_1,\ \{h\}^T[M]\{h\}\sim M_1H_1^2 \tag{11.15}$$

THIS PAGE LEFT BLANK

have been used in the deriviation of Eq. (11.6). For most structure , $\beta_1 \sim 1.3 - 1.5$, $H_1/H \sim 0.6 - 0.7$ and $M_1/M_b \sim 0.6 - 0.8$ where M_b is the total mass.

An approximate solution of Eq. 11.6 obtained by neglecting terms involving products of the small quantities ξ_1, ξ_s, ξ_R and ξ_H is given by

$$\begin{Bmatrix} U_b \\ U_s \\ H\phi_s \end{Bmatrix} = \frac{(\omega/\tilde{\omega}_1)^2}{\Delta_o(\omega)} \begin{Bmatrix} \beta_1(\tilde{\omega}_1/\omega_1)^2 & & \\ (1 - 2i[\xi_s - (\omega/\omega_1)\xi_1 + (\omega/\omega_H)\xi_H]) & (\omega_1/\omega_H)^2 & \\ (1 - 2i[\xi_s - (\omega/\omega_1)\xi_1 + (\omega/\omega_R)\xi_R]) & (\omega_1/\omega_R)^2(H/H_1) & \end{Bmatrix} U_g \qquad (11.16)$$

in which H is the height of the structure and

$$\Delta_o(\omega) = 1 - (\omega/\tilde{\omega}_1)^2 + 2i\tilde{\xi}_1 \qquad (11.17)$$

where

$$1/\tilde{\omega}_1^2 = 1/\omega_1^2 + 1/\omega_R^2 + 1/\omega_H^2 \qquad (11.18)$$

and

$$\tilde{\xi}_1(\omega) = (\omega/\omega_1)^3\tilde{\xi}_1 + [1 - (\omega/\omega_1)^2]\xi_s + (\omega/\omega_H)^3\xi_H + (\omega/\omega_R)^3\xi_R + [1 - (\omega/\tilde{\omega}_1)^2](\xi_1\omega/\omega_1 - \xi_s). \qquad (11.19)$$

It is apparent from Eqs. (11.16) and (11.17) that the peak response of the system occurs in the vicinity of the frequency $\tilde{\omega}_1$, given by Eq. (11 18), which corresponds to the fundamental frequency of the complete soil-structure system. The equivalent damping ratio for the complete system corresponds to $\tilde{\xi}_1(\tilde{\omega}_1)$ which can be obtained from Eq. (11.19) by setting $\omega = \tilde{\omega}_1$. In the particular case of a single-story structure ($\beta_1 = 1$, $H_1 = H$, $M_1 = M_b$), the results given by Eq. (11.16) are equivalent to those obtained by Jennings and Bielak (1973). In the general case of multistory structures the expressions for U_s and ϕ_s given above differ from those presented by Jennings and Bielak. The corresponding expressions obtained by Jennings and Bielak (1973) erroneously include an additional factor β_1.

The first of Eqs. (11.16) indicates that the relative response of the superstructure U_b, including the effects of soil-structure interaction, can be assimilated to the relative response of an equivalent one degree-of-freedom oscillator with natural frequency $\tilde{\omega}_1$ and damping ratio $\tilde{\xi}_1(\tilde{\omega}_1)$ when subjected to a base translation given by $\beta_1(\tilde{\omega}_1/\omega_1)^2 U_g$.

Having obtained a solution for U_b, U_s and $H\phi_s$ in terms of the free-field motion U_g it is possible to obtain other quantities of interest, such as the total translational response at foundation level, $U_{To} = U_g + U_s$, the total translational response at the top of the structure, $U_{Tb} = U_{To} + H\phi_s + U_b$, and the translational response at the top relative to the total translation of the base, $U_{Tb} - U_{To}$. The resulting expressions are

$$U_{To} = [1 - (\omega/\tilde{\omega}_1^*)^2 + 2i\tilde{\xi}_1^*] U_g/\Delta_o(\omega) \qquad (11.20)$$

$$U_{Tb} = \{\beta_1(\omega/\tilde{\omega}_1^*)^2 + 1 - (\omega/\tilde{\omega}_1^*)^2 + 2i\tilde{\xi}_1^* + (\omega/\omega_R)^2(H/H_1 - \beta_1) + 2i(H/H_1)[(\omega/\omega_1)\xi_1 - \tilde{\xi}_1^*]\} U_g/\Delta_o(\omega) \qquad (11.21)$$

$$U_{Tb} - U_{To} = \{\beta_1(\omega/\tilde{\omega}_1^*)^2 + (\omega/\omega_R)^2(H/H_1 - \beta_1) + 2i(H/H_1)[(\omega/\omega_1)\xi_1 - \tilde{\xi}_1^*] U_g/\Delta_o(\omega) \qquad (11.22)$$

in which $\tilde{\omega}_1^*$ and $\tilde{\xi}_1^*(\omega)$ are defined by

$$(\tilde{\omega}_1^*)^{-2} = (\omega_1)^{-2} + (\omega_R)^{-2} \tag{11.23}$$

and

$$\tilde{\xi}_1^*(\omega) = (\omega/\omega_1)^3\xi_1 + [1-(\omega/\omega_1)^2]\xi_s + (\omega/\omega_R)^3\xi_R + [1-(\omega/\tilde{\omega}_1^*)^2]\,(\xi_1\omega/\omega_1 - \xi_s). \tag{11.24}$$

Eq. (11.20) indicates that the total translational response of the base U_{To} will exhibit a peak in the vicinity of the system frequency $\tilde{\omega}_1$ and a minimum in the vicinity of the frequency $\tilde{\omega}_1^*$ given by Eq. (11.23).

Finally, it is interesting to note that $U_{To} + H_1\phi_s$ given by

$$U_{To} + H_1\phi_s = [1 - (\omega/\omega_1)^2 + 2i\xi_1(\omega/\omega_1)]U_g/\Delta_o(\omega) \tag{11.25}$$

exhibits a minimum in the vicinity of the fixed-base natural frequency ω_1.

The basic results given by Eqs. (11.16), (11.20), (11.21), (11.22), and (11.25) have been used by Luco (1980) to interpret the results of structural identification techniques which neglect the effects of soil-structure interaction. It is convenient to consider first a hypothetical identification technique based on the transfer function between the free-field motion U_g and the total translational response at the top of the structure U_{Tb}. This is a hypothetical situation since the free-field motion is rarely recorded. In this case, and neglecting the effects of soil-structure interaction, the transfer function would be given by

$$\left(\frac{U_{Tb}}{U_g}\right)_{r.s.} = \frac{\beta_1(\omega/\omega_1)^2 + 1 - (\omega/\omega_1)^2 + 2i\xi_1(\omega/\omega_1)}{1 - (\omega/\omega_1)^2 + 2i(\omega/\omega_1)\xi_1} \tag{11.26}$$

The actual transfer function, given by Eq. (11.21), is

$$\frac{U_{Tb}}{U_g} = \frac{\beta_1(\omega/\tilde{\omega}_1^*)^2 + 1 - (\omega/\tilde{\omega}_1^*)^2 + 2i\tilde{\xi}_1^*}{1 - (\omega/\tilde{\omega}_1)^2 + 2i\tilde{\xi}_1} \tag{11.27}$$

where the last two terms appearing in Eq. (11.21) have been neglected. Comparison of Eq. (11.26) and (11.27) reveals that the modal frequency and modal damping ratio calculated by this identification technique would actually correspond to the system frequency $\tilde{\omega}_1$ and to the equivalent system damping ratio $\tilde{\xi}_1(\tilde{\omega}_1)$. Since $\tilde{\omega}_1^*$ is not very different from $\tilde{\omega}_1$, the calculated participation factor would correspond to the actual participation factor β_1. It should be noted that the typical identification techniques when applied to forced or ambient vibration tests also lead to estimates of $\tilde{\omega}_1$ and $\tilde{\xi}_1$ (Luco, Wong and Trifunac, 1980).

As a second case, consider a more common identification technique based on the transfer function between the total translational motion at foundation level U_{To} and the total translational response at the top of the structure U_{Tb} (Udwadia and Trifunac, 1974). The transfer function, if the effects of soil-structure interaction are neglected, is also given by Eq. (11.26) (when soil-structure interaction is neglected, U_{To} is assumed to be equal to U_g). The actual transfer function as obtained from Eqs. (11.20) and (11.21) is

$$\frac{U_{Tb}}{U_{To}} = \frac{\beta_1(\omega/\tilde{\omega}_1^*)^2 + 1 - (\omega/\tilde{\omega}_1^*)^2 + 2i\tilde{\xi}_1^*}{1 - (\omega/\tilde{\omega}_1^*)^2 + 2i\tilde{\xi}_1^*} \tag{11.28}$$

where, again, the last two terms in Eq. (11.21) have been neglected. Comparison of Eqs. (11.26) and (11.28) indicates that, in this case, the calculated modal frequency and damping ratio would correspond to the apparent system frequency $\tilde{\omega}_1^*$ and to the apparent system damping ratio $\tilde{\xi}_1^*(\tilde{\omega}_1^*)$. In this case, the calculated participation factor would also correspond to the actual participation factor.

An identification technique based on the transfer function between the total translation of the base U_{To} and the relative translation $U_{Tb} - U_{To}$ at the top, leads to similar results, i.e., the calculated modal quantities correspond to $\tilde{\omega}_1^*$, $\tilde{\xi}_1^*(\tilde{\omega}_1^*)$ and β_1.

To isolate the modal characteristics of the superstructure it would be necessary to consider the transfer function between $U_{To} + H_1\phi_s$ and $U_b = U_{Tb} - (U_{To} + H\phi_s)$. From Eqs. (11.16) and (11.25), the transfer function in this case is

$$\frac{U_b}{U_{To} + H_1\phi_s} = \frac{\beta_1(\omega/\omega_1)^2}{1 - (\omega/\omega_1)^2 + 2i\xi_1(\omega/\omega_1)} \tag{11.29}$$

in which only structural properties are involved. For this technique to be used it is necessary to record U_{Tb}, U_{To}, and the rocking angle ϕ_s (on a common time basis). The typical instrumentation of buildings, which does not contain provisions for the recording of the rocking response at foundation level, eliminates this possibility of isolating the structural characteristics.

The previous discussion indicates the important role that the system frequency $\tilde{\omega}_1$ and the apparent system frequency $\tilde{\omega}_1^*$ play in the calculation of the response of the system. It is of particular interest to determine the deviation of $\tilde{\omega}_1$ and $\tilde{\omega}_1^*$ from the fixed-base frequency of the supersturcture ω_1. Eqs. (11.18) and (11.23),

$$\left(\frac{\omega_1}{\tilde{\omega}_1}\right)^2 = 1 + \left(\frac{\omega_1}{\omega_R}\right)^2 + \left(\frac{\omega_1}{\omega_H}\right)^2 \tag{11.30}$$

$$\left(\frac{\omega_1}{\tilde{\omega}_1^*}\right)^2 = 1 + \left(\frac{\omega_1}{\omega_R}\right)^2 \tag{11.31}$$

indicate that the deviations of $\tilde{\omega}_1$ and $\tilde{\omega}_1^*$ from ω_1 depend on the ratios (ω_1/ω_R) and (ω_1/ω_H). At this point it should be noted that ω_R corresponds to the frequency of the system if the superstructure is rigid and the foundation is prevented from translating. Similarly, the frequency ω_H corresponds to the resonant frequency of the system if the superstructure is rigid and the foundation is prevented from rocking. The frequency $[\omega_R^{-2} + \omega_H^{-2}]^{-1/2}$ corresponds to the frequency of the system if the superstructure is rigid and the foundation is free to translate and rotate.

The ratios (ω_1/ω_R) and (ω_1/ω_H), calculated by use of Eqs. (11.10, and (11.11), are given by

$$(\omega_1/\omega_R)^2 = (\omega_1 r/\beta)^2 (M_1/\pi r^2 \varrho_s H_1)(H_1/r)^3 (\pi/k_R) \tag{11.32}$$

$$(\omega_1/\omega_H)^2 = (\omega_1 r/\beta)^2 (M_1/\pi r^2 \varrho_s H_1)(H_1/r)(\pi/k_H) \tag{11.33}$$

where β is a shear wave velocity of reference for the soil and ϱ_s is the soil density ($G = \varrho_s\beta^2$). Eqs. (11.32) and (11.33) indicate that the deviations of $\tilde{\omega}_1$ and $\tilde{\omega}_1^*$ from ω_1 will depend on the relative stiffness of the structure measured by $(\omega_1 r/\beta)$, on the mass ratio $(M_1/\pi r^2 \varrho_s H_1)$ and on the slenderness ratio H_1/r. The slenderness ratio H_1/r is approximately equal to 0.67 H/r and takes values in the range from 0.5 to 3.0. The mass ratio $(M_1/\pi r^2 \varrho_s H_1)$ is approximately equal to $(M_b/\pi r^2 \varrho_s H)$, and, for most structures, has a value of the order of 0.2. The relative stiffness parameter $(\omega_1 r/\beta)$ typically varies in the

range from 0. to 2. For a ten - story building with a fixed-base frequency of 1 Hz, resting on a foundation with an equivalent radius r = 15 m supported on a soil with a characteristic shear wave velocity β = 400 m/sec, the value of $\omega_1 r/\beta$ is 0.24. For a containment structure in a nuclear power plant (f_1 = 5 Hz, r = 23 m) supported on a soil with a shear wave velocity of 800 m/sec, the corresponding value of $\omega_1 r/\beta$ is 0.9. The normalized stiffness coefficients k_R and k_H appearing in Eqs. (11.32) and (11.33) depend on the characteristics of the soil deposit and on the dimensionless frequency $\omega r/\beta$. This dimensionless frequency must be set equal to $\tilde{\omega}_1 r/\beta$ to calculate $\tilde{\omega}_1$, and to $\tilde{\omega}_1^* r/\beta$ to calculate $\tilde{\omega}_1^*$. For this reason, an iterative process may be required to obtain $\tilde{\omega}_1$ and $\tilde{\omega}_1^*$. For a circular foundation supported on a uniform elastic half-space (υ = 0.33), the foundation stiffness coefficients, at low frequencies, take values of the order of $k_R \sim 4$ and $k_H \sim 5$.

The deviations of the system frequency $\tilde{\omega}_1$ and of the apparent system frequency $\tilde{\omega}_1^*$ from the fixed-base frequency ω_1 are illustrated in Fig. 11.1. In this figure the ratios $\tilde{\omega}_1/\omega_1$ and $\tilde{\omega}_1^*/\omega_1$ are presented versus the relative stiffness $\omega_1 r/\beta$ for three values of the slenderness ratio H_1/r. The results presented in Fig. 11.1 are based on a mass ratio $(M_1/\pi r^2 \varrho_s H_1 = 0.2$ and on the foundation stiffness coefficients obtained by Luco and Westmann (1971) for a rigid circular foundation resting on a uniform half-space (υ = 0.33). The results presented in Fig. 11.1 indicate that the system frequencies $\tilde{\omega}_1$ and $\tilde{\omega}_1^*$ can be significantly lower than the fixed-base frequency ω_1. The deviations increase with relative stiffness ($\omega_1 r/\beta$) and with slenderness ratio H_1/r. The apparent system frequency $\tilde{\omega}_1^*$ is slightly higher than the true system frequency $\tilde{\omega}_1$. The difference between $\tilde{\omega}_1$ and $\tilde{\omega}_1^*$ decreases as the slenderness ratio increases. Similar results for $\tilde{\omega}_1$ have been presented by Jennings and Bielak (1973).

In many cases the fixed-base natural frequency ω_1 is not known and must be determined from the observed values of $\tilde{\omega}_1$ or $\tilde{\omega}_1^*$. The results presented in Fig. (11.2) can be utilized for that purpose. In Fig. 11.2, the ratio $\omega_1/\tilde{\omega}_1$ is presented versus $\tilde{\omega}_1 r/\beta$ for four values of the slenderness ratio. The ratio $\omega_1/\tilde{\omega}_1^*$ versus $\omega_1^* r/\beta$ is also shown in Fig. 11.2. To utilize the results presented in Fig. 11.2 it is necessary to have an estimate of the characteristic shear wave velocity in the soil and of the equivalent radius of the foundation. It is interesting to notice that $\tilde{\omega}_1 r/\beta$ and $\tilde{\omega}_1^* r/\beta$ cannot exceed the values

$$\frac{\tilde{\omega}_1 r}{\beta} = \left\{ \left(\frac{M_1}{\pi \varrho_s r^2 H_1} \right) \left[\left(\frac{H_1}{r} \right)^3 \frac{\pi}{k_R} + \left(\frac{H_1}{r} \right) \frac{\pi}{k_H} \right] \right\}^{-1/2} \tag{11.34}$$

$$\frac{\tilde{\omega}_1^* r}{\beta} = \left\{ \left(\frac{M_1}{\pi \varrho_s r^2 H_1} \right) \left(\frac{H_1}{r} \right)^3 \left(\frac{\pi}{k_R} \right) \right\}^{-1/2} \tag{11.35}$$

These limiting values correspond to the system frequencies when the superstructure is rigid.

During moderate and strong seismic excitations significant strains are induced in the soil. These strains cause a marked reduction in the effective shear modulus and on the shear wave velocity of the soil. The effects of such changes on the frequency of the soil-structure system are illustrated in Fig. 11.3. In this figure, the ratio of the system frequency $\tilde{\omega}_1(\beta')$, when the shear wave velocity has been reduced by 33 percent ($\beta' = 0.67\beta$), to the system frequency $\tilde{\omega}_1(\beta)$ for the initial soil conditions is shown versus $\omega_1 r/\beta$ for different values of the slenderness ratio. The results shown in Fig. 11.3 indicate that a variation in soil properties, as a result of the seismic excitation, may lead to a significant reduction of the system frequency. The variation of the apparent system frequency $\tilde{\omega}_1^*$ is similar to that of ω_1. Reductions of the shear wave velocity of the order of 30 percent can be produced by shear strains in the soil of the order of 0.1 percent. For very stiff structures, Eq. (11.34) indicates that $\tilde{\omega}_1(\beta')/\tilde{\omega}_1(\beta)$

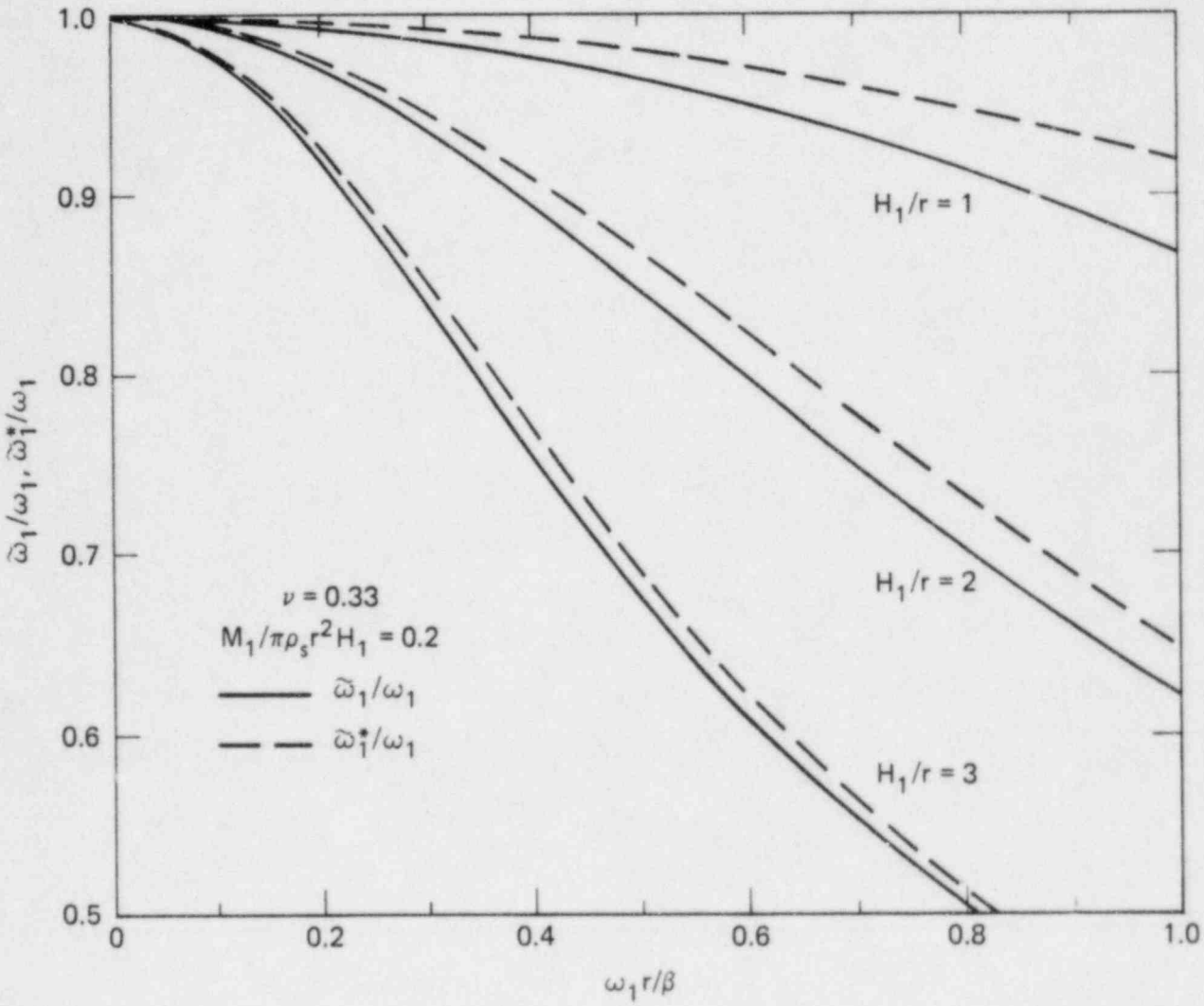

FIG. 11.1 System frequency and apparent system frequency versus relative stiffness and slenderness ratio (after Luco, 1980).

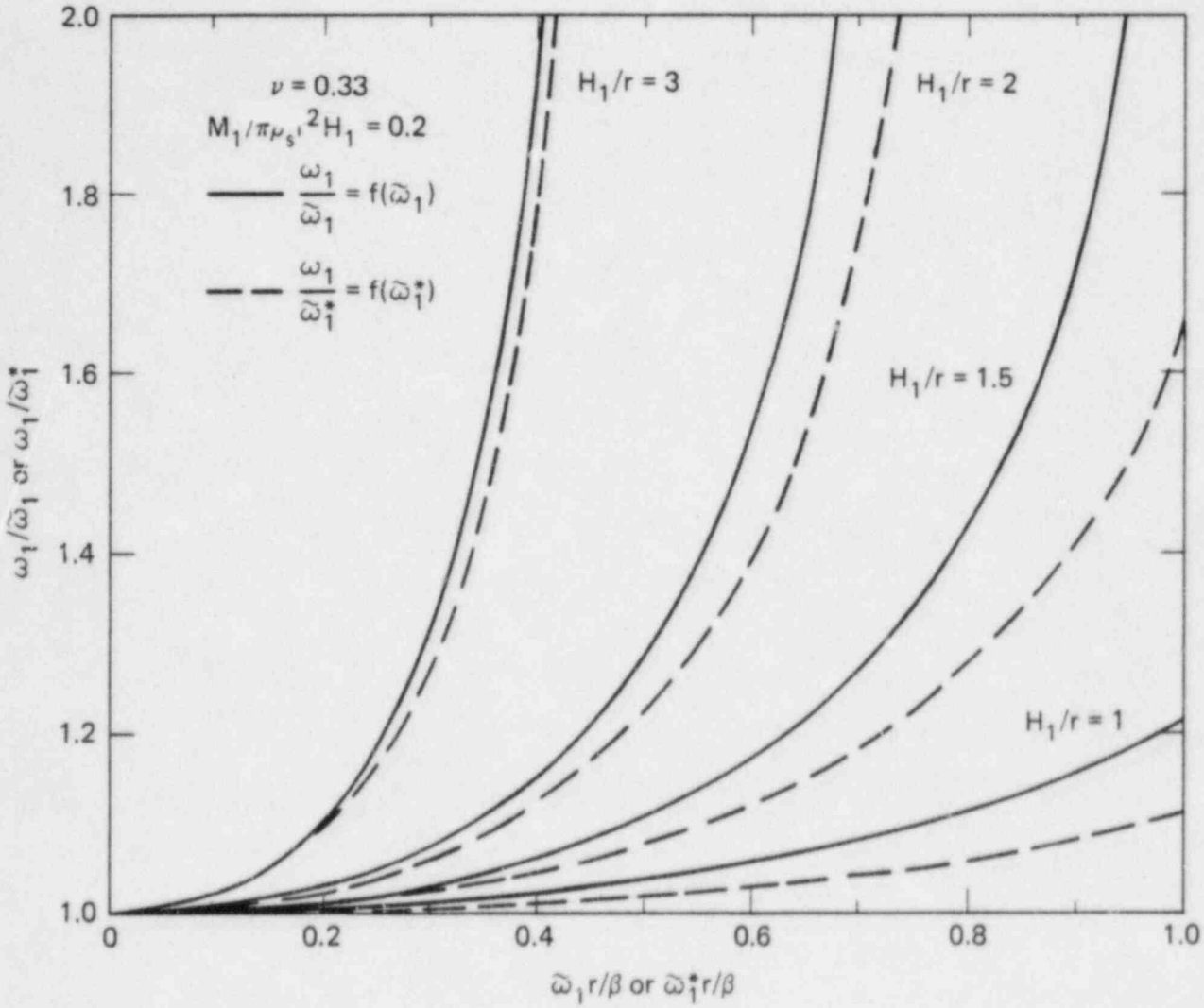

FIG. 11.2. Fixed-base natural frequency in terms of the system frequency or of the apparent system frequency (after Luco, 1980).

$= \beta'/\beta$ and the change in system frequency would provide a measure of the variation in soil properties.

The effect described above explains, in part, the temporary changes in system frequencies observed by Udwadia and Trifunac (1974) on the Millikan Library building (50 percent reduction) and on the administration building at the Jet Propulsion Laboratory in Pasadena (20 percent reduction) during the San Fernando earthquake of 1971 (Luco, 1980).

It has been shown that the common structural identification techniques do not determine the damping in the superstructure but rather provide a measure of the overall system damping $\tilde{\xi}_1(\tilde{\omega}_1)$ or of the apparent system damping $\tilde{\xi}_1^*(\tilde{\omega}_1^*)$. Apparent damping ratios as high as 10 percent of critical for moderate seismic excitation have been reported in several studies (Hart et al., 1973, Iemura and Jennings, 1973, Hart and Vasudevan, 1975). It is of interest to describe the effects of soil-structure interaction on the apparent damping ratios.

In the first place, it should be mentioned that Eq. 11.19 indicates that the energy dissipation for the complete system does not follow a viscous or hysteretic type of model but a more complete frequency-dependent behavior. The approximate equivalent system damping ratio is given by

$$\tilde{\xi}_1(\tilde{\omega}_1) = (\tilde{\omega}_1/\omega_1)^3\xi_1 + [1-(\tilde{\omega}_1/\omega_1)^2]\xi_s + (\tilde{\omega}_1/\omega_H)^3\xi_H + (\tilde{\omega}_1/\omega_R)^3\xi_R \tag{11.36}$$

while the apparent equivalent system damping ratio is given by

$$\tilde{\xi}_1^*(\tilde{\omega}_1^*) = (\tilde{\omega}_1^*/\omega_1)^3\xi_1 + [1-(\tilde{\omega}_1^*/\omega_1)^2]\xi_s + (\tilde{\omega}_1^*/\omega_R)^3\xi_R \tag{11.37}$$

The first terms in Eqs. (11.36) and (11.37) correspond to the contribution of attenuation in the superstructure, the second terms represent the contribution of material damping in the soil, while the remaining terms reflect the attenuation by radiation of energy into the soil.

It is apparent from Eqs. (11.36) and (11.37) that as the effects of soil-structure interaction become more important ($\tilde{\omega}_1 < \omega_1$, $\tilde{\omega}_1^* < \omega_1$), the contribution of attenuation in the structure to the overall damping decreases drastically. On the other hand, the contributions of material damping in the soil and of the radiation damping increase significantly and become dominant. These effects are illustrated in Figs. 11.4 and 11.5. In Fig. 11.4, the factors $(\tilde{\omega}_1/\omega_1)^3$ and $(\tilde{\omega}_1^*/\omega_1)^3$ which multiply ξ_1 and the factors $[1-(\tilde{\omega}_1/\omega_1)^2]$ and $[1-\tilde{\omega}_1^*/\omega_1)^2]$ which multiply ξ_s are presented versus the relative stiffness $\omega_1 r/\beta$ for various values of the slenderness ratio. For a relatively stiff structure ($\omega_1 r/\beta = 1.0$) and a slenderness ratio $H_1/r = 2$, the factor multiplying ξ_1 is 0.25, while that multiplying ξ_s is 0.62.

The contributions of radiation damping to the overall system damping $\tilde{\xi}_1$ and to the apparent system damping $\tilde{\xi}_1^*$ are shown in Fig. 11.5 versus the relative stiffness $\omega_1 r/\beta$. In general, the contribution of radiation damping to $\tilde{\xi}_1$ is larger than that to $\tilde{\xi}_1^*$. For sufficiently stiff structures (relative to the soil) radiation damping may contribute in excess of one percent of the overall critical damping. For a relative stiffness $\omega_1 r/\beta = 2$, radiation damping may contribute from 5 to 15 percent of the overall critical damping depending on the slenderness ratio (Jennings and Bielak, 1973).

The variation of the system damping ratio $\tilde{\xi}_1$ and of the apparent damping ratio $\tilde{\xi}_1^*$ versus the relative stiffness parameter $\omega_1 r/\beta$ are shown in Fig. 11.6 for $\xi_1 = 0.05$ and for three values of ξ_s ($H_1/r = 2$, $M_1/\pi\varrho_s r^2 H_1 = 0.2$). It can be observed that, in general, $\tilde{\xi}_1^* < \tilde{\xi}_1$. If $\xi_s < \xi_1$, the system damping ratios may be lower than the damping on the structure. This possibility has been noted previously by Jennings and Bielak (1973). On the other hand if $\xi_s > \xi_1$, the system damping ratios for relatively stiff structures can be significantly higher than ξ_1.

It is important to notice that for relatively stiff structures (or for soft soils) the system damping ratio $\tilde{\xi}_1$ and the apparent damping ratio ξ_1^* provide poor measures of the attenuation in the superstructure. Large variations in the value of $\tilde{\xi}_1$ could have little effect on the values of $\tilde{\xi}_1$ and $\tilde{\xi}_1^*$ and, consequently, it becomes difficult to estimate ξ_1 from observed values of $\tilde{\xi}_1$ or ξ_1^*.

During seismic excitation the strains induced in the soil produce not only a reduction in shear wave velocity but also a significant increase in the equivalent hysteretic damping in the soil. The reduction of β coupled with an increase in ξ_s may lead to a large increase in the value of the system damping. Con-

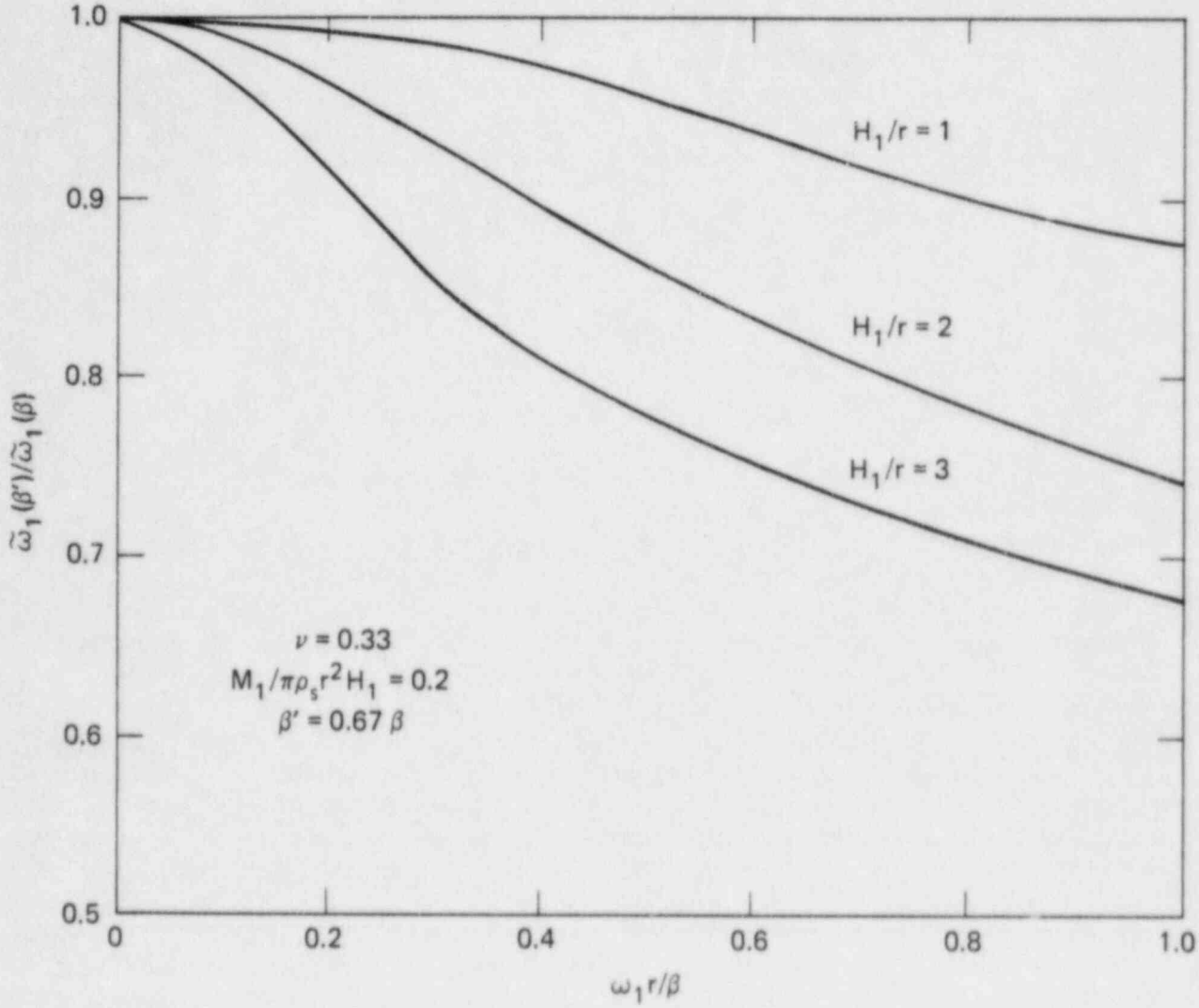

FIG. 11.3. Effect of a reduction of the soil shear wave velocity on the system frequency (after Luco, 1980).

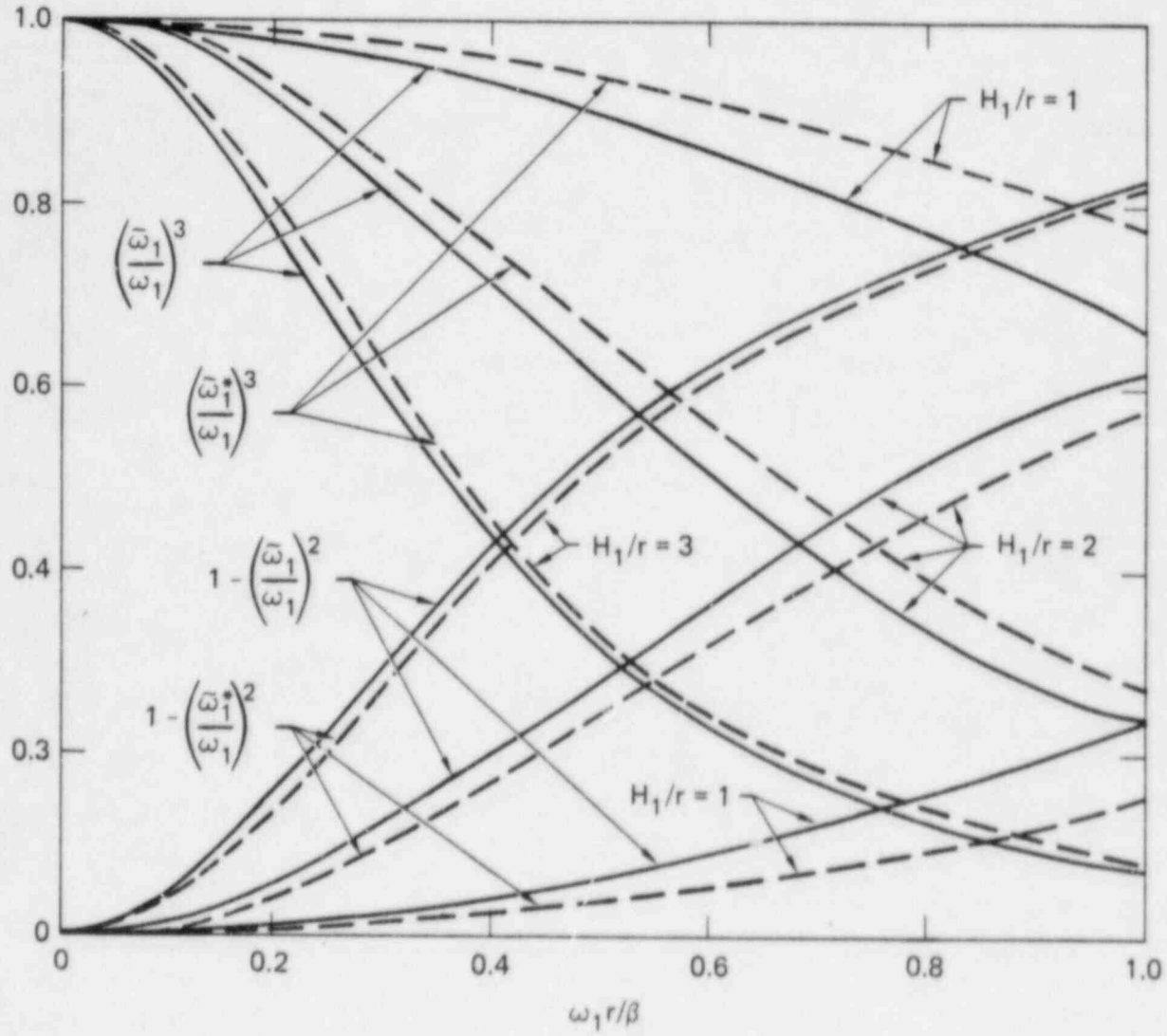

FIG. 11.4. Participation factors of the structural and material soil damping to the system damping and to the apparent system damping ($M_1/\pi\varrho_s r^2 H_1 = 0.2, \upsilon = 0.33$)(after Luco, 1980).

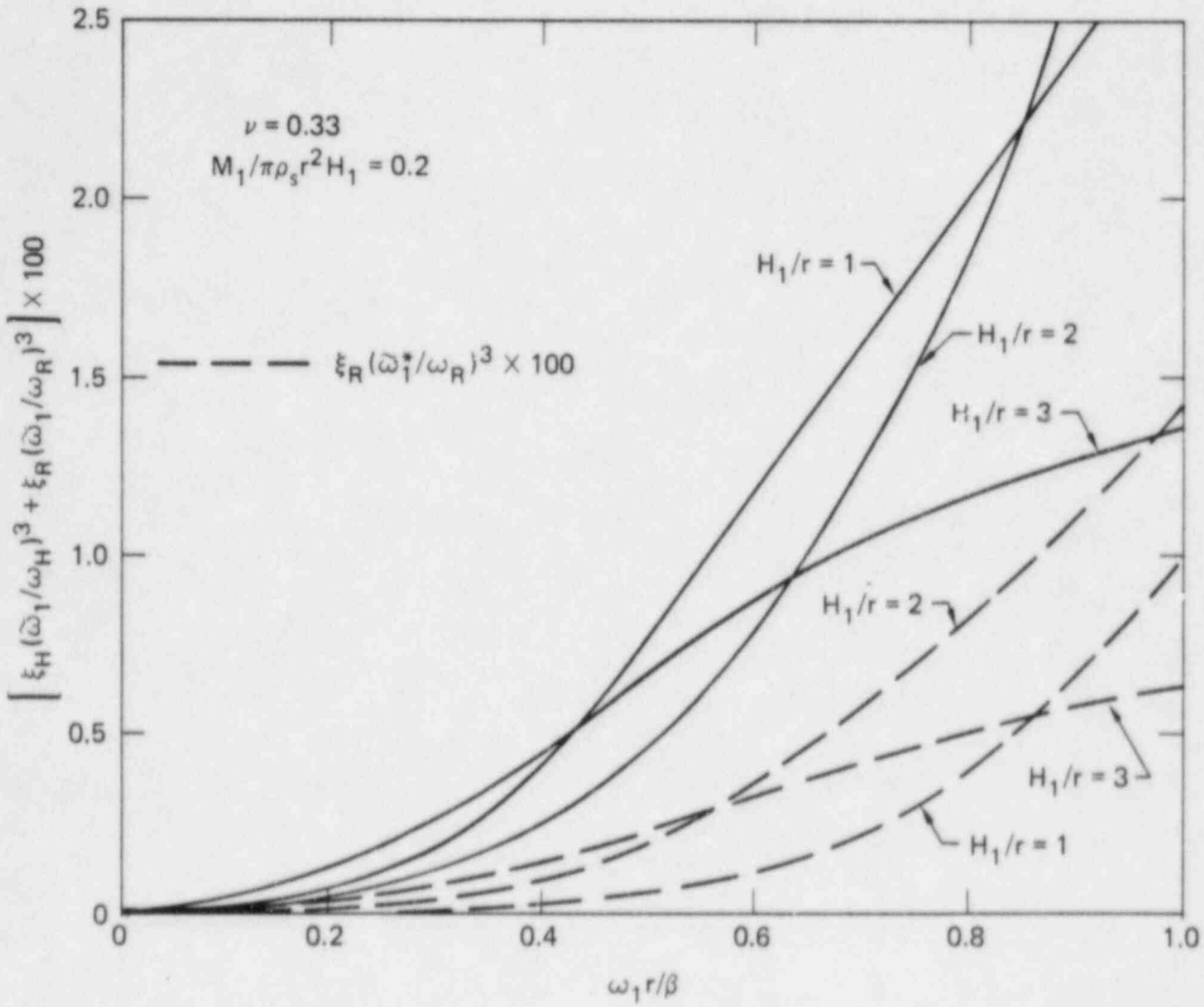

FIG. 11.5. Contribution of radiation damping to the overall system damping and to the apparent system damping (after Luco, 1980).

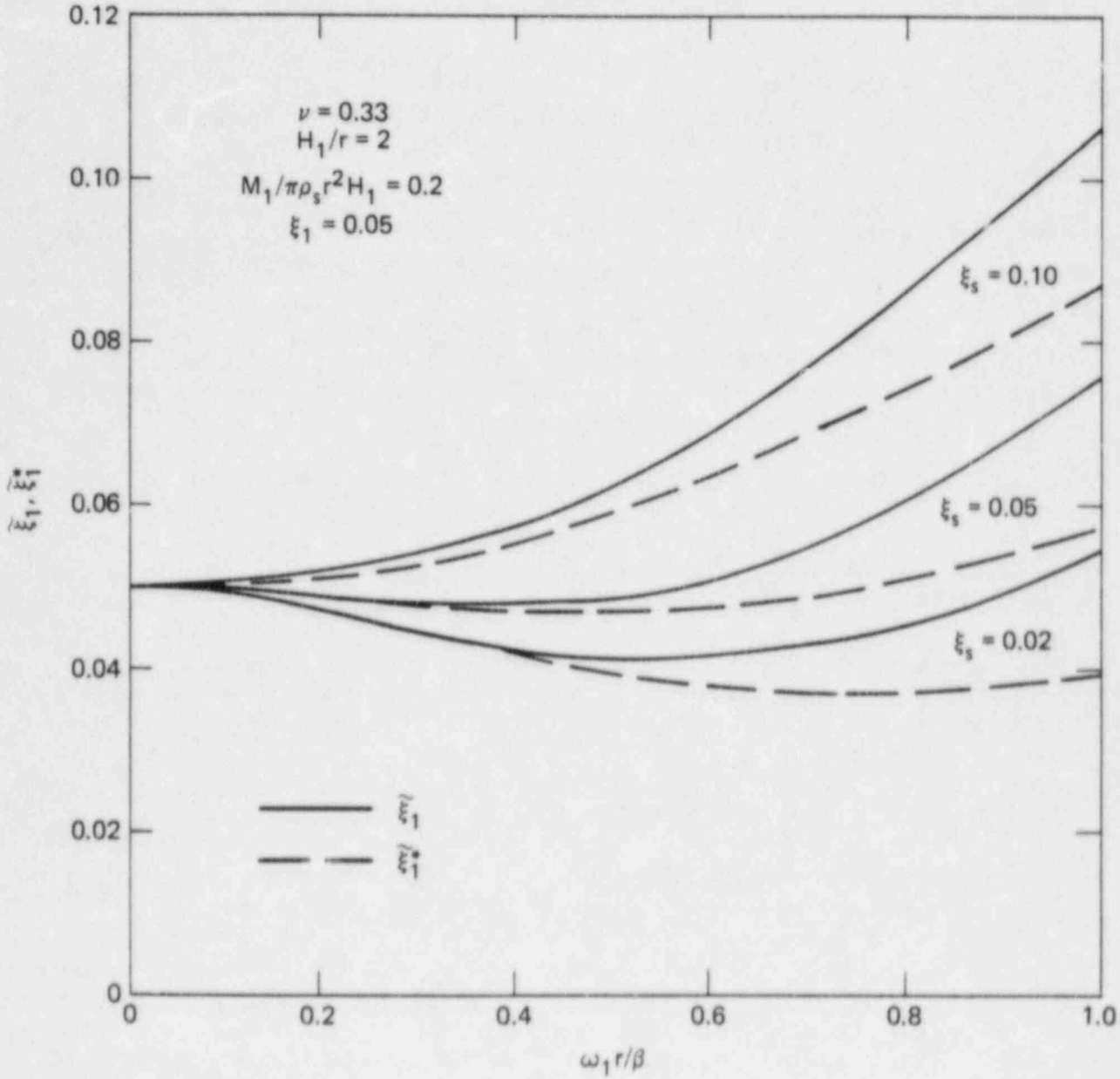

FIG. 11.6. Effect of the relative stiffness and of the material soil damping on the overall system damping and on the apparent system damping (after Luco, 1980).

sider an initial situation in which $\xi_1 = 0.05$, $\xi_s = 0.02$ and $\omega_1 r/\beta = 0.6$. In this case from Fig. 11.6 it is found that $\widetilde{\xi}_1 = 0.04$. If the seismic excitation induces shear strains in the soil of the order of 0.1 percent, β would suffer a reduction of 33 percent and ξ_s would increase to 0.10. Under these conditions, $\omega_1 r/\beta \sim 0.9$ and $\widetilde{\xi}_1$ would reach a value of 0.09. This mechanism may explain in part the large damping values obtained by various studies of the seismic response of structures.

REFERENCES (11)

Bielak, J. (1971). Earthquake Response of Building-Foundation Systems, *Report EERL 71-04, Earthquake Engineering Research Laboratory,* California Institute of Technology, Pasadena, California.

Foutch, D. A., Luco, J. E., Trifunac, M. D., and Udwadia, F. E. (1975). Full-Scale, Three-Dimensional Tests of Structural Deformations During Forced Excitation of a Nine-Story Reinforced Concrete Building, *Proc. U.S. National Conference on Earthquake Engineering,* Ann Arbor, Michigan, pp. 206-215.

Hart, G. C., Lew, M., and DiJulio, R. (1973). High-Rise Building Response: Damping and Period Nonlinearities, *Proc. Fifth World Conference on Earthquake Engineering,* Vol. 2, Rome, Italy.

Hart, G. C., and Vasudevan, R. (1975). Earthquake Design of Buildings: Damping, *Journal of the Structures Division,* ASCE, Vol. 101, ST 1, Jan., pp. 11-30.

Iemura, H., and Jennings, P.C. (1974). Hysteretic Response of a Nine-Story Reinforced Concrete Building, *International Journal of Earthquake Engineering and Structural Dynamics,* Vol. 3, No. 2, Oct.-Dec., pp. 183-202.

Jennings, P. C., and Bielak, J. (1973). Dynamics of Building-Soil Interaction, *Bulletin of the Seismological Society of America,* Vol. 63, pp. 9-48.

Luco, J. E., Wong, H. L., and Trifunac, M. D. (1980). Soil-Structure Interaction Effects on Forced Vibration Tests, *Report,* Dept. of Civil Engineering, Univ. So. Calif., Los Angeles, Calif.

Luco, J. E., and Westmann, R. A. (1971). Dynamic Response of Circular Footings, *Journal of the Engineering Mechanics Division,* ASCE, Vol. 97, pp. 1381-1395.

Luco, J. E. (1980). Soil-Structure Interaction and Identification of Structural Models. *Proc. ASCE Specialty Conference,* Knoxville, Tennessee.

Udwadia, F. E., and Trifunac, M. D. (1974). Time and Amplitude Dependent Response of Structures, *International Journal of Earthquake Engineering and Structural Dynamics,* Vol. 2, pp. 359-378.

12. FINAL COMMENTS

Since the pioneering studies of Sezawa and Kanai (1935, 1936) and, particularly, in the last ten years, the field of soil-structure interaction has experienced a tremendous growth. At the present time, it is possible to analyze with some confidence a number of configurations involving interaction with and through the soil. Significant advances have been made in the incorporation of the effects of soil layering, foundation embedment and nonvertically incident seismic excitation. A number of alternative analytical techniques and some user-oriented computer programs are available. Additional development of user-oriented computer programs in the areas of three-dimensional embedded foundations of arbitrary shape, flexible embedded foundations, pile-supported structures and through-the-soil coupling for embedded foundations is required.

The opportunities created by these developments in modeling and analysis techniques are somewhat limited by the uncertainties in the characterization of the free-field motion and of some structural and soil properties. It is expected that improved instrumentation of structures and the use of more refined soil-structure models will permit the identification of these properties.

Finally, it should be mentioned that the introduction of more refined modeling and analysis techniques may upset, temporarily, the balance in which some seismic hazard reduction recommendations are based. Some seismic codes are based on a balance of the predictions calculated by use of the analysis techniques prescribed by the code and observed damage. Since, in many cases, the effects of soil-structure interaction tend to reduce the calculated response, it may be necessary to adjust some of the code requirements to attain the same level of risk.

REFERENCES (12)

Sezawa, K. and K. Kanai (1935). Decay in the Seismic Vibration of a Simple or Tall Structure by Dissipation of Their Energy into the Ground, *Bull. Earth. Res. Inst.*, XIII, Part 3, 681-697.

Sezawa, K. and K. Kanai (1936). Improved Theory of Energy Dissipation in Seismic Vibrations on a Structure, *Bull. Earth. Res. Inst.*, XIV, Part 2, 164-168.

ACKNOWLEDGMENTS

This study was sponsored by the Lawrence Livermore Laboratory as part of the Seismic Safety Margins Research Program (U. S. Nuclear Regulatory Commission, U. S. Department of Energy, Contract No. W-7405-ENG-08). Partial support from Grant PFR 79.00006 from the National Science Foundation is also acknowledged.

The author would like to express his gratitude to J. J. Johnson of the Lawrence Livermore Laboratory for his continued interest in the work and for editing the original manuscript. Finally, the author is indebted to Prof. H. L. Wong of the University of Southern California for his generous contribution to almost every aspect of this work.

Technical Information Department · Lawrence Livermore Laboratory
University of California · Livermore, California 94550